Investigation of the Surface Relief Grating formation on amorphous azobenzene polymer films

DISSERTATION

zur Erlangung des Grades eines Doktors

der Naturwissenschaften

vorgelegt von

M.Sc

Padmanabh U. Veer

geb. am 07.02.1980 in solapur (INDIA)

Eingereicht beim Fachbereich-7, Physik

der Universität Siegen

Siegen 2009.

Table of Contents

Preface

The optically sensitive chromophore containing polymeric films has number of applications in optoelectronic and photonic industries. Due to this fact the research on such optically sensitive chromophores containing polymeric films has exploded during last few years. The linear and non linear optical effects are of much importance in such photo-reactive organic polymer films which are induced because of the photo-orientation of the chromophores. Light can manipulate chromophores orientation by photoisomerization. Second order non linear optical effects have also been recorded in such photosensitive films which are due to the optical poling technique. Because of all these applications, the photosensitive organic thin films are of much importance in industrial area. The understanding of the basic phenomenon behind these effects would help in new applications in the similar area.

The most staggering effect in photosensitive organic thin films is the formation of surface relief gratings (SRGs) onto thin azobenzene polymer films. The phenomenon was reported independently by two different groups in 1995. [1][2] These gratings can be inscribed onto thin films of azobenzene polymer films using intensity or polarisation modulations resulting from an interference pattern. Using a wavelength corresponding to the absorption maxima of the azobenzene moiety, grating of several hundreds of nanometre heights, depending upon initial film thickness, can be easily written well below the glass transition temperature.

Several models [3-7] have been proposed to describe the process of grating formation and to explain the origin of the force, forming these gratings but none of these theories could explain the complete process depending upon various parameters like polarisation, photo-induced softening and the origin of the inscribing force.

The scope of this thesis work is to find out the origin of the stress which leads to the formation of grating onto the azobenzene polymer film and to support the experimental data with an appropriate model. From all the theories and previously reported scientific papers, it has been seen that trans-cis-trans photo-isomerization is the initiative of the orientation phenomenon within azobenzene polymer. Considering this fact, the interaction of azobenzene chromophores with the polarised light leads to the orientation of the whole polymer chain along with the azobenzene chromophores was our assumption about the formation process. The orientation of azo chromophores leads to the generation of the mechanical stress necessary for the formation of the gratings. To verify the orientation mechanism, I studied the formation of surface relief grating by continuous and pulsed exposure techniques with respect

to temperature. The temperature dependent continuous exposure measurements have revealed the ordering of chromophores at room temperature and disordering at higher temperature whereas the temperature dependent pulsed exposure measurements have revealed the orientation and relaxation of chromophores. The experimental results were found to support the assumption of orientation mechanism. The orientation mechanism was also studied in the context of the dipole moment of the two different azobenzene polymers namely pDR1M and pMEA having dipole moments $\mu=7.0D$ and $\mu=0.05D$ respectively. From this study it was found that the orientation rate is higher for high dipole moment pDR1M compared to low dipole pMEA.

Most of the theories support the assumption of softening of the azobenzene polymer film under visible irradiation,[3-7] at least three orders of magnitude less compared to the room temperature as found near the glass transition temperature of the polymer and hence predict a light induced stress of $\sigma<1Kpa$ for the inscription of grating. The logical consequence of this assumption is that inscription of surface relief gratings should become more effective upon approaching the glass transition region of the azobenzene polymer. The temperature dependent continuous and pulsed exposure results are contradictory to the above statement. The grating formation diminishes approaching the glass transition temperature of the polymer.

Also in this study, I was able to predict the magnitude of the stress generated during the orientation mechanism of azobenzene and its relation to the laser power. The magnitude of the stress is found to be enough to deform the glassy polymer at room temperature during the process of grating formation. The stress is higher than the yield stress of the typical polymer like pDR1M, $(\sigma_Y=50MPa)$[7a,7b].

The obtained data of the temperature dependent measurements can be very well explained in frame of the viscoelastic model [7a]. Further the decomposition of the total external stress obtained from the simulation data into yield stress and viscoplastic stress can lead to the up-gradation of viscoelastic model into viscoplastic model[8] which is found to be the appropriate model for the description of deformation of a polymers in its glassy state.

Finally, we report the alteration of the mechanical properties of the polymer film during the process of grating formation by ex-situ investigation of the inscribed gratings. The ex-situ investigation was carried out by spatially resolved hardness measurements using atomic force microscope (AFM) to clarify the process at microscopic level. It can be concluded that the polymer chains are uniformly arranged with respect to each other at the crests of the grating. This uniformity and higher density increases the hardness of the polymer material at crests compared to the non uniform arrangement at troughs.

Chapter 1

Structure and properties of azobenzene polymers

1.1 Introduction

Azobenzene and many of its derivatives have been known and studied for a long time. The rigid, rod like azobenzene moiety is well suited to spontaneous organisation into thermotropic mesophases, therefore research has centred on the potential applications of the polymers doped or functionalized with azobenzene based chromophores. The azo chromophores have also been used extensively in designing nonlinear optical polymers [9,10] and in liquid crystalline (LC) displays [11]. One of the most important and known properties of azo chromophore however, is the photochemical trans ↔ cis isomerisation induced by UV or visible light [12]. In azo polymer, the photoisomerization induces conformational changes in the polymer chains, which in turn lead to macroscopic variations in the chemical and physical properties of the surrounding and media. This photoisomerization allows systems containing azo molecules to be employed as photoswitches that could control rapidly and reversibly the material properties [12-14]. In 1984 it was seen that when a thin polymer film of azo dye is exposed to linearly polarised light (LPL), optical anisotropy is generated as a result of photo isomerisation and photoorientation of the chromophores perpendicular to the laser polarisation direction to give birefringent and dichroic films [15]. Later on, authors[16,17] reported another unexpected effect of photoisomerization. Irradiation of thin azo polymer film with an interference pattern of coherent light can induce not only photoorientation chromophores through the volume of the material (birefringence gratings), but also a controlled modification of the film surface that results in micrometer deep surface relief gratings (SRGs).

1.2 Light induced motion in azopolymer

Due to the number application in optoelectronics and photonic industry and in optical signal processing, the photo-orientation mechanism has been studied by number of researchers. This photo-orientation of azobenzene molecule occurs in the cyclic trans ↔ cis photoisomerization process where the photo-chromic azo molecules are selected by a polarized light of proper wavelength. The azobenzene molecule then undergoes a cyclic trans cis trans isomerization and finally align perpendicular to the light polarization direction. [17a] In solutions, the photoisomerization phenomenon can be neglected because in solution

rotational diffusion has enough time to randomize induced molecular orientation. [17a] Depending upon the viscosity of solution, small molecule undergoes diffusion. In case of solid polymer films, the mobility can be reduced depending upon factors like temperature, pressure and the photo-orientation effects are appreciable. [17a] One should consider at least three distinct features of photo-orientation by photo-isomerization.[17a]

A first feature would be consideration of photo-orientation by photo chemical basis.

A second feature would be consideration of photo orientation depending upon various factors like film configuration, polymer structure, molecular environment etc.

A third feature would be consideration of dynamics of photo-orientation.

Photo-orientation by photoisomerization occurs through a polarization sensitive photo-excitation, i.e. photo-selection. The probability of exciting a transition in an isomer in between its two states is proportional to the cosine square of the angle between that transition and the polarization of the excitation light[40]. Here the transition means converting from trans state to cis state.

The azobenzene chromophores that lie along the light polarization direction are excited with highest probability and the molecules may be isomerized and oriented. Since photo-isomerizable molecule has two forms that can be interconverted into each other by light and heat one can think of variety of question like, why does the molecule change orientation upon isomerization? Which isomer is oriented during which isomerization reaction? Do isomer orients upon photo-selection without isomerization? How many photoisomerization quantum yields influence photo-orientation? etc.

These questions are discussed in the following sections.

1.3 Geometric isomers of azobenzene

It is well known that azobenzene molecules can exist in two geometric isomers: trans and cis. These two configurations can easily be interconverted by light and heat as shown in figure1[17a]. The isomerization process is induced by electronic excitation of an electron from either the highest occupied non bonded orbital (n) or the highest occupied π orbital to the lowest unoccupied π orbital (π*). A non-radiative decay from the excited states puts the molecule back to the ground state either in the cis or trans state.
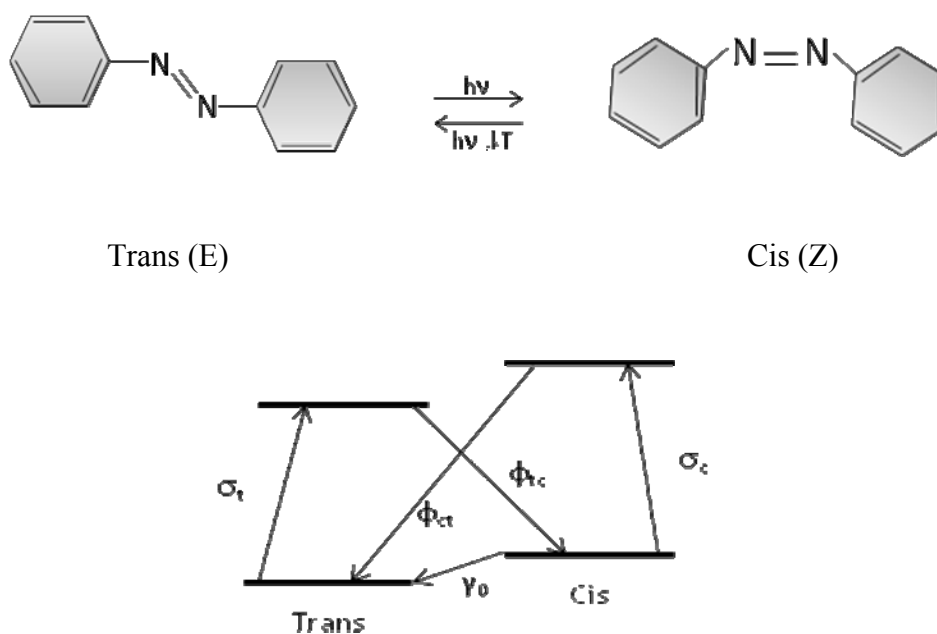
Figure1.1- (Top) Trans (E) ↔ Cis (Z) isomers of azobenzene.

(Bottom) Simplified model of the molecular states

The trans isomer is thermodynamically more stable than the cis isomer- the energy barrier at room temperature is about 50kJ/mol for the azobenzene and generally, the thermal isomerization is in cis→trans direction. Since the trans ground state lies lower in the energy than that of the cis isomer, any cis species created return to trans state photochemically and or thermally. The rate and extent of isomerization as well as the composition of the photostationary state depends on the ring substituents [12]. For most common azobenzene, the two photochemical conversions occur on a picoseconds time scale, whereas the thermal relaxation from cis to trans is much slower on the order of seconds or hours [12]. When the azobenzenes are bound to or doped into polymer matrix, this constant and rapid trans-cis-trans photoisomerization activity results in a series of motions. Depending on the level at which they occur, these motions could be classified into three types: at molecular, nanoscale, and micrometer level. On E-Z conversion (see figure 1.1), the isomer changes its molecular shape, reducing the distance between the azobenzene rings from 1.0nm to 0.59nm and increasing the dipole moment from 0 to ca. 3 Debye[18]. It has also been seen that donor acceptor substituted azobenzenes, which have large second and third order non linear optical properties, show a fast thermal Z-E (cis-trans) conversion.

The simplified model of excited states is shown in the lower part of figure 1.[17a] Two excited states i.e. trans and cis are presented here. σ_t and σ_c form the cross section for absorption of

one photon by the trans and the cis isomer, respectively. The cross sections are proportional to the isomers extinction coefficient. γ is the thermal relaxation rate; it is equal to the reciprocal of the life time of the cis isomer (τc). Φ_{ct} and Φ_{tc} are the quantum yields (QYs) of photoisomerisation; they represent the efficiency of the trans$\rightarrow$cis and cis$\rightarrow$trans photochemical conversion per absorbed photon, respectively. The process of photoisomerization can be represented by two mechanisms, first from high energy π-π^* transition, which leads to the rotation around the azo group, i.e. –N=N- double bond, and second form low-energy n- π^* transition, which induces isomerization by inversion through one of the nitrogen nuclei. Both these process leads to the same conformational change still the process of photoisomerization is different. In case of inversion mechanism, the free volume needed is lower as compared to rotation mechanism.

1.4 Structure and properties of pDR1M and pMEA

The polymers used in the study were poly [4-nitrophenyl-4´-[[2-(methacryloyloxy) ethyl] ethyl-amino] phenyldiazene] pDR1M and poly [4-(2-methacryloyloxy) ethylazobenzene] pMEA. The chemical structure of the polymers is as shown in the figure2 below.

(a) pDR1M   (b) pMEA
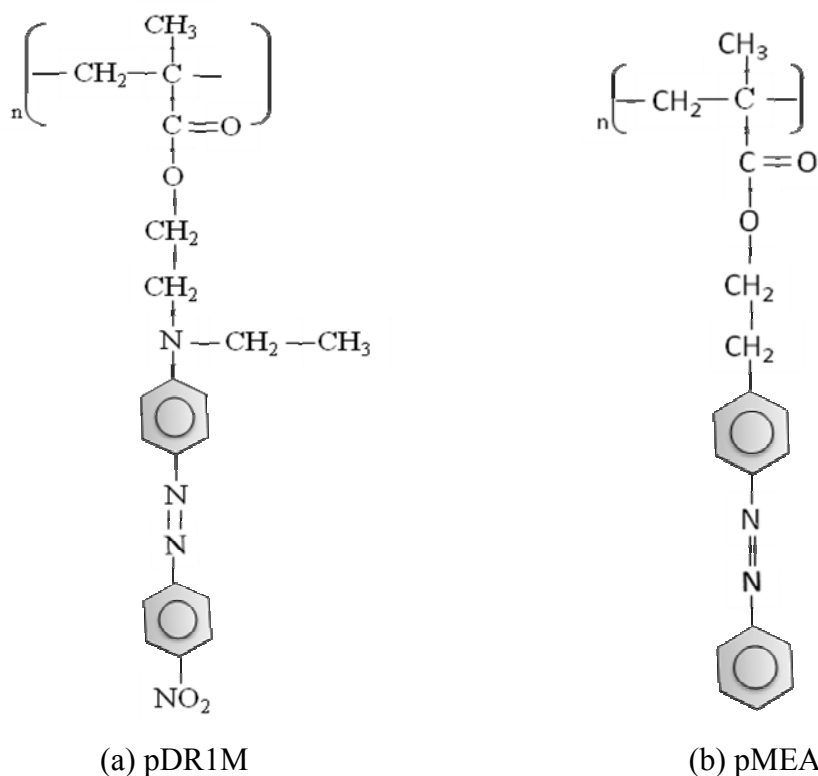
Figure1.2:- The chemical structure of amorphous azobenzene polymers used in the study.

The absorption spectrum of these two polymers is as shown in the figure below.
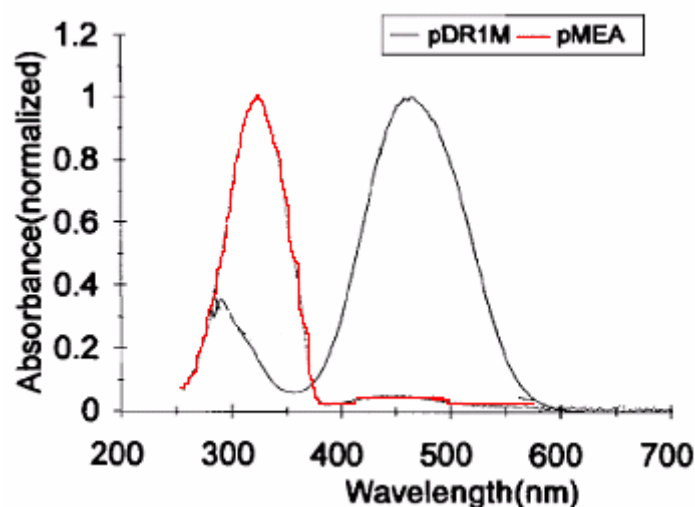
Figure1.3:- Absorption spectra of azobenzene

The chemical structure and the absorption spectra of the polymers used for the grating inscription study are as shown in the figure 1.2 and figure 1.3. pDR1M has a glass transition temperature (T_G) of about 120°C and absorption maximum of λ_{max}=458nm where as pMEA has a glass transition temperature (T_G) of about 80°C and absorption maximum of λ_{max}=324nm[19] as shown in the figure 1.3. In terms of the nature of the azo group, the azobenzene is classified into three categories: azobenzene, amino substituted azobenzene and pseudo stilbene[12] can be applied to the photo induced orientation behavior as well. The chromophore bearing the strong NO_2 group as the electron withdrawing substituent, pDR1M shows highest permanent dipole moment 7.0D as compared to pMEA 0.05D. Moreover, pDR1M belongs to pseudo stilbene class in which the cis and the trans spectra are superimposed i.e. π-π^* and n- π^* transitions over lap each other, irradiation with an argon laser (usually 514nm or 488nm) activates both trans cis and cis trans isomerization processes. This leads to the large number of trans-cis-trans isomerization cycles per unit time[19]. For simple azobenzene like pMEA, the trans-isomer absorbs in the UV region, whereas the cis-isomer absorbs in the visible region. This result in an efficient cis-trans isomerization at 488nm (or 514nm) while the trans-cis experiences only the tail of the absorption band. Consequently, little photoinduced orientation occurs in these materials[20].

1.5 Theory of photo-orientation[7b]

Many optoelectronic applications of linear and nonlinear optical properties of dye doped polymers need some special ordering of anisotropic or polar active molecules. The traditional method for ordering of the molecules is thermally assisted electrical poling (TAEP) in which first the sample is heated upto the glass transition temperature (T_g), in order to increase the mobility of chromophores (reduced viscosity) then a DC electric field is applied, which orients the permanent dipoles of the molecules, and finally the sample is cooled in order to freeze the molecular order, by restoring the high viscosity of the sample. The mobility of the chromophores depends upon the availability of free volume. Alternatively, there are many possible techniques available for the ordering of the chrormophores viz. -Photoinduced anisotropy or Weigert effect[21, 22]: birefringence and dichroism are induced by resonant excitation with polarized light beam. This effect is often used for writing waveguides or holographic gratings [23, 24], -Photoassisted electrical poling (PAEP)[25] in which molecular mobility is increased by optical pumping which can then be oriented by DC field, -All optical poling (AOP)[26] in which the material is coherently pumped by the fundamental frequency and the second harmonic of a laser beam. The reversible trans-cis photoisomerization (E-Z isomerization[27]) of azobenzene induced by resonant excitation with a polarized laser beam is the most efficient mechanism among all because of the good stability of the azo dyes. The polarized light imposes on anisotropic dye molecules an angular selective optical pumping that results in a macroscopic alignment perpendicular to the light polarization [28,29]. Only in the case of such orientation further absorption of photon is prevented and, hence a steady state is reached [30,31]. The model is based on the work carried out by M. Dumont and E. Osman, named as "hole burning model for the photoorientation of azo dyes in amorphous polymers [32,33]".

From steric point of view, the azobenzene moiety in the trans state can be considered as a rigid rod of length $\sim 15A^0$ and a width $\sim 5A^0$.[34] the axis of the rod is labeled by the unit vector **e** and the rod is assumed to have a complete cylindrical symmetry about **e**. Under illumination with visible of ultraviolet light the photoisomerization takes place, and the angular distribution of trans isomers, $n_T(\theta, t)$ and that of the cis isomer, $n_C(\theta, t)$ are described by the following set of differential equation[7b]

$$\frac{\partial n_T(\theta,t)}{\partial t} = -\Phi_{TC} P_T(\theta) n_T(\theta,t) + \Phi_{CT} \int P_{CT}^{ph}(\theta',\theta) P_C(\theta') n_c(\theta',t) d\Omega'$$

$$+ \gamma \int P_{CT}^{ph}(\theta',\theta) n_C(\theta',t) d\Omega' + \left(\frac{\partial n_T(\theta,t)}{\partial t} \right)_{Diff}$$

(1.1)

$$\frac{\partial n_C(\theta,t)}{\partial t} = -\Phi_{CT} P_C(\theta) n_C(\theta,t) + \Phi_{TC} \int P_{TC}^{ph}(\theta',\theta) P_T(\theta') n_T(\theta',t) d\Omega'$$

$$- \gamma n_C(\theta,t) + \left(\frac{\partial n_C(\theta,t)}{\partial t} \right)_{Diff}$$

(1.2)

With the normalization condition

$$\int \left[n_T(\theta,t) + n_C(\theta,t) \right] d\Omega = N$$

(1.3)

Here N is the total molecular density of chromophores, $d\Omega = \sin\theta d\theta$ and θ is the angle between **e** and the electric field vector of the electromagnetic wave, **E**. Φ_{TC} and Φ_{CT} are the quantum yields of the direct trans-cis and reverse cis-trans isomerization, respectively. P_T and P_C are probabilities of the absorption of a photon by a molecule in the trans and the cis state, respectively, and $\gamma = \tau_C^{-1}$ is the rate of the cis-trans thermal back relaxation. $P_{JK}^{ph}(\theta', \theta)$ and $P_{JK}^{th}(\theta', \theta)$ are the probability of rotation from θ' to θ during photoinduced (thermal) J-K isomerization (J(K)= C or T). The last term in each equation is the thermal orientational diffusion.

The authors supposed that the molecular axis of cis (trans) isomers is distributed around that of trans (cis) isomers before the photoisomerization, with an angular distribution only dependent of the polar angle, α, between two isomers [35]

$$P_{JK}^{PH}(\alpha) \equiv F(\alpha) = \frac{1}{2} \sum_P (2p+1) F_p P_p(\cos\alpha)$$

(1.4)

where $P_p(\cos\alpha)$ are Legendre polynomials.
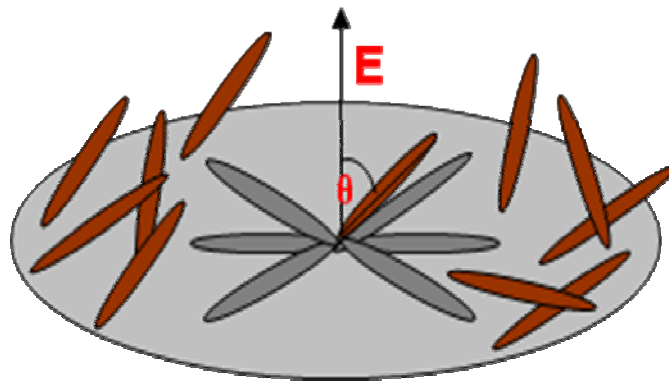
Fig1.4:- Angular selection of chromophore.

The mechanism of angular hole-burning model can be understood intuitively if one considers the probability of absorption. It is given by

$$P_J(\theta) = I_P \sigma_J \left[1 + \varepsilon a_J P_2(\cos\theta) \right] \qquad (1.5)$$

where I_p is the pumping intensity in W/cm², σ_j and a_j are the average absorption cross section and molecular anisotropy of trans (J=T) and cis (J=C) isomers, respectively. $\varepsilon = 2$ for linear polarized light and $\varepsilon = -1$ for circular polarized light.[35] Let us consider irradiation with linearly polarized light and assume for simplicity $a_T = a_C = 1$, we can write

$$P_J(\theta) = 3 I_P \sigma_J \cos^2\theta \qquad (1.6)$$

Hence the probability of excitation by the linear polarized light is proportional to cos²θ. Therefore starting from a sample with an isotropic angular distribution of the chromophores, multiple trans-cis-trans photoisomerisation with linearly polarized light will result in a preferential orientation of the long axis of the chromophores. After some time a dynamic steady state will be reached which is characterized by a rather small fraction of the chromophores pointing in the polarization direction and thus a small photoisomerization rate.

1.6 Photoisomerisation kinetics[7b]

In some experiments considered in this thesis, for example when the film is illuminated by sequence of very short pulses followed by a longer relaxation pauses,[8,36] light induced reorientation of the chromophores is proved to be negligible. In this case the change in the cis isomers with time can be calculated by integrating equation (1.5) over θ. Then the probability of absorption can be expressed as

$$P_J = 2 I_P \sigma_J \quad \text{Since} \quad \int_0^\pi P_2(\cos\theta)\sin\theta d\theta = 0 \qquad (1.7)$$

and equation (1.2) can be transformed into

$$\frac{\partial n_c(t)}{\partial t} = -\left(k_{TC}I_P + k_{CT}I_P + \gamma\right)n_c(t) + k_{TC}I_P N \qquad (1.8)$$

Here, $K_{TC} = \Phi_{TC}\sigma_T$ is the rate constant of the trans-cis photoisomerisation and $K_{CTt} = \Phi_{CT}\sigma_C$ is the rate constant of the reverse cis-trans photoisomerisation. If we define the cis fraction as

$f_C(t) = n_C(t)/N$, then Eq. (1.8) can be rewritten for the cis fraction as

$$\frac{df_c(t)}{dt} = -\tau_p^{-1}f_c(t) + k_{TC}I_P \qquad (1.9)$$

Here, we have introduced $\tau_p = \left[\left(k_{TC} + k_{CT}\right)I_P + \gamma\right]^{-1}$ as the characteristic time of the isomerization process. For the situation where light is switched on at t=0, Eq. (1.9) results into

$$f_C(t) = k_{TC}I_P\tau_P(1 - \exp(-t/\tau_P)) \qquad (1.10)$$

On the other hand, the isomerization rate $\dot{f}_{iso} \equiv df_{iso}/dt,$ is given by

$$\dot{f}_{iso}(t) = \left[\left(k_{CT} - k_{TC}\right)I_P + \gamma\right]f_c(t) + k_{TC}I_P \qquad (1.11)$$

Thus, we define $\dot{f}_{iso}$ as the number of all isomerization events per unit of time, accounting for both trans-cis and cis-trans isomerization. When the photostationary state is reached (**t=∞**), the following two relations are obtained

$$f_{C,\infty} = k_{TC}I_P\tau_P \qquad \text{and}$$

$$\dot{f}_{iso,\infty} = 2f_{C,\infty}\tau_C^{-1}$$

where $\tau_c = \left[k_{CT}I_P + \gamma\right]^{-1}$ is the effective lifetime of the cis isomer under illumination.

Both trans-cis and cis-trans photoisomerisation processes stop immediately when the inscribing laser is switched off. The only process that is still continuing in the absence of irradiation is a much slower cis-trans thermal relaxation. The rate of thermal relaxation mostly depends upon the type of the chromophore and type of it´s attachment to the polymer backbone.[37] it is usually a multiexponential decay on a very short time scale (1 s) followed by a monoexponential decay for which relaxation times between 10s and 12 hrs have been estimated for a variety of azobenzene polymers. [37, 38, 39] The rate of thermal relaxation differs considerably between the two polymers used in this study. pDR1M belongs to the pseudo stilbene group and pMEA belongs to the azobenzene type group of the azobenzene

classification. The rate of thermal relaxation is in seconds for pseudo stilbene type azobenzene and in hours for that of azobenzene type molecules.

1.7 Types of motion during photo-orientation

Under illumination, azobenzene undergoes photoisomerization[12]. When the azobenzenes are bound to or doped into a polymer matrix, this constant and rapid photoisomerization activity results in a series of motions, which intern exploited in photonic applications. These motions can be classified into molecular, nanoscale and micrometer level depending upon the level at which they occur[40].

The motion at molecular level is due to the chromophore motion. This motion results due to the interaction between mesogenic azo molecules and polarized light. The polarized light activates the photoisomerization in selective manner due to the highly anisotropic shape of the trans azobenzene. As the transition dipole moment of the chromophore is directed along its principal axis, the azo unit probability (P) to absorb a photon and subsequently isomerizes is proportional to $\cos^2\varphi$ where φ is the angle between the polarization direction of the light and azobenzene transition dipole moment. Thus only azobenzene group having component dipole moment parallel to the light polarization direction will absorb and photoisomerize. While undergoing multiple trans-cis-trans isomerization cycles the chromophores move and slightly orient their optical transition movement axis and hence their long axis. At the end of the isomerization cycles, if they fall perpendicular to the light polarization direction they become inert to light. As long as light is on the concentration of azobenzene chromophores perpendicular to light polarization increases steadily and reaches the saturation level. Thus optical birefringence and dichroism is induced in the polymer film.

The second type of motion, at nanoscale level is the motion of the chromophore in an organized environment such as LC or crystalline domains. When these organized structures are irradiated with light there is a competition between two types of ordering. First, the ordering impact of polarized light tends to align the chromophores perpendicular to the light polarization direction. On the other hand the initial order of the system opposes this alignment. The high photoisomerization quantum yield coupled with strong driving force leads to the orientation of the whole domain perpendicular to light polarization. Since these motions occurs at the domain level, which has a size of nanometers, the amount of moved material is greater than in the first type of motion.

When the polymer films was exposed to a circularly polarized light, it was found that the photoisomerization process is accompanied my mass movement of polymer material over

several micrometer distances[40]. This is the third type of motion. Since the volume affected by such type of movement is of the order of several cubic microns, one can conclude that this type of motion is not limited to chromophores but involves polymer chains. This motion occurs well below the glass transition temperature of polymer and produce controlled and stable relief pattern on the polymer film.

References

[1] P. Rochon, E. Batalla, A. Natansohn. Appl. Phys. Lett., 66, 136, (1995).

[2] D. Y. Kim, S. K. Tripathy, L. Li, J. Kumar. Appl. Phys. Lett., 66, 166, (1995).

[3] C. J. Barrett, A. L. Natansohn, P. L. Rochon. *J. Phys. Chem.*, **100**, 8836, (1996).

[4] X. L. Jiang, L. Li, J. Kumar, D. Y. Kim, V. Shivshankar, S. K. Tripathy, *Appl. Phys. Lett.*, **68**, 2618, (1996).

[5] P. Lefin, C. Fiorini, J. M. Nunzi, *Pure Appl. Opt.*, **7**, 71, (1998).

[6] D. Bublitz, B. Fleck, L. Wenke. *Appl. Phys. B*, **72**, 931, (2001).

[7] T. G. Pedersen, P. M. Johnsen, N. C. R. Holme, P.S. Ramanujam, S. Hvilsted. *Phys. Rev. Lett.*, **80**, 89, (1998).

[7a] Saphiannikova M, Geue T. M., Henneberg O, Morawetz K, Pietsch U, J. Chem. Phys. 2004, 120, 4039-4045.

[7b] Grenzer M, *Photoinduced material transport in amorphous azobenzene polymer films*. Habil. Thesis, Potsdam, University of Potsdam, 2007.

[8] P. Veer, U. Pietsch, P. Rochon, M. Saphiannikova, *Mol. Cryst. Liq. Cryst.* 486, 66/[1114]-78/[1126], 2008.

 [9] D. M. Burland, R. D. Miller, C. A. Walsh. *Chem. Rev*. 93, 31, (1994).

[10] J. A. Delaire and K. Nakatani. *Chem. Rev*. 100, 1817, (2000).

[11] K. Ichimura. In Polymers as Electrooptical Components, V.P. Shibaev (Ed.), Vol. 138, Springer Verlag, New York (1996).

[12] H. Rau. Photochemistry and photophysics, Vol. 2, J. K. Rabek (Ed.), p. 119, Crc Press, BocaRaton, FL (1990).

[13] G. S. Kumar and D. C. Neckers. *Chem. Rev*. 89, 1915 (1989).

[14] S. Xie, A. Natansohn, P. Rochon. *Chem. Mater*. 5, 403, (1993).

[15] T. todorov, L. Nikolova, N. Tomova. *Appl. Opt*. 23, 4309, (1984).

[16] P. Rochon, E. Batalla, A. Natansohn. *Appl. Phys. Lett*. 66,136,(1995).

[17] D. Kim, S. Tripathy, L. Liam, J. Kumar. *Appl. Phys. Lett*. 66, 1166 (1995).

[17a] Zouheir Sekkat and Wolfgang Knoll, *Photoreactive Organic Thin Films*, Acadamic Press, Elsevier Science (2002).

[18] De Lange J. J., Robertson, J. M., and Woodward, I. (1939). X ray crystal analysis of Azobenzene. Proc. Roy. Soc. London, Sec. A 171, 398-410.

 [19] M. S. Ho, A. Natansohn, C. Barrett, P. Rochon. *Can. J. Chem.* 73, 1773 (1995).

[20] A. Natansohn, P. Rochon, M.S. Ho, C. Barrett. *Macromolecules* 28, 4179, (1995).

[21] F. Weigert, Verh. *Phys. Ges.* 21, 485, (1919).

[22] F. Weigert, Z. *Phys.* 5, 410, (1921).

[23] S. D. Kakichashvili, Kvant. *Electron* 1, 1435, (1974).

[24] T. Todorov, L. Nikolova, N. Tomova, *Appl. Opt.* 23, 4309, (1984).

[25] Z. Sekkat, M. Dumont, *Appl. Phys.* B 54, 486-489, (1992).

[26] F. Charra, F. Kajzar, J. M. Nunzi, P. Raimond, E. Idiart, *Opt. Lett.* 18, 941, (1993).

[27] Geue, T. Lichtinduzierte Eigenschaftsänderungen in ultradünnen organischen Filmsystemen. PhD thesis, Humboldt University, Berlin 1995.

[28] Geue, T.; Ziegler, A.; Stumpe J. *Macromolecules* 30, 5729-5738, (1997).

[29] Jung, C. C.; Rosenhauer, R.; Rutloh, M.; Kempe, C.; Stumpe, J.; *Macromolecules,* 38, 4324-4330, (2005).

[30] Kulinna, C.; Hvilsted, S.; Hendannm, C,; Siesler, H. W.; Ramanujam, P. S. *Macromolecules,* 31, 2141-2151, (1998)

[31] Yaroschuk, O;, Sergan, T;, Lindau, J,; Lee, S. N.; Kelly, J.; chien, L. C. J. *Chem. Phys.* 114, 5330-5337, (2001).

[32] Sekkat, Z,; Dumont, M.; *Synth. Met.* 54, 373-381, (1993)

[33] Dumont, M.; Osman, A. E. *Chem. Phys.* 245, 437-462, 1999.

[34] Saphiannikova, M.; Radtchenko, I.; Sukhorukov, G,; Shchukin, D.; Yakimansky, A.; Ilnytskyi, J. *J. Chem. Phys.* 118, 9007-9014, (2003).

[35] Dumont M, Osman A. E. *Chem. phys.* 245, 437-462, **1999**

[36] Saphiannikova M., Henneberg O., Geue T.M., Pietsch U., Rochon P., *J. Phys. Chem. B,* 108, 15084-15089, (2004) .

[37] Barrett C, Natansohn A, Rochon P, *Chem. Mater.*, 7, 899-903, (1995)

[38] Ramanujam P. S., Hvilsted S, Zebger, I, Siesler H. W. Macromol. *Rapid commun.*, 16, 455-461, (1995)

[39] Buffeteau T, Lagugne-Labarthet F, Pezolet M, Sourisseau C, *Macromolecules,* 34, 7514-7521, (2001)

[40] Cristina Cojocariu and Paul Rochon Pure Appl. Chem. **76**, 1479, (2004)

Chapter 2

Formation of surface relief gratings on azobenzene polymer thin films

2.1 Introduction

The discovery of surface relief grating (SRG) formation on azopolymers occurred in high T_g polymers through the exposure of the sample to an interference pattern from relatively low intensities of a writing laser.[2.1,2.2] As subsequent studies confirmed[2.3,2.4], under low intensity writing conditions the surface modulation basically arises from light driven mass transport, with negligible thermal effects. Thus, it is an entirely photonic process. It is based on the ability of azobenzene chromophores to undergo trans-cis-trans isomerizations, which are followed by molecular orientation. The molecular orientation follows the isomerization associated with the thermal relaxation from the high energy cis to low energy trans configuration. The probability of molecular orientation upon interaction of the chromophore with the polarized light is maximum when their dipole moment is parallel to the laser light polarization and minimum when their dipole moment is perpendicular. Upon thermal relaxation, the chromophores can adopt any orientation, including the perpendicular direction to the light polarization, in which case they will no longer be affected by the light electric field. It indicates in particular that the chromophores aligned perpendicular to the laser light polarization has much smaller transition dipole moments.

2.2 Photo-induced Mass Transport

In most of the studies, the grating formation has been studied on high T_G amorphous polymers using modest light intensities. The origin of the grating formation is concluded to the light driven mass transport with negligible thermal effects.[2.4a] It has been observed that efficient surface relief gratings can only be formed when there is variation in both light intensity and resultant electric field vector on the sample film. Here are some experimental results which show that thermal effects and photo degradation doesn´t contribute to the SRG formation process.

It has been seen that SRG are formed only on the azobenzene polymer films due to the light driven mass transport. Hence one can conclude that trans-cis-trans photoisomerization is an essential phenomenon.[2.4a,2.12] Also it has been seen that polymers which contain chromophores like biphenyls which undergoes photoisomerization do not from SRGs. This

can be due to the fact that free volume required by them which is much higher than the azobenzene chromophore hinders the photoisomerization reaction in the thin films.[2.4a,2.12] The conclusion that thermal effects are negligible is drawn from the facts that an absorbing, non isomerizable dye (rhodamine 6G) do not form SRGs. [2.4a,2.13] The optical origin of the light driven mass transport has also been proved experimentally. Irradiating a polymer film with low intensities, the diffraction efficiency is found independent of the inscription intensity.[2.4a,2.14]

It has been seen that the azobenzene must be covalently attached to the polymer chain, either in its side chain or in main chain. Very small surface modulations have been recorded for guest-host systems.[2.4a,2.15,2.16] In these systems photoisomerization is possible but efficient SRG inscription was not possible. This effect can be attributed to the facts that polymer chains are not induced to move unless they are covalently attached. In the comparative of doped system to the grafted system containing azobenzene unit, it has been seen that compared to grafted system doped system is less efficient.[2.4a,2.17] Increasing the chain length by adding two azo groups enhances the photo-induced birefringence and orientation stability in comparison to similar homo-polymers containing only one azo bond. But in this case, the photo-induced orientation process is relatively slow as both the azo groups have to photoisomerize with respect to its initial orientation [2.17a].

The mobility of the polymer chains also plays an important role in the mass transport phenomenon. This mobility i.e. viscosity of the polymer material found to depend upon glass transition temperature T_G and molecular weight. SRG inscription on polyureas[2.4a,2.18] and polydiacetylenes[2.19] is found difficult due to the rigidity of the polymer matrix. Also due to this same reason SRG formation was found difficult on high molecular weight polymers[2.4a,2.20] and azobenzene containing gel.[2.4a,2.21]

The surface relief grating formation is a surface initiated process[2.4a]. This conclusion has been drawn from the experimental evidence. When the azobenzene polymer film is coated with another polymer film of thickness around 25nm, the grating formation mechanism was found to be hindered completely. Without that top layer, it was possible to write deep gratings on the same sample. Also it has been seen that with increasing number of deposited bilayers, the surface modulation goes on decreasing.

It has also been seen that light driven mass transport is not related to only azobenzene containing material. Indandione containing guest-host polymer films have been found to show mass transport effect and were used for grating inscription by optical method.[2.23]

2.3 Inscription of SRG

2.3.1 Sample preparation

To inscribe such SRGs, thin films of polymer pDR1M poly[4-nitrophenyl-4´-[[2-(methacryloyloxy)ethyl]ethyl-amino]phenyldiazene] and pMEA poly[4-(2-methacryloyloxy)ethylazobenzene] were prepared by dissolving 6% of the each powdered sample in tetrahydrofuran (THF) and spin coated over glass substrate at 500rpm. The obtained film thickness was around 500nm for both types of the polymer films measured using DEKTAK IIA surface profile measurement unit. The samples were heated in an oven near respective T_g for 1 hour to remove any solvent content and to achieve uniformity within the films.

2.3.2 Experimental Setup

SRGs were inscribed on pDR1M thin films using a semiconductor disc laser operating at a green wavelength of 514 nm and on pMEA thin films using Ar^+ laser operating at a blue wavelength of 488nm because of the difference in the absorption maxima. As described in chapter 1, the absorption a maximum of pDR1M is 458nm and that of pMEA is 324nm hence two different wavelengths were used for SRG inscription which were close to the absorption maximum of respective azobenzene chromophores.

The formation of SRG is probed using a P polarized low power He-Ne laser operating at a red wavelength of 632.8nm and having an output power >5mw/cm². The wavelength of the probe laser was outside the absorption maxima of azobenzene chromophores and thus has no influence on the process of grating formation.

Figure 2.1 shows a typical experimental setup employed for inscribing SRGs. It consists of the inscribing laser followed by a lens system to expand the beam and a quarter wave plate ($\lambda/4$) to create the circular polarization of the light. The vacuum chamber hosts a mirror and the sample equipped on a Peltier plate. The mirror and the sample on peltier plate are arranged perpendicular to each other. The 488/514 nm line of an Ar^+/semiconductor disc laser is split into two beams of equal intensity with appropriate polarizations using a mirror and was made to impinge on the sample surface. The periodicity, Λ, of the resulting grating can be predicted using the relation

$$\Lambda = 2\,\pi/k = \lambda\,/\,[2\sin(\theta)],$$

and it can be varied by changing the angle between the writing beams, θ. Λ is the wavelength of the writing beam. The largest amplitude of surface modulation, and hence the best

diffraction efficiency is obtained when θ=14°-15° and circularly polarized light (CPL) is used for writing[2.20] in agreement with other reports [2.12] which was also observed in this experimental setup. For the used angles of reflection at mirror the polarization state of the reflected wave was circular.[2.5] Thus, the interference of two contra circularly polarized beams results in a periodic rotation of electric field vector while the intensity remains nearly constant, which produces the gratings of the highest diffraction efficiency and surface modulations.[2.6,2.7,2.8] The initially flat polymer film forms a sinusoidal shaped surface relief grating after few minutes of exposure. A typical sinusoidal shaped surface relief grating inscribed on the polymer pDR1M is as shown in Figure 2.3. The depth of the surface relief grating can be controlled with reasonable accuracy by varying the fluence since it has been seen that the SRG depth increases linearly with time at the beginning of the irradiation, before slowing down and reaching saturation at certain depth which depends upon the initial film thickness. It has also been seen that the fabrication time of the SRG could be shortened by varying the laser intensity used for grating inscription.

The formation of SRG was probed in-situ using a He-Ne laser by monitoring the scattered first order diffraction and the specular signal.

The signals were detected in reflection geometry using a pair of photodiodes (see figure 2.1). Figure 2.3 shows the typical surface relief grating inscription setup.

To study the temperature dependence of the grating formation, the sample was heated steadily using a Peltier plate. During the preliminary measurements, at a certain temperature above the room temperature it was found that the wave front close to the sample surface was disturbed by the turbulence of hot air which led to attenuation of the grating formation process which was also observed in the previous studies of temperature dependent grating formation.[2.9] To avoid the air turbulence, the experiment was performed inside a closed chamber at pressure of about 1000 Pa created by a vacuum pump (Vacuubrand GmbH). The designed vacuum chamber is as shown in the figure 2.2(b). The sample temperature was measured by means of a thermistor placed on the Peltier plate inside the vacuum chamber and which was calibrated for change in the resistance with accuracy of one degree.
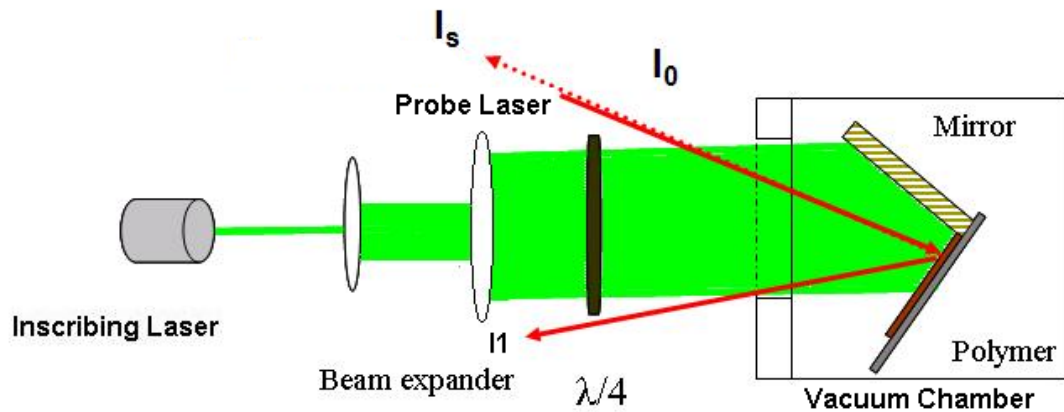
Figure 2.1- Holographic setup for inscription of surface relief gratings on azopolymers films.

In figure 2.2, picture (a) shows the grating of different periodicity written on pDR1M thin film and picture (b) shows the designed vacuum chamber used for the temperature dependent grating formation study.
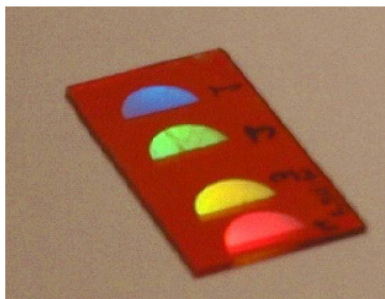
(a)   (b)

Figure2.2- (a) SRGs with different grating period, (b) Vacuum chamber for temperature dependent measurements

The inscribed surface relief gratings were ex-situ investigated using atomic force microscope (AFM). After inscription the grating profile can be described as follows.

$$h(x) = h_0 + A\cos(x/D)$$

where, h(x) is the height of SRG from the substrate, h_0 is the initial film thickness, A is the grating amplitude and D is the grating period.
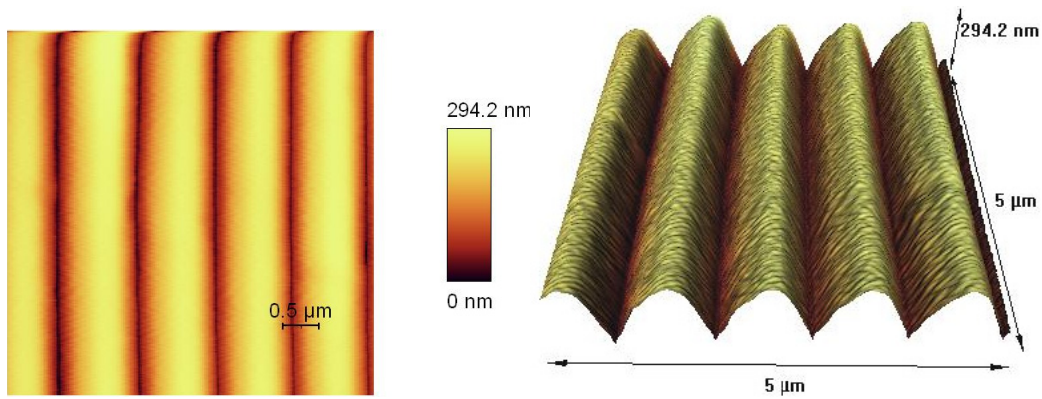
Figure2.3- A typical sinusoidal shaped SRG inscribed on azobenzene polymer film.

In this thesis work, to study the grating formation phenomenon temperature dependent continuous exposure and pulsed exposure measurements were carried on thin films containing azopolymer.

2.4 Continuous exposure measurements

Initially the interference pattern of the laser light is formed over the Peltier plate which is fixed perpendicular to the mirror. The polymer sample is then placed at the position of the interference pattern. The laser is again switched on to inscribe the surface relief gratings onto the polymer film. The first order diffraction intensity is then measured as a function of time using a photodiode as shown in the scheme below.
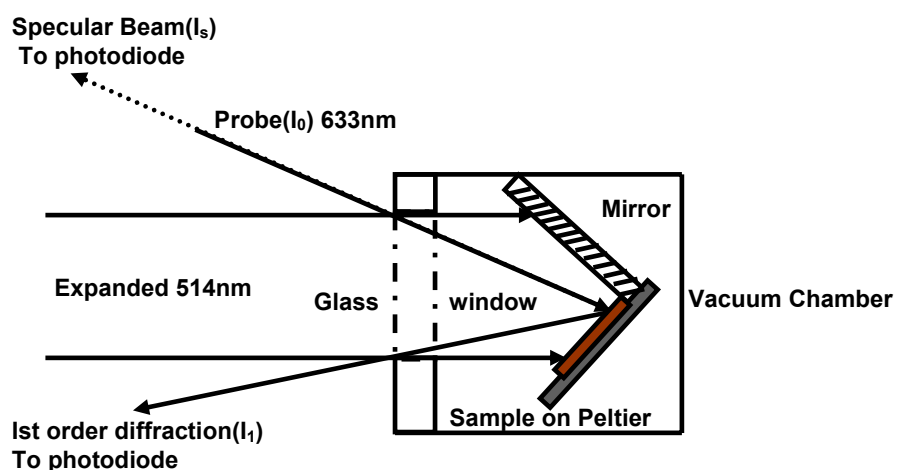
Scheme of the inscription geometry

The initial laser power before expanding the beam was 750mW/cm². After the beam expansion, the laser power at sample surface is typically 10% of the initial power, per square centimeter.

Figure 2.4 shows a typical response of I[st] order diffraction intensity during the process of surface relief grating formation at room temperature. The diffraction intensity roughly correlates with the grating height. The diffraction intensity increases with increase in grating heights and finally achieves saturation. The saturation of the grating heights depend upon the initial film thickness and the time required till saturation depends upon the inscription power at the sample surface.

Figure 2.4:- Typical response of first order diffraction intensity at room temperature during the process of grating formation under continuous exposure.

In continuous exposure measurements, the polymer sample is subjected to the constant stress generated due to the orientation mechanism of the polymer chains as a consequence of the interaction of the azochromophore with the polarized light leading to the multiple trans-cis-trans isomerization cycles. The temperature dependence of SRG formation using continuous exposure method is studied by heating polymer above the room temperature till the glass transition temperature (T_g), increasing the temperature by few tens of degree. The experiment was performed at variable inscription intensities and is discussed separately in the following chapters.

2.5 Pulsed exposure measurements

The chromophore orientation and relaxation has seen to be strongly affected by the presence of light.[2.10,2.11] To study this behavior, pulse exposure technique has been exploited. In this technique the polymer sample was subjected to a cyclic inscribing force unlike continuous exposure measurements. This is achieved by designing an electro-mechanical shutter that was allowing light to fall on a sample for a particular time period.

The inscription process was initiated by a short light pulse followed by much longer relaxation time in dark. The formation of SRG was studied under pulse like illumination at sample temperatures varying between roo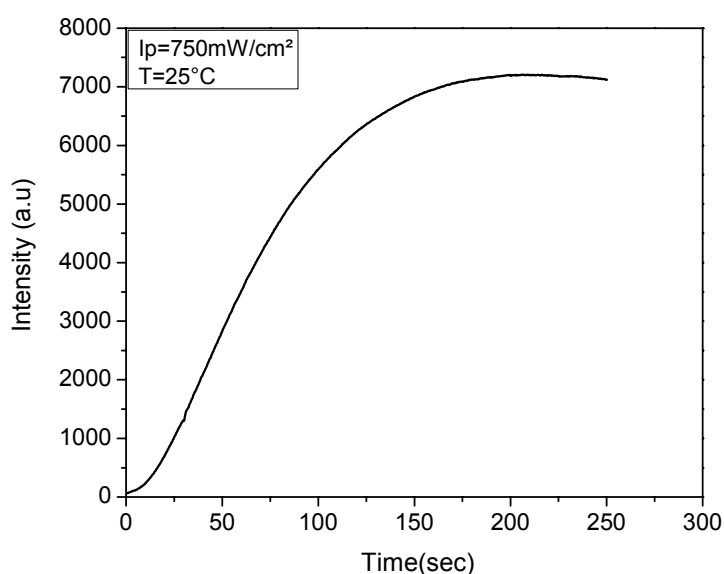m temperature and T_G similar to the continuous exposure method. Figure 2.5 shows a typical response of a first order diffraction intensity at room temperature during the process of grating formation under pulse like exposure. The exposure time of the sample was 2sec and the dark time was 20sec.
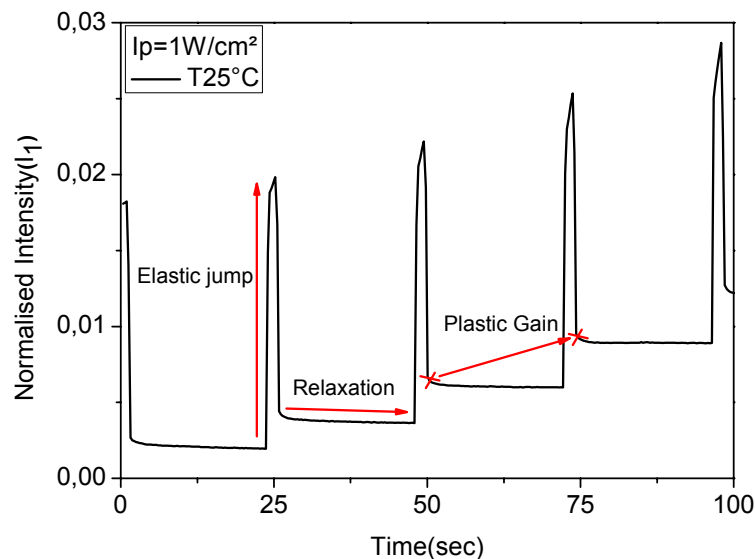
Figure 2.5:- Typical response of first order diffraction efficiency at room temperature, during the process of grating formation under pulse like exposure technique.

The pulse exposure technique has reveled 3 different responses of the polymer material. We assume the responses as the elastic jump under light exposure, relaxation in the dark and plastic gain in every successive pulse as shown in the figure 2.5. The degree of plastic gain induced in successive pulse depends upon the light intensity used for the inscription of gratings. Like continuous exposure measurements, temperature dependent pulsed exposure

measurements were carried out. The three different responses of the polymer mentioned above have been found to alter with temperature. The temperature dependent of SRG formation under pulse exposure will be discussed in following topic.

As discussed in the section 2.2, since the formation of SRGs is the light driven mass transport, one important question lies in whether there is any difference in orientation of chromophores between the peaks and valleys of SRGs at the film surface. A conclusive answer would probably bring important information on the mechanism of the mass transport. This question is separately answered in a proceeding chapter, in which ex-situ investigation of the surface relief gratings inscribed on pDR1M polymer film was carried out.

References

[2.1] P. Rochon, E. Batalla, A. Natansohn. *Appl. Phys. Lett*., 66, 136, (1995).

[2.2] D. Y. Kim, S. K. Tripathy, L. Li, J. Kumar. *Appl. Phys. Lett*., 66, 166, (1995).

[2.3] Tripathy S.K., Kumar J., kim D.Y., Li L., *Naval research reviews*, 2, 1-9, (2002).

[2.4] Viswanathan N.K., Balasubramanian S, Li L., Tripathy S., Kumar J., Japanese *J. Appl. Phys., Part 1*, 38, 5928-5937, (1999).

[2.4a] Zouheir Sekkat and Wolfgang Knoll, *Photoreactive Organic Thin Films*, Acadamic Press, Elsevier Science (2002).

[2.5] F.Lagugne, T.Buffeteau, C.Sourisseau. *Appl. Phys. B*, **74**, 129, (2002).

[2.6] X. L. Jiang, L. Li, J. Kumar, D. Y. Kim, V. Shivshankar, S. K. Tripathy, *Appl. Phys. Lett.*, **68**, 2618, (1996).

[2.7] O. Henneberg, T. Panzner, U. Pietsch, T. Geue, M. Saphiannikova, P. Rochon, K. Finkelstein. *Z. Kristallogr.*, **219**, 218, (2004).

[2.8] N.K. Viswanathan, D.Y. Kim, S. Bian, J. Williams, W. Liu, L. Li, L. Samuelson, J. Kumar, S.K. Tripathy. *J. Mater. Chem.*, **9**, 1941, (1999).

[2.9] O. Henneberg, In-situ Untersuchungen zur Entstehung von Oberflächengittern in Polymeren. PhD-Thesis Universität Potsdam, (2004)

[2.10] T. Geue, M. Saphiannikova, O. Henneberg, U. Pietsch, P.L Rochon, A.L. Natansohn. *Phys. Rev. E*, **65**, 052801, (2002).

[2.11] M. Saphiannikova, O. Henneberg, T. M. Geue, U. Pietsch, and P. Rochon, *J. Phys. Chem. B, 108, 15084, (2004).*

[2.12] Kim D. Y., Li L., Jiang, X. L., Shivshankar V., Kumar J., and Tripathy S. K., *Macromolecules*, **28,** 8835-8839, (1995).

[2.13] Barrett C. J., Natansohn A. L. and Rochon P.L, *J. Phys. Chem*. **100**, 8836-8842, (1996).

[2.14] Tripathy S.K., Kumar J., Kim D. Y., Li, L. and Xiang, X. L., *Naval Research Reviews*, **2**, pp. 1-9, (1997).

[2.15] Hattori T., shibata T., Onodera S.,and Kaino T., *J. Appl. Phys*. **87**, pp. 3240-3244, (2000).

[2.16] Fiorini C., Prudhomme N., de Veyrac G., Maurin I., Raimond P., and Nunzi J. M., *Synthetic Met*, **115**, pp. 121-125, (2000)

[2.17] Chen J. P., Labarther F. L., Natansohn A., Rochon P., *Macromolecules* **32**, pp. 8572-8579, (1999).

[2.17a] Cristina Cojocariu and Paul Rochon, *Pur Appl. Chem.* **76**, 1479, (2004).

[2.18] Lee T. S., Kim D. Y., Jiang X. L., Li L. A., Kumar J., and Tripathy S., *macromolecular Chem. and Phys*, **198**, pp 2279-2289, (1997).

[2.19] Sukwattanasinitt M., Lee D. C., Kim M., Wang X. G., Li L., Yang K., Kumar J., Tripathy S.K., and Sandman D. J. *Macromolecules* **32**, 7361-7369, (1999)

[2.20] Barrett C. J., Rochon P. L., and natansohn A. L., *J. Chem. Phys*. **109**, pp. 1505-1516, (1999).

[2.21] Darracq B., Chaput F., Lahlil K., Levy Y., and Boilot J. P., *Advanced Materials* **10**, pp. 1333-1336, (1998)

[2.22] Viswanathan N.K., Balasubramanian S., Li L., Kumar J., Tripathy S. K., *J. Phys. Chem. B*, **102**, pp. 6064-6070, (1998).

[2.23] B. Stiller, M. Saphiannikova, K. Morawetz, J. Ilnytskyi, D. Neher, I. Muzikante, P. Pastors, V. Kampars, *Thin solid films* **516**, 8893, (2008).

Chapter3

Alteration of mechanical properties of azopolymer film in the process of surface relief grating formation

3.1 Introduction

There is an important question regarding the arrangement of the chromophores and the polymer chains at the crests and trough of the gratings. Is the arrangement same or different at these locations?? The answer to this question will help to clarify the process of SRG formation and its mass transport. Here in this introduction section, I will explain the outcome of some of the earlier studies.

Consider the SRG inscription with linearly polarized light. It was considered that the mass transport occurs to remove the polymer material away from the light.[3.1a] Hence one can say that the chromophores that are removed away from light are those which were in the light polarization direction. Contrary to this, in the trough of the gratings one can expect the chromophores with perpendicular orientation with respect to the light polarization direction. At the crests one expect that the chromophores should be oriented along the light polarization direction. The relaxation of the polymer chains is accompanied by molecular orientation; hence the chromophore alignment may be that strong. Under these circumstances chromophore would be more orientated in the trough of the gratings, perpendicular to the light polarization. Another assumption that is quite possible is that due to the thermal relaxation which occurs when the inscription laser light is switched off the chromophores at the crests and trough of the gratings gets randomly oriented and hence there is no special ordering at crests and troughs of the gratings.

To probe the position of the chromophores at crests and troughs Raman spectroscopy measurements have been performed, but the results are conflicting. The probing on spin coated azobenzene polymer film by Labarthet et. al. [3.1, 3.1a] showed that the polymer removed from the trough of the grating has more ordering, perpendicular to the light polarization than the material that is aggregated at the crests of the grating. In the intermediate region the author reports alternate weak and strong orientation effects which are then attributed to the more or less cooperative movements. An analysis drawn from the information entropy theory[3.2, 3.1a] suggests that the chromophore orientation should be different at crests and troughs.

Another conclusion drawn from the surface enhanced Raman spectroscopy by Constantino et. al.[3.1a,3.3] states that the arrangement of the molecules at the crests and trough of the grating is the same on LB films form an amorphous azobenzene containing polymer. These results were contradictory to the earlier study.

From the above two studies one can say that the systems that are investigated are different but the common thing is the light driven mass transport. The polymer was amorphous and SRG were inscribed using modest light intensity. But both the studies agree that there is a gradient of the azobenzene chromophore exists at the crests and at the troughs of the grating which could be due to the light driven mass transport.

In this study, to investigate the changes in the material properties due to mass transport upon visible illumination, specially resolved hardness measurements were carried out on SRGs i.e. ex-situ investigation of the inscribed SRGs was carried out using atomic force microscope, AFM. The measurements were performed at room temperature. The conclusions of these measurements have allowed us to conclude the possible alignment of the polymer chains at crests and troughs.[3.3a]

3.2 Atomic force microscope studies

The experiments discussed in this thesis support the assumption that the origin of the surface relief grating formation is the photoorientation and ordering of azobenzene groups along with its main chain with respect to light polarisation direction.[3.4] The direction of final chain alignment is perpendicular to the direction of grating vector. [3.5,3.6,3.7] The earlier atomic force microscope (AFM) study of these surface relief gratings by force distance curve measurement has revealed the changes in the local mechanical properties of the material along the grating period.[3.8, 3.9] The SRGs were found to be stiff at the crests and were more adhesive in the trough. This variation of the local mechanical property was then related to the polymer chains density variation along the grating period.[3.8] But, it was not possible to predict the arrangement of the polymer chains at crests and troughs of the gratings.

3.3 Hardness analysis of SRGs using AFM

3.3.1 Experiment

For hardness measurements the atomic force microscope AFM which operates by measuring force between a probe and a sample which has electronic, electrostatic and magnetic origins

was operated in the force modulation mode by monitoring both the lateral and vertical deflection of the cantilever. The force modulation mode of operation of AFM is similar to the contact mode of operation, in which the tip is physically in contact with the sample. As the tip approaches the sample surface the interatomic forces become very strongly repulsive and, since the cantilever has the low force constant (lower than the effective spring constant holding the atoms of the sample together), the force will cause the cantilever to bend following the topography of the sample. Therefore, the detection of the position of the cantilever leads to the topographic map of the sample surface. In most AFMs the position of the cantilever is detected with optical techniques. The most common scheme is with a laser beam reflected off the back of the cantilever onto a position-sensitive photo-detector (photodiode) as shown in the figure 3.1(a). Figure 3.1(b) shows the AFM device used for the scanning purpose.

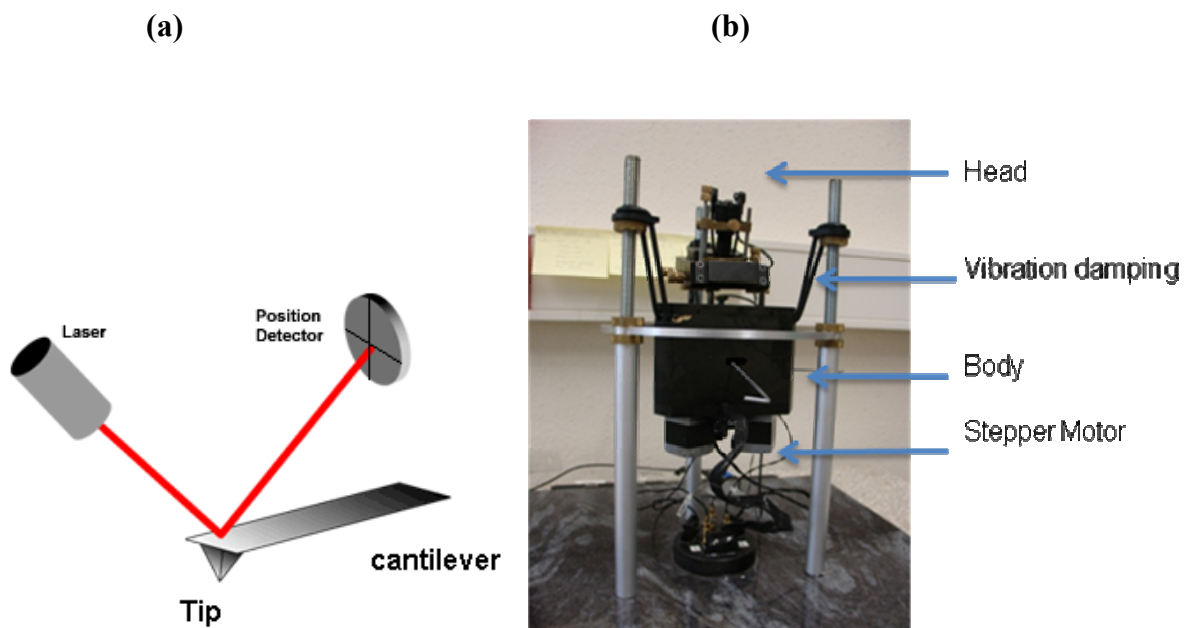**(a)**   **(b)**

Figure3.1(a) : Most common scheme of AFM, (b) AFM from Anfatec instruments used for scanning

The tip sample force is given by Hooke's law

$$F = -k_c \delta_c$$

where k_c is the spring constant of the cantilever and δ_c is the cantilever deflection.

In force modulation mode, the AFM tip is scanned in contact with the sample and the z feedback loop maintains a constant cantilever deflection. In addition, a periodic signal is applied to the cantilever (tip). The amplitude of cantilever modulation that results from this applied signal varies according to the elastic properties of the sample. This technique is thus helpful to characterize the sample´s mechanical properties. Very soft cantilevers having blunt tip (NSC17) with a force constant of 0.15N/m were used for scanning. The samples were scanned with a speed of 0.3lines/sec in order to avoid the friction effects in the signal which could add contrast to the final signal. The selected scanning frequency was 220Hz. The X direction of scanning was perpendicular to the grating vector and in this way the blunt tip of the cantilever was passing over successive crests and troughs while scanning. The estimated contact force was 1.322nN, which is too low to affects the scanning process.

In present study, hardness measurements at SRGs formed at different temperatures varying from room temperature upto about 20 degrees below the glass transition temperature, T_g, have been performed. As discussed, measurements of local hardness have been performed using force modulation mode of AFM for SRGs formed on pDR1M and pMEA which were the test polymers used for the grating inscription study. In order to quantify the results, the similar hardness measurements were performed on the plane films of pDR1M and pMEA and also on the polymer film of pMMA having similar thickness and with known stiffness constant. Also, hardness measurements have been performed on SRGs inscribed using P polarization of inscription laser light to investigate the difference in the local hardness at crests and troughs of the gratings compared to one inscribed using circular polarization of the inscription laser light.

3.3.2 Hardness measurements of SRGs on pDR1M

Hardness refers to various properties of matter in the solid phase that gives it high resistance to various kinds of shape change i.e deformation when force is applied. In short, hardness is the resistance of the material to the external force. The hardness analysis was done by measuring the contrast in the amplitude signal recorded in the amplitude image along with the topography image. Figure 3.2 shows alterations of both surface height and local hardness at samples of pDR1M formed at 25°C and at 100°C. Large alterations in the surface profile and hardness were recorded for the samples formed at room temperature, contrary to the values for samples formed near T_g. The average height amplitude was measured to be 150nm at temperature 25°C, figure3.2(a) and only 20nm at temperature 100°C, figure3.2(c). Visible hardness contrast is found at the room temperature sample only (Fig.3.2b) but not for the

sample formed at 100°C (Fig.3.2d). The pictures shown in figure 3.2 are only the extreme case pictures, whereas the visible contrast was found to be decreasing slowly with increasing temperature.
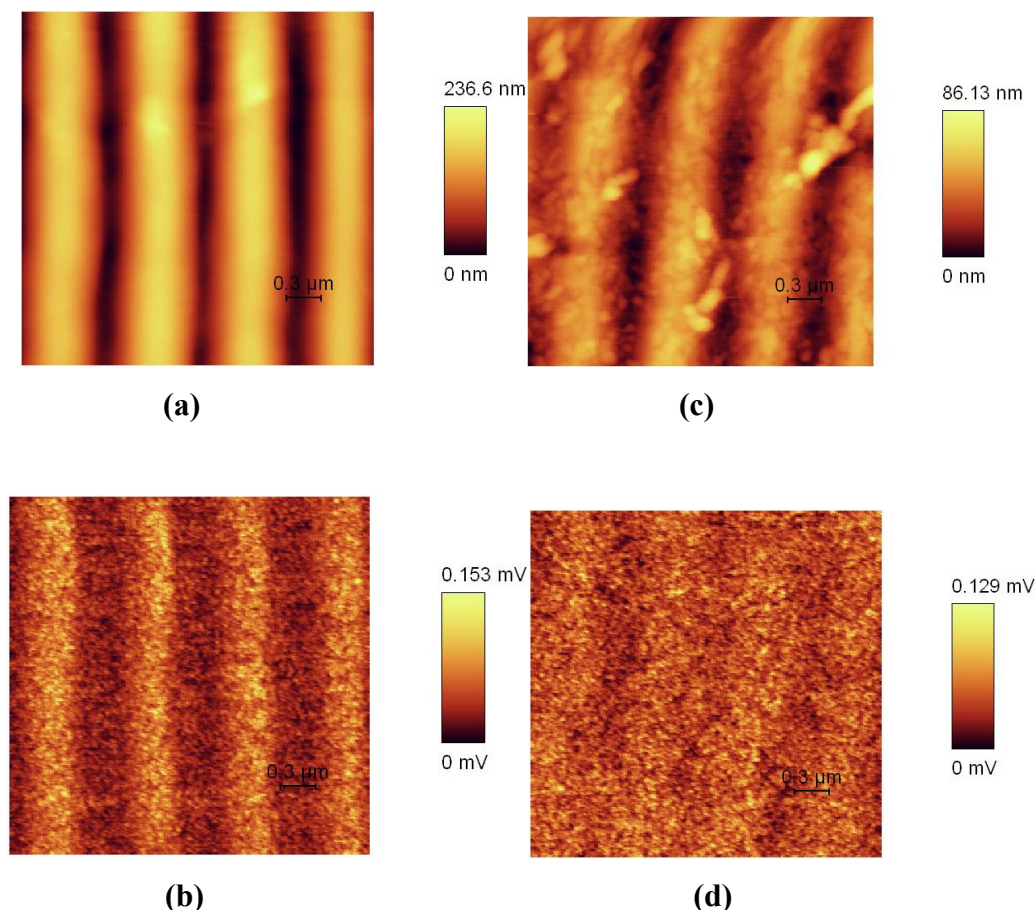

(a)

(c)

(b)

(d)

Figure3.2:- AFM pattern of SRG samples, (a) Topography (b) Hardness signal, at T=25°C (c) Topography (d) Hardness signal, at T=100°C

The hardness of the material is nothing but its stiffness constant and is measured in the units of mega Pascal or giga Pascal. In the above discussed AFM measurements, the hardness/stiffness of the material is recorded as a change in an amplitude signal of the cantilever. Hence figure 3.2b and figure 3.2d are scaled in millivolts. This change in the amplitude signal is plotted against the sample scan area as shown in figure 3.3a.

In order to quantify the measurements a bunch of line scans taken parallel to the grating vector were selected and averaged. Figure 3.3(a) shows the variation of hardness contrast for SRGs recorded on pDR1m at various temperatures. The periodicity observed in the plot is equal to that of the grating spacing recorded in the topography image. The hardness contrast decreases nearly linear with increasing temperature of formation. The plot also

includes the hardness measurements of the plane polymer film of pDR1M at room temperature without grating and also the measurements of the plane pMMA film with known stiffness constant at room temperature. Comparing to the plane pDR1M film at room temperature without gratings, it can be seen that the maxima and minima differ by approximately same amount relative to the hardness of virgin sample.
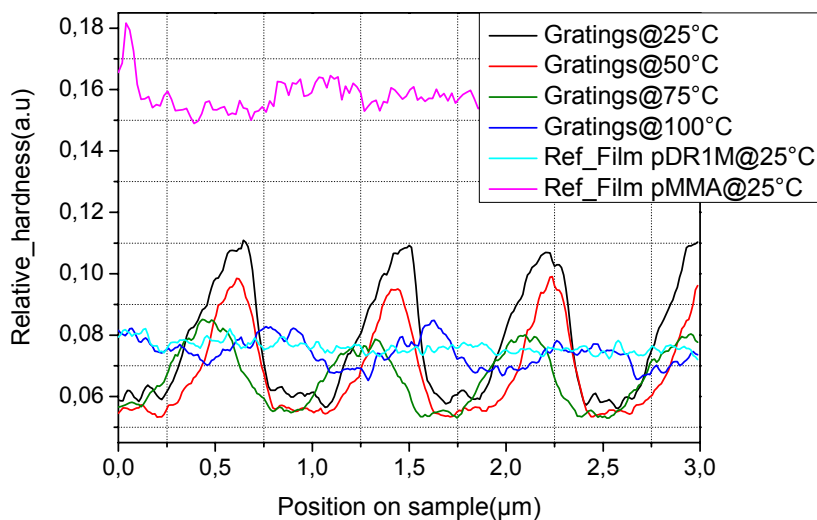
Figure 3.3(a):- Hardness variation on grating sample at various temperatures, pDR1M

The gratings formed at 25°C shows about 50% variation in hardness compared to the non patterned sample. Less then 5% variation is recorded for gratings formed at 100°C in case of pDR1m.

3.3.3 Hardness measurements of SRGs on pMEA

Similar hardness measurements were also performed on the second test polymer pMEA and the results are qualitatively same, compared to pDR1M as shown in figure 3.3(b).
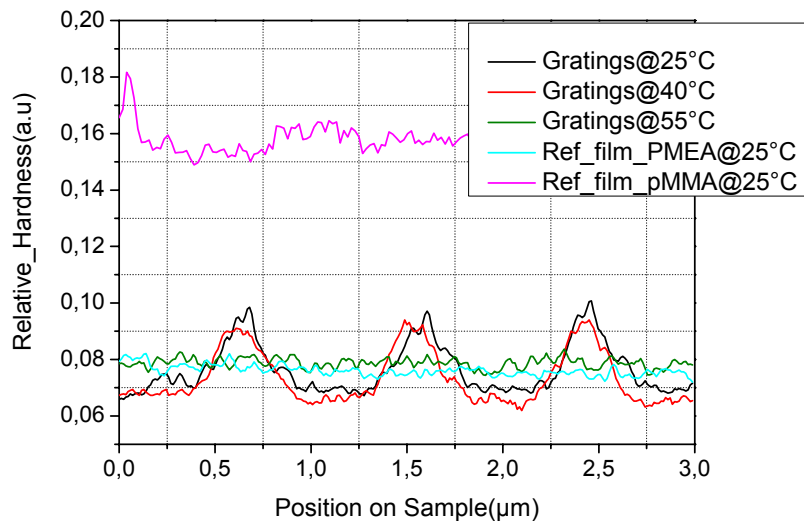
Figure 3.3(b):- Hardness variation on grating sample at various temperatures, pMEA

3.3.4 Hardness Analysis

From the hardness measurements of pDR1M and pMEA, the value of the relative hardness was calculated by considering the difference between the maxima and minima. That change in the hardness is plotted along with the average grating height against temperature as shown in figure 3.4.
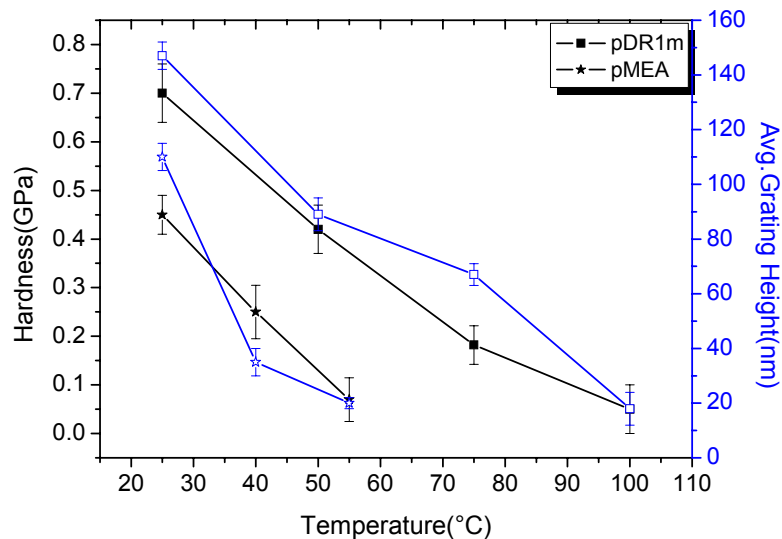
Figure3.4:- Hardness variation with respect to temperature and grating height.

As seen in figure 3.4, both the quantities i.e. the hardness and the grating height decrease with increasing temperature. Both the quantities show the same linear dependence. The decrease in the relative hardness with grating heights could be an indication of crests of

the gratings corresponds to the increased hardness compared to the trough. To investigate exactly which part of the grating corresponds to the increased value of hardness, separate experiments have been performed which are discussed in the proceeding sections of the chapter.

In order to quantify the results similar hardness measurements at polymer films made from pMMA have been performed. Since the pMMA film was isotropic at room temperature, negligible variation in the hardness for pMMA was observed and the hardness value is almost constant. On relative hardness scale in figure 3.3, the hardness of pMMA falls at 0.16 compared to pDR1m and pMEA. To compare this hardness value with the actual physical parameter of pMMA, the stiffness constant i.e. youngs modulus (also called as modulus of elasticity) of the film was taken into consideration. The high-molecular weight of pMMA (M_w=199Kg/mol) has a stiffness constant of about 2.944GPa[3.10,3.11]. Assuming linear relation between the measured hardness and the stiffness of polymer material the virgin pDR1m film (M_w=11.5Kg/mol) is estimated to be about 1.4GPa. Subsequently 50% variation of this value corresponds to an alteration of stiffness between crests and troughs of about 0.7GPa after grating inscription at 25°C (see fig.3.4). The stiffness modulation has a value of ±0.05GPa for sample formed at 100°C which corresponds to a decrease of 0.0086 GPa/K. The hardness modulation for pMEA formed at 25°C amounts to 0.45GPa and decrease to 0.07GPa for sample formed at 55°C corresponding to a decrease of 0.013 GPa/K.

3.3.5 Locating the hardness position

From the above measurements, it cannot be concluded directly whether the maxima of hardness corresponds to crests or trough of the grating. This confusion is due to the delay in the recording of the topography and amplitude signal. The maxima can either refer to crests or troughs of the height profile of SRG. To correlate the maxima of hardness with features of SRG, a scan has been performed through the boundary line of the grating pattern separating light patterned and virgin polymer material as shown in inset of figure 3.5. This boundary line is created due to the particular setup of a mirror to create the interference pattern at the film surface. [3.4]
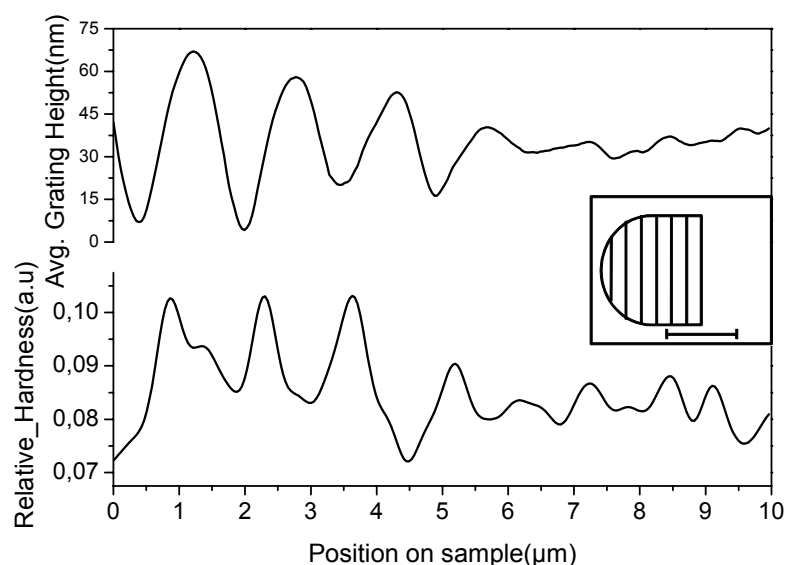
Figure3.5:- Line scans through border between patterned and non patterned polymer film; top line – surface profile, bottom line – hardness profile

The topography analysis of the selected scan area shows three distinct grating crests of about 60nm height separated by 1.5 μm followed by an almost flat surface with certain uncorrelated surface roughness. The corresponding amplitude signal of hardness shows the three equally spaced maxima as well followed by uncorrelated smaller variations. Both line scans provide reasonable mutual correlation, i.e. maxima of hardness coincide with maxima of height profile and vice versa. A slight offset along X direction in the signal is caused by the small time delay between read out of surface height profile and that of the hardness and has no physical relevance. Thus it can be concluded that crests of the grating corresponds to the increased hardness area of the polymer after grating inscription. The results are in accordance with the conclusions of B. Stiller et. al.[3.9]

3.3.6 P Polarised grating analysis

For the gratings inscribed using different polarisation of the inscribing light other than circular polarisation, (which was used to inscribe grating throughout the experiment discussed in this thesis) it was assumed that the maxima of hardness will correspond to a location other than that of observed for gratings inscribed using circular polarisation of light. The assumption was made on the basis of polarisation dependence of the inscription of surface relief gratings.[3.13] For this investigation, SRGs were inscribed using P polarisation of the laser light and were scanned under the similar conditions as per the previous samples for its hardness analysis. In

P polarization inscription, the E field vector of the inscribing light is parallel to the plane of incidence. The measurements show qualitatively similar results.
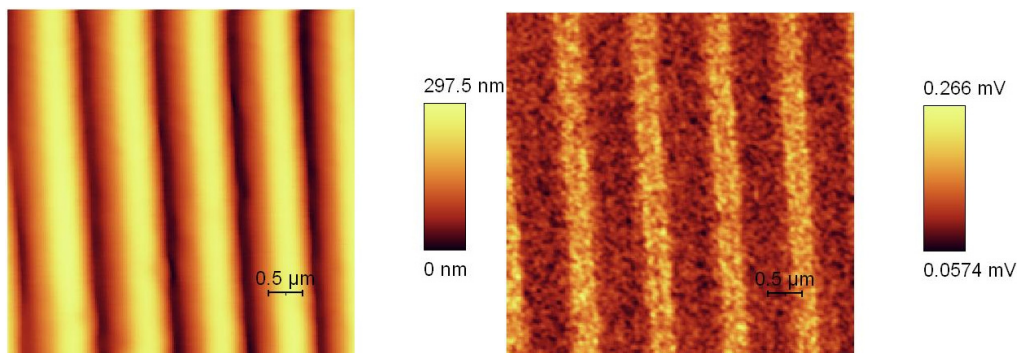
Figure 3.6(a):- AFM pattern of SRG sample inscribed using P polarization of laser light.
(a) Topography (b) Hardness signal; at T25°C

The hardness signal was analyzed and plotted against the scan area of the sample as shown in figure 3.6(b). The pattern of the hardness variation for the gratings recorded using P polarization of inscribing light is found similar to the pattern of the SRG samples recorded using circular polarization of inscribing light (figure3.3). The pattern shows similar maxima and minima of the recorded hardness. The periodicity of the gratings matches with the periodicity of the hardness pattern.
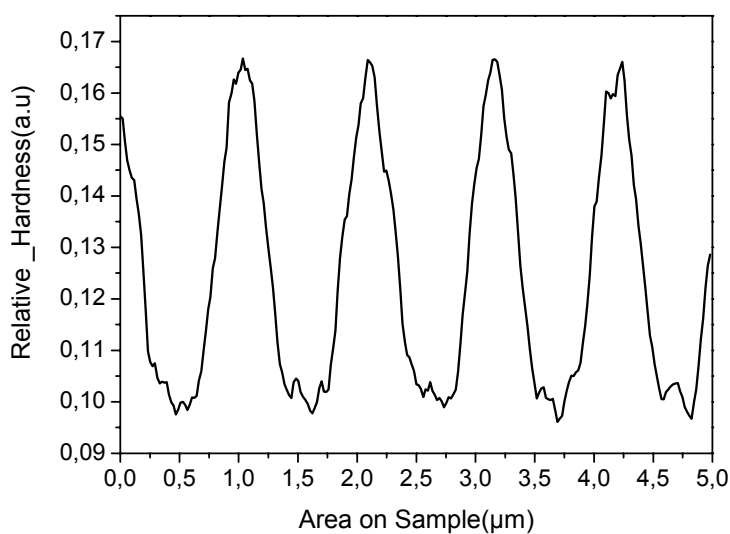
Figure 3.6(b):- Hardness variation on grating sample inscribed using P polarized light.

The maxima of hardness can either correspond to crests or trough of the height profile of the SRG. To correlate the maxima of hardness with the features of SRG, a scan has been performed on a selected area of the SRG. For this purpose, a single crest of the grating has been selected for scanning. The topography analysis of selected scan area is as shown in the figure 3.7(a)
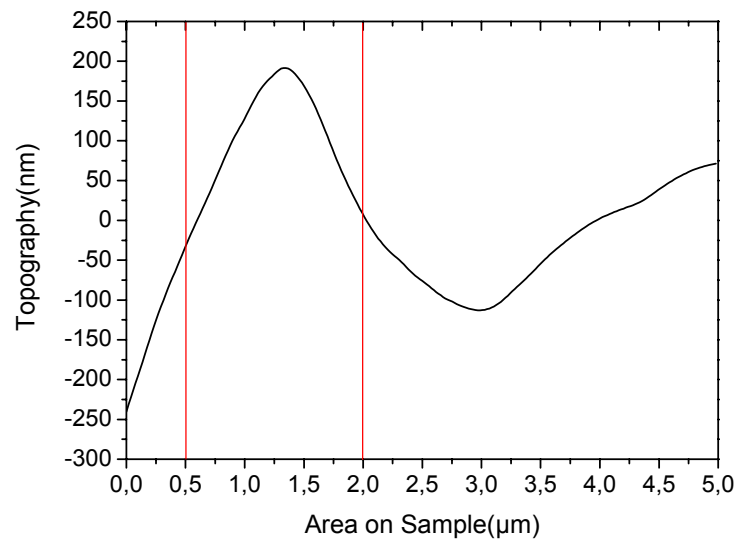
Figure 3.7(a):- Line scan of a single crest of the grating, surface profile

The topography analysis of the selected scan area shows a crest of the grating about 190nm high above the film surface. The corresponding amplitude signal of hardness shows a sharp peak corresponding to the crest of the grating as shown in the figure 3.7(b).
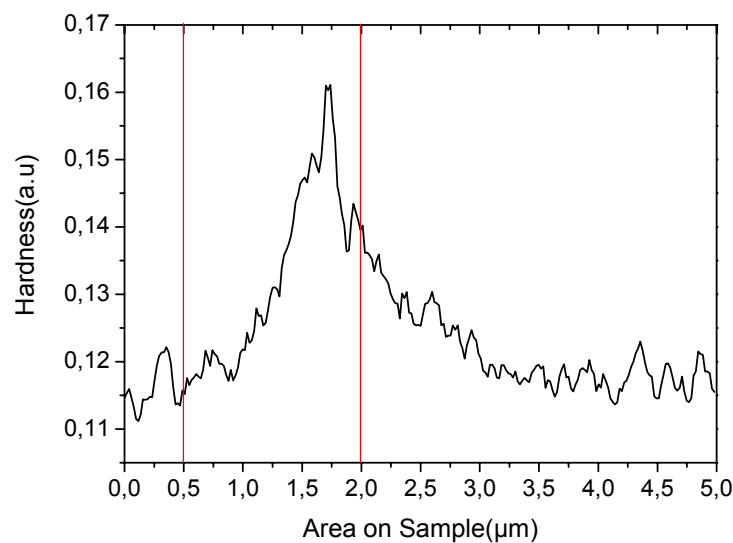
Figure 3.7(b):- Line scan of a single crest of the grating, Hardness profile

Both line scans provide reasonable mutual correlation, i.e. maxima of hardness coincide with maxima of SRG height. Thus it can be concluded that crests of the grating corresponds to the increased hardness area of the polymer after grating inscription despite of the changes in the polarisation states of the writing beam.

3.4 Discussion

The photo-orientation of azobenzene units during SRG formation is an angular sensitive process where the azobenzene chains become oriented with respect to the light polarization direction.[3.14] The rotation is induced by the permanent trans-cis-trans isomerisation of the azobenzene molecule implemented in the side chain of the polymer. Considering angular dependence of dipole force the orientation rotation of the entire azobenzene side chain saturates since the dipole moment of azobenzene unit coincides with the local polarisation vector of the incident light. Subsequently the spatially periodic variation of the polarization vector of inscribing light finally leads to a certain arrangement of azobenzene polymer side chains in parallel. Photoelectron spectroscopy has revealed that after SRG formation a large amount of azobenzene chain are aligned perpendicular to the grating vector but it was not possible to identify whether the chain density is larger in crests or in troughs.[3.15] Parallel alignment of polymer chains will increase to the Van der Waals interaction between neighboured chains and subsequently increase the local stiffness, resp. hardness, of the material. In uniaxially oriented polyethylene terephthalate a clear difference in stiffness was found compared to isotropic samples that lack ordering and show increased hardness for ordered phase, confirmed by micro indentation studies.[3.16] The enhancement in the stiffness is also found due to the confinement phase under mechanical stress in pMMA and other chain polymers.[3.17] Previous calculations in terms of finite element have shown that crests of SRG always show higher density compared to the troughs[3.18]. Subsequently from our measurement we can conclude that regions with high density showing increased hardness are hosting a large number of parallel arranged chains. In contrast to this one can conclude that regions with lower hardness compared to the virgin sample must have less number of parallel arranged chains. Therefore our results give direct evidence for the redistribution of azobenzene chains within SRG during grating formation. This process is more effective for polar polymer pDR1m compared to non-polar pMEA. The presence of higher hardness at crests is an indication of induced plasticity within the polymer during the process of grating formation.

Moreover, the observation that for sample formed at 20°C below T_g the hardness modulation nearly vanishes demonstrates the competition between light induced photo-orientation due to permanent trans-cis-trans isomerisation of azobenzene units and the thermal induced disorder of chain alignment. Whereas the first process is independent on temperature the second one increases exponential with raising temperature. At certain temperature both terms become equal which makes it impossible to form a SRG.

3.5 Summary

The ex-situ investigation of SRGs using force modulation mode of atomic force microscope has revealed the alteration of the mechanical properties of the azopolymer, after the inscription of surface relief gratings.

The uniform arrangement of the polymer chains with respect to each other at the crests of the grating leads to the increased hardness of the material, contrary to this; regions with lowered hardness correspond to random arrangement of polymer chains.

The variable hardness location is independent of the light polarization used for grating inscription. In both, circular-circular and P-P inscription geometry, the crest of the grating always corresponds to the increased hardness. From this one can conclude that the final arrangement of the polymer chains in any inscription geometry is the same but varies along crests and troughs.

References

[3.1a] Photoreactive organic thin films, Z. Sekkat and W. Knoll, ed., (Academic press, USA) (2002).

[3.1] Labarthet F. L., Buffeteau T., Sourisseau C., *J. Phys. Chem. B*, **102**, pp.5754-5765, (1998).

[3.2] Labarthet F. L., Buffete au T., Sourisseau C., *Applied Spectroscopy,* **54**, pp. 699-705, (2000).

[3.3] Constantino C. J. L., Aroca R. F., Mendonca, C. R., Mello S. V., Balogh D. T., Zilio S. C., and Oliveria, Jr. O.N. *Advanced Functional Materials*, **1**, pp.1-5, (2001).

[3.3a] Padmanabh U. Veer, Ullrich Pietsch, Anne D. Mueller *Appl. Phys. Lett.* **94**, 231911, (2009) .

[3.4] P. Veer, U. Pietsch, P. Rochon, and M. Saphiannikova Mol. Cryst. Liq. Cryst. 486, 66/[1114]-78/[1126], 2008.

[3.5] H. Ishitobi, M. Tanabe, Z. Sekkat and S. Kawata Optics Express, Vol. 15 (2), 652 (2007).

[3.6] P. Karageorgiev, D. Neher, B. Schulz, B. Stiller, U. Pietsch, M. Giersig, and L. Brehmer, Nature Materials 4,699-703 (2005).

[3.7] Photoreactive organic thin films, Z. Sekkat and W. Knoll, ed., (Academic press, USA) (2002).

[3.8] B. Stiller, P. Karageorgiev, T. Geue, K. Morawetz, M. Saphiannikova, N. Mechau, and D. Neher, Phys. Low-Dim. Struct. 1/2, 129, (2004).

[3.9] B. Stiller, T. Geue, K. Morawetz and M. Saphiannikova J. Microscopy, 219, 109-114, (2005).

[3.10] S.B. Sane and W.G. Knauss, Mechanics of time-dependent materials **5**, 325-343, (2001).

[3.11] 6.777J/2.751J *Material Property Database.]*

[3.13] Jiang X. L., Li L., Kumar J., Kim D. Y., Shivshankar V., Tripathy S.K. *Appl. Phys. Lett.* **68**, pp. 2618-2620, (1996).

[3.14] Dumont M, Osman A. E. Chem. Phys. **245**, 437 (1999)

[3.15] O. Henneberg, Th. Geue, U. Pietsch, M. Saphiannikova and B. Winter Appl. Phys. Lett. **84**, 1561 (2004).

[3.16] Ahmed I. Abou – Kandil, A. Flores, F.J. Balta Calleja and A. H. Windle J. Polym. Res. **15**, 373-379, (2008).

[3.17] Catherine A. Tweedie, Georgios Constantinides, Karl E. Lehman, Donald J. Brill, Gregory S. Blackman, and Krystyn J. Van Vliet, Adv. Mater. **19**, 2540–2546, (2007).

[3.18] T. M. Geue, M. Saphiannikova, O. Henneberg, U. Pietsch, P. Rochon and A. Natansohn Phys. Rev. E, **65**, 52801 (2002).

Chapter 4

Theoretical models

4.1 Introduction

Number of models has been developed to explain the process of surface relief grating formation on azobenzene polymer thin films[4.1a]. Herewith, I will be explaining basic assumptions and the drawbacks of those models briefly. The mechanism involved in the SRG formation depends upon variety of experimental conditions like polarization of the writing beam, laser power used for the inscription and also on the polymer architecture.

4.2 Free Volume model

This model is proposed by Barrett et. al.,[4.1a,4.1] In this model, the driving force for the grating formation was considered to be arise from pressure gradients due to the photoisomerization of the chromophores. The model states that the regions of high isomerization would be created next to the regions of the low isomerization. The isomerization requires free volume within the polymer vicinity and hence the pressure gradients are created. The generated pressure should be above the yield point of the polymer material. The mass transport takes place from the regions of high isomerization which possesses high pressure to the regions of low isomerization which possesses less pressure. Thus the gratings of sinusoidal shape are formed. To describe the flow of the material the author used the Navier-Stokes equations for laminar flow of a viscous fluid[4.2] as

$$\rho \frac{\partial \overline{v}}{\partial t} = -gradP + \mu \Delta \overline{v}$$

According to this equation, the product of mass and acceleration of a unit volume of a fluid is equal to the sum of the forces acting upon it. The equation states that the internal forces are composed of pressure gradients and has opposite sign. The term $\mu \Delta \overline{v}$ in the equation is called as the viscosity term and it describes the momentum transfer between adjacent thin layers of a fluid under shear flow.

Further, boundary layer conditions have been defined considering the nature of the writing beam and the physical state of the system to relate the velocity components in the film to the pressure gradients. This model can explain number of experimental findings like increase in the rate of the grating formation with increase in the intensity of the writing laser

and the inverse relation of the rate of the grating formation to the molecular weight of the polymer below the limit of entanglement. The model has also predicted a relation for the rate of the grating inscription and the initial thickness of the film. This model has provided good results which were consistent with the known values of the free volume required for the isomerization and bulk viscosity of the polymer matrix. The model also predicts that the crests of the surface relief grating correspond to the non illuminated region of the polymer film i.e. the gratings are π shifted in relation to the interference pattern. This prediction was observed experimentally.

4.3 Field Gradient model

The field gradient approach is based on the forces that are resulted due to the electric field gradient.[4.1a,4.3, 4.4] The electric field gradient is induced optically. According to this model, the deformation of the polymer film is caused by the lateral movement of the polymer chains. The experimental results of this model show no volume change in the polymer film during deformation. The force required for the mass transport is predicted to be a combination of the forces due to the change in the susceptibility due to the light and the field gradient. The time average of the gradient force density is given by[4.3]

$$f(r) = \langle [P(r,t).\nabla]E(r,t) \rangle = \langle [\varepsilon_0 \chi E(r,t).\nabla]E(r,t) \rangle = \frac{1}{2}\varepsilon_0 \chi' \acute{E}(r).\nabla E(r)$$

(4.1)

where P(r, t) is the polarization, E(r, t) is the optical electric field, $< >$ represents the time average, ε_0 is the vacuum permittivity and χ' is the optically induced change in the susceptibility of the film.[4.3]

From this equation 4.1 it can be seen that the polymer chains are subjected to force only in the direction where the component of the field gradient exists. When the polarization of the light is perpendicular to the gradient; the force is nil. It has been seen that under visible illumination, the polymer film becomes dichroic and birefringent. This dichroism and the induced birefringence induces a change in the susceptibility in the polymer film. The change in the susceptibility depends upon the direction of the total field which results from the interference pattern.

The model states that in the formation of surface relief gratings the direction of the resultant force is parallel to the grating vector in the experiments with the single laser beam. Considering a single Gaussian beam and a sample in XY plane, the laser polarization is in the

X direction. The light penetration depth for typical polymer is 0.1-0.3µm. thus the force density exerted on the chromophore is given by

$$f(x,y,z) = \frac{1}{4}\varepsilon_0\chi^{'}\exp(-\alpha z)\frac{\partial I(x,y)}{\partial x}x_0$$ (4.2)

where I(x, y) is the Gaussian distribution of the intensities in the focal plane, and x_0 is the unit vector in the direction x.[4.5] From the π shift of the grating formation in relation to the interference pattern it is suggested that the force is directed outward from the high intensity region to the low intensity region. The model treats the polymer surface as a thin mobile layer in which the polymers viscosity is dominated by the force f(x,y,z). The velocity due to this force is given by

$$v_s(x,y,z) = \mu f(x,y,z)$$ (4.3)

where μ is the coefficient that depends on the viscoelasticity of the photo-altered polymer. μ is related to the confirmation of the polymer chains. In this model μ was taken constant independent of the time and light intensity. The model also neglects the transient regions where the velocity changes because of the reason that the time required for the transient is very smaller than the one required for the writing of surface relief gratings.

According to this model the surface deformation caused by the linearly polarized Gaussian beam is given by

$$S(x,y,t) = \int_0^t v_z(x,y,0)dt^{'} = \frac{1}{4}h\mu\varepsilon_0\chi^{'}\frac{\partial^2 I(x,y)}{\partial x^2}t$$ (4.5)

And the surface deformation caused by the circularly polarized Gaussian beam, according to above analysis is

$$S(r,t) = \frac{1}{4}h\mu\varepsilon_0\chi^{'}\frac{\partial^2 I(x,y)}{\partial x^2}t$$ (4.6)

From equation 4.5 and 4.6, it can be seen that the surface deformation profile is proportional to the second derivative of the intensity with respect to the direction of polarization.
This model predicts the pattern of surface relief grating from the interference pattern.

4.4 Mean-Field Theory Model

The mean field theory is based on the assumption that the mean field potential is responsible for the alignment of the chromophores along the director according to the Maier-Saupe theory. It is also responsible to attract the chromophores with parallel orientation.[4.1a,4.6] Under illumination with linearly polarized light, the azobenzene chromophores will orient

parallel to each other and, according to the Maier-Saupe theory. According to this theory the attractive interaction between the chromophores will have different effects depending upon their alignment i.e. side by side or end to end. When the chromophores are aligned side by side there is a mass transport because in this case the direction of the attractive force coincides with the direction of grating vector. With this assumption the author could explain the polarization dependence of the grating formation and the special periodicity of surface relief gratings inscribed on the liquid crystalline polymer films. The model predicts that the chromophores should be attracted to the illuminated region of the interference pattern of the sample. This observation was found consistent with the experimental results of the surface relief grating formation on liquid crystalline polymer films and is contradictory to the observations of surface relief grating formation on amorphous azobenzene polymer films. Hence the model cannot be used or extended to explain the grating formation on amorphous azobenzene polymer films.

Also this mean field model does not consider any possible thermal effects. The thermal effects may arise from the high laser power required to inscribe gratings on liquid crystalline polymer films unlike amorphous polymers. Hence there is a possibility of the contribution of the thermal effects. In case of amorphous polymers it has been already showed that the thermal effects are not negligible.[4.5]

4.5 Diffusion model

The diffusion model assumes that the bulk diffusion of the molecules is responsible for the surface relief grating formation.[4.1a,4.7] The basic assumption of the model are as follows:

The model neglects the rotational and translational coupling of the molecules while diffusion. That is translational motion doesn´t involve rotation of the molecules and vice versa.

The model predicts that the molecules are allowed to move randomly forward and backward.

The angular distribution of the molecules was considered to be time independent during the diffusion. The time scale for orientation was considered to be 0.1 to few seconds while for the diffusion it was considered to be 10 min or more.

According to this model, the probability of collision of an excited molecule during its motion decreases exponentially with the distance it moves divided by the molecules diffusion length. This distance is typically of the order of molecular size and is smaller than the grating period. Thus the diffusion flow has contribution of probability and that of number of chromophores that cross a given area section per unit time. Such a number of chromophores depend upon variety of factors like light intensity, the angle between the light polarization, the quantum

efficiency of the translation process and the molecular axis. The theoretical results shown by this model agrees with the experimental findings of Jiang et.al.[4.8] in which it has been shown that the P polarized beams are more efficient in writing gratings than S polarized beam.

The surface modulation is then calculated from the number density of chromophores. Another feature of this model that is observed experimentally is that the azochromophore molecules are directed outwards from the illuminated regions.[4.7]

4.6 Comments on the models

The free volume model[4.1,4.2] could explain number of experimental findings of surface relief gratings on high T_g polymers. According to this model the origin of grating formation is the light induced mass transport. But this model cannot explain the polarization dependence of the grating formation. The mass transport based on the pressure difference should be insensitive to the P or S polarized writing laser beams. Thus this model explains the dynamics of the mass transport but cannot explain the origin of the force for the mass transport[4.1a,].

The diffusion model by Lefin et. al.[4.7] explains the polarization dependence of the grating formation. This model predicts the worm like mechanism within the azobenzene polymer for the mass transport. But such worm like movement could simply be due to the pressure gradients and cannot be the origin of the process[4.1a,]. Also, the free volume model assumes that the viscous flow of the polymer material arises from the bulk of the polymer material whereas the experiments had showed that the grating formation is a surface initiated process.[4.1a,4,10]
.

The field gradient model[4.4] explains the grating formation phenomenon by giving the origin of the force required for the mass transport. This model can also explain the polarization dependence of the grating formation. But this model failed to explain the mechanism for the dynamics of the mass transport. Also this model cannot explain the reason for viscoelastic flow of the polymer material which leads to the grating formation[4.1a,]. The further extension to this study was done by Viswanathan et. al.[4.10]. In this study the author has quantitatively predicted the polarization of the surface relief grating. They also showed that the shape of the experimentally observed SRG could be reproduced theoretically. But the force density calculated from the predicted approach is found two orders of magnitude smaller than the density of gravitational force[4.11] and thus it is small enough for the inscription of the surface relief gratings.

The calculations are as follows

The optically induced force density (averaged over time) is given by[4.4,4.5]

$$f(r) = \langle [P(r,t).\nabla]E(r,t) \rangle \tag{4.7}$$

where $p(r,t) = \varepsilon_0 \chi E(r,t)$ is the medium polarization,

$\varepsilon_0 = 8.854 \times 10^{-12} C^2 /(Nm^2)$ is the permittivity of vacuum, and

$|\chi| \sim 1$ is the medium susceptibility.

For a case of two counter circularly polarized beams, the resultant force acts in the direction x parallel to the grating vector, and its density is equal to

$$f = -k\varepsilon_0 \chi E_0^2 \sin\theta(1 + \cos^2\theta)\sin(kx\sin\theta), \tag{4.8}$$

where 2θ is the angle between two beams and the term k=2π/λ appears due to the ∇ derivative in equation 4.7. Taking into account that $E_0^2 = 2Iz_0$ (I is the laser intensity and z₀=377Ω is the vacuum impidence) the upper estimate of f will be

$$f_{max} = \frac{4\pi}{\lambda} \varepsilon_0 z_0 \chi I. \tag{4.9}$$

Typically for a laser power I=100mW/cm² and wavelength of λ=488nm. This gives a force density of about 100N/m³, which is two orders of magnitude smaller than the density of gravitational force. Thus the force is not enough to deform the polymer in glassy state.

The results of the model by Pedersen et. al.[4.6] which is based on the mean field theory are in good agreement with the experimental findings for the grating inscription on liquid crystalline polymers. This model predicts that the surface relief gratings should be phase with the interference pattern. This statement could be valid for the liquid crystalline polymers because of the pronounced cooperative movements of the molecules. However this model cannot be considered to explain the grating formation on amorphous azobenzene polymer films since the gratings on amorphous polymer films have π phase shift with respect to the interference pattern.

A model based upon statistical reorientation of side chains in the polymer by repeated trans-cis-trans isomerization process[4.9] explains the SRG formation in different types of polymers. But this model couldn´t give a detailed microscopic process leading to the deformation of the polymer sample.

4.7 Summary

Thus, despite of several models developed to explain the process of surface relief grating formation on amorphous azopolymer films, none of them could explain the complete process of SRG formation depending upon the parameters like, writing beam polarization, photo-induced softening, origin of the force and the strength of the force, direction of the migration of the polymer chains and the final alignment of the polymer chains etc.

The experiments performed in the scope of this thesis work (temperature dependent continuous and pulsed exposure), and the results obtained from those experiments are satisfactorily explained by a suitable model which is described in the following chapter.

References

[4.1a] Photoreactive organic thin films, Z. Sekkat and W. Knoll, ed., (Academic press, USA) (2002).

[4.1] Barrett C. J., Natansohn A. L., and Rochon P. L., *J. Phys. Chem.*, **100**, pp. 8836-8842, (1996).

[4.2] Christopher J. Barrett, Paul L. Rochon, Almeria L. Natansohn, *J. Chem. Phys.*, **109**, pp. 1505-1516, (1998).

[4.3] A. Ashkin, J. M. Dziedzic, J. E. Bjorkholm, and S. Chu, Opt. Lett. **11**, pp. 288-290, (1986).

[4.4] Jayant Kumar, Lian L., X. L. Jiang, D. Y. Kim, T. S. Lee, and S. Tripathy, *Appl. Phys. Lett.*, **72,** pp.2096-2098, (1998).

[4.5] Bian S.P., Williams J. M., Kim D.Y., Li L. A., Balasubramanian S., Kumar J., and Tripathy S., *J. Appl. Phys.* **86**, pp. 4498-4508, (1999).

[4.6] Pedersen T. G., Johansen P. M., Holme N. C. R., and Ramanajum P.S., *Phys. Rev. Lett.* **80**, pp. 89-92, (1998).

[4.7] Lefin P., Fiorini C., and Nunzi J., M., *Optical Materials* **9**, pp. 323-328, (1998).

[4.8] Jiang X. L., Kumar J., Kim D. Y., Shivshankar V., and Tripathy S. K., *Appl. Phys. Lett.* **68**, pp. 2618-2620, (1996).

[4.9] D. Bublitz, B. Fleck, L. Wenke *Appl. Phys. B* **72**, pp. 931-936, (2001)

[4.10] Viswannathan N. K., Balasubramanian S., Li L., Kumar J., and Tripathy S. K., *J. Phys. Chem. B*, **102**, pp. 6064-6070, (1998).

[4.11] M. Saphiannikova, T. M. Gaue, O. Henneberg, K. Morawetz, and U. Pietsch *J. Chem. Phys.* **120**, pp.1-7, (2004).

Chapter 5

Time and Temperature Dependence of Surface Relief Grating Formation

5.1 Introduction

In this chapter, the results of the surface relief grating formation under time and temperature dependent deformation will be presented. As discussed in chapter 2, in temperature dependent technique, the sample was heated from room temperature till the glass transition temperature of the polymer with the steps of few degrees and then the grating formation was studied under continuous exposure till the saturation of the process. Also in time dependent study, the polymer sample was heated from room temperature till the glass transition temperature with the steps of few degrees whereas the illumination was pulse like using an electromechanical shutter operating in time scale of seconds.

In spite of the number of theories, the formation of surface relief grating is still a controversial issue taking into account the parameters like photo-induced softening of the polymer material, microscopic origin of the process and the dependence of the molecular architecture. To explain the process several theories assume considerable degree of light induced softening comparable to the softening found near glass transition temperature or even a fluid state which is characterized by zero value of young's modulus[5.1,5.2,5.3] or the theories predict small magnitude of force required for the inscription process assuming the photo-induced softening[5.4,5.5]. The logical consequence of this assumption is that inscription of SRG should become much more effective following the increase in the temperature approaching the glass transition. Whereas number of experiments has showed that there is no considerable softening of the azobenzene layer under illumination.[5.5a]

Hence to verify this assumption, temperature resolved continuous and pulsed exposure measurements have been performed on azobenzene polymer thin films of pDR1M (poly [4-nitrophenyl-4´-[[2-(methacryloyloxy) ethyl] ethyl-amino] phenyldiazene]). To study the effect of the molecular architecture on the inscription process, the SRG formation on thin films of pMEA (poly [4-(2-methacryloyloxy) ethylazobenzene]) having low dipole moments compared to pDR1M have been studied. Also to study the grating formation process at microscopic level, the ex-situ investigation of the inscribed grating samples were carried out using an atomic force microscope and it was already discussed in the previous chapter.

5.2 Continuous exposure measurements

Continuous exposure measurements were performed on high dipole moment pDR1M and low dipole moment pMEA to study the effect of molecule architecture on the grating inscription process. Dipole moment being the measure of polarity of a molecule was assumed to affect the rate of the grating formation. The chromophore bearing the strong-NO_2 group as the electron –withdrawing substituent at the end of the side chain in pDR1M causes a permanent dipole moment μ=7.0D and showed higher level, rate and stability of photo-induced birefringence than that of having –SO_2 group. This is attributed to its larger optical density at the writing wavelength and shorter cis life time, which means it cycles more in the same time scale.[5.7] The azobenzene moiety in pMEA has a permanent dipole moment of μ=0.05D. It was already observed that the high dipole moment in pDR1M resulted in faster and higher degree of birefringence compared to low dipole pMEA[5.6,5.7] due to effective higher orientation of chromophores, still increasing the strength of the azo dipole is not always beneficial to photo-orientation as irreversible photo-bleaching (photo-degradation) process may accompany the orientation process.[5.7] A low dipole moment molecule will undergo less number of isomerization cycles compared to that of the high dipole moment molecule.

The absorption maxima of pDR1M and pMEA correspond to the wavelength of 458nm and 324nm, respectively. Hence in the case of pDR1M, the grating inscription was carried out at the green wavelength of 514nm, for which the absorption coefficient is $3.6 \times 10^4 cm^{-1}$. [5.8] The absorption coefficient of pMEA at this wavelength is extremely low ($5.8 \times 10^2 cm^{-1}$).[5.8] Therefore, for pMEA grating inscription was performed at the blue wavelength of 488nm.

To overcome the effect of different wavelengths used for the inscription of gratings, the obtained data were normalised with respect to the absorption maxima of respective polymer. From UV-VIS spectra[5.8] the normalization factors calculated for pDR1M and pMEA were 1.53 and 20 respectively (factor 13), which corresponds to the difference in the absorption coefficient at used wavelengths in the experiment. For quantitative comparison between pDR1M and pMEA the obtained data were normalised with this factor.

The effect of glass transition temperature in the comparative study of pDR1M (T_G=120°C) and pMEA (T_G=80°C) was neglected for room temperature measurements because the T_G of the material was far above the room temperature.[5.9] Above room temperature till glass transition temperature, diffraction efficiency shows similar trend in pDR1M and pMEA without significantly showing any additional effect.

5.2.1 Continuous exposure measurements on pDR1M

Continuous exposure measurements were performed on thin films of pDR1M with increasing steps of temperature from room temperature up to the glass transition. The initial experiments were performed monitoring only the first order diffraction intensity signal using a single photo-diode. The experiments were performed at four different intensities of inscribing laser with respect to increasing temperature to verify the behavior of the diffraction intensity at different grating inscription conditions.
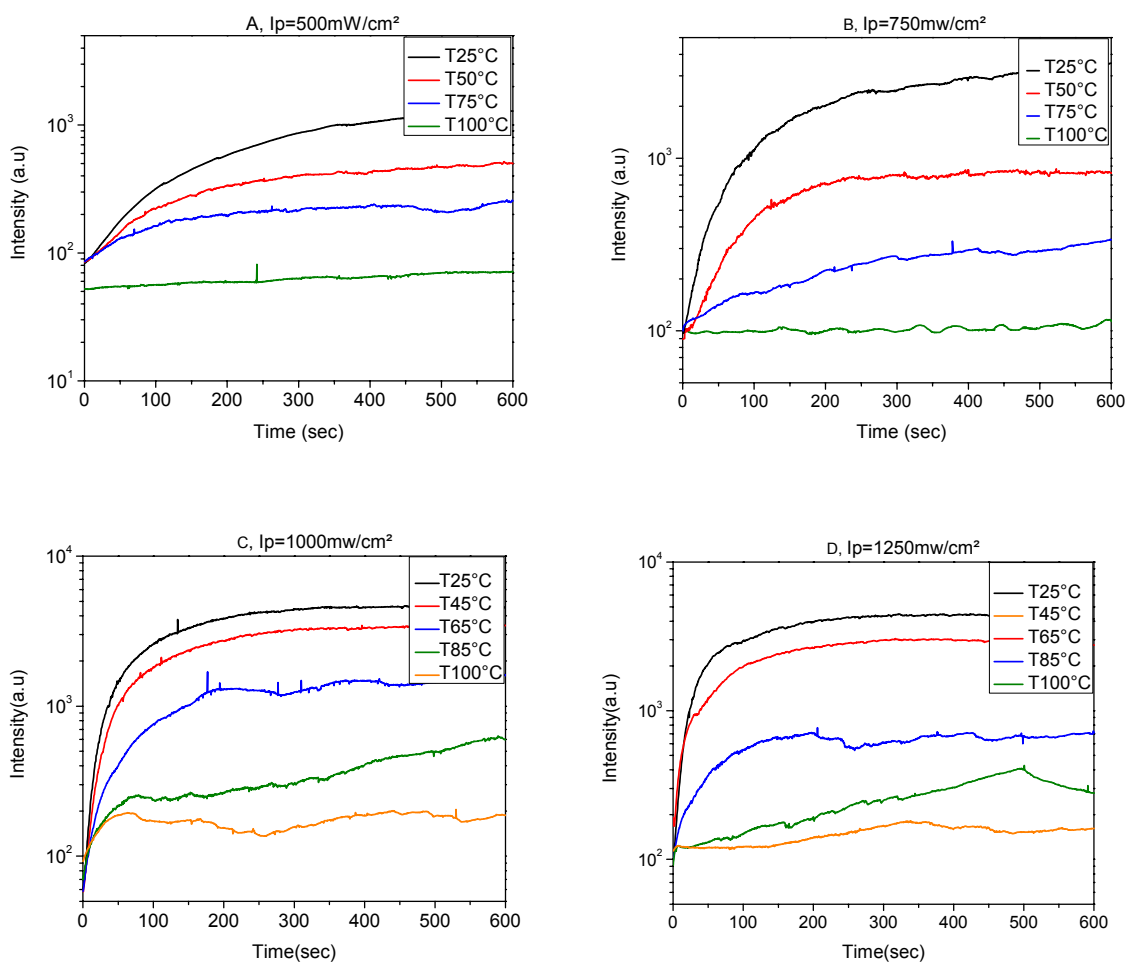

Figure 5.1- Temperature dependence of SRG formation at various power densities of the inscribing laser, A=500mW/cm², B=750mW/cm², C=1000mW/cm², D=1250mW/cm².

Figure 5.1 A, B, C, and D shows the first order diffraction intensity measured during the formation of the surface relief gratings at various temperature and inscription intensities of the laser viz. 500mW/cm², 750mW/cm², 1000mW/cm², and 1250mW/cm² respectively. The intensity in mW/cm² indicates the initial intensity of the inscribing laser before the expansion of the beam. After the beam expansion the intensity at the sample surface is about 10% of the initial laser power and is increases almost linearly with increase in the initial laser intensity.

Further to verify the exact changes in the recording of the intensity, the measured first order diffraction intensity (I_1) is then normalized with respect to the intensity of the incoming light (I_0). For this purpose the, specular reflected intensity was also measured using another photodiode simultaneously. The recording of the first order diffracted and specular reflected intensity was carried out for two different sets of the laser intensity with respect to temperatures. The plots are as shown in figure 5.2.
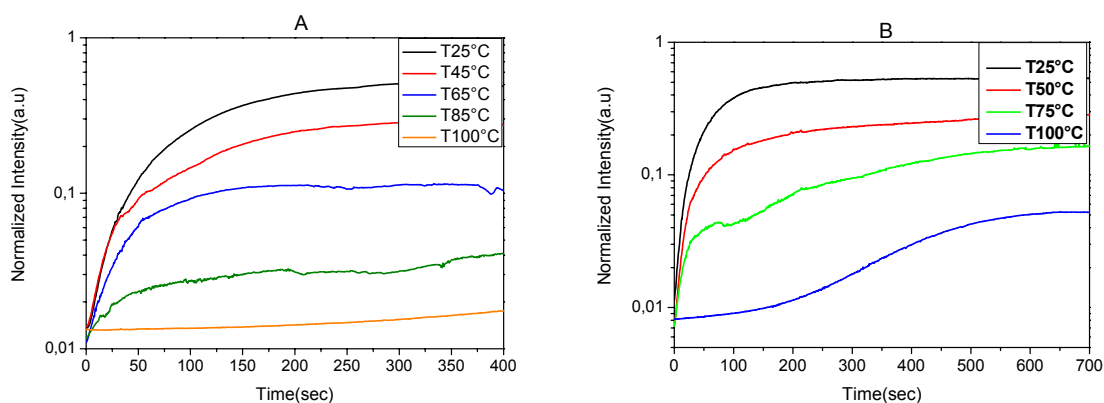

Figure 5.2- Normalized first order diffraction intensity at various temperature during SRG formation, (A)Laser Intensity=500mW/cm², (B)Laser Intensity=1000mW/cm²

The first order diffraction intensity reflects the state of the grating formation, where the intensity increases with increase in the grating heights with respect to the inscription time. From figure 5.1 and 5.2 it has been seen that the diffraction intensity of the first order peak varies significantly with temperature. At room temperature one observes a typical behavior of diffraction intensity known from the grating formation at room temperature.[5.10,5.11] The intensity increases exponentially in the beginning and reaches saturation later. The intensity at the saturation level reflects the achieved formation of nearly sinusoidal SRG. The exponential shape of the curve disappears about 20° below the glass transition temperature.

In contrast to the room temperature, the efficiency of the grating formation is strongly reduced at higher temperature. This is seen in the considerably reduced value of the intensity at the saturation, I_{sat} and in the lower slope of the diffraction curves at the beginning of the illumination following the successive increase in the temperature. At T=100°C, 20°C below T_G which is the closest temperature to the glass transition in the temperature dependent inscription study, no gain in the diffraction intensity is observed i.e. gratings were not inscribed.

5.2.2 Continuous exposure measurements on pMEA

Continuous exposure measurements were performed on a low dipole moment pMEA in the similar way as that of pDR1M. The glass transition temperature of pMEA was lower than pDR1M hence the temperature steps were according to that difference.
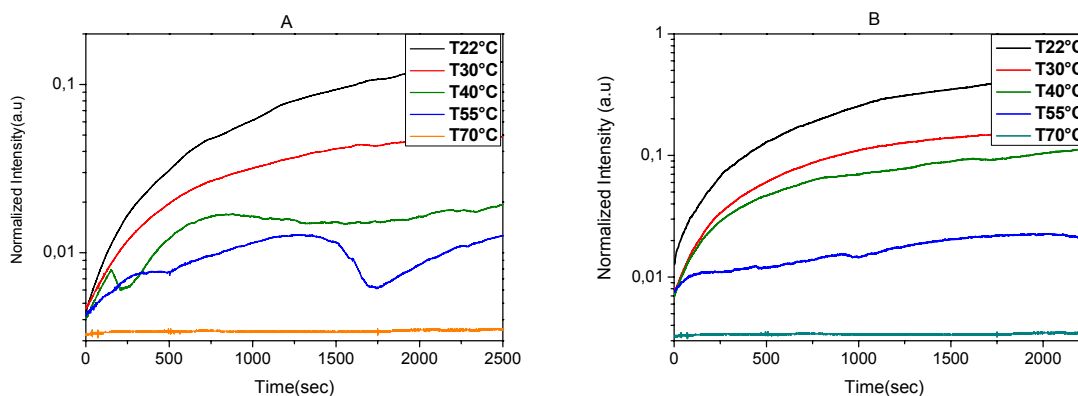

Figure 5.3- Normalized first order diffraction intensity at various temperature and power density, A=2.5W/cm², B=5W/cm²

Figure 5.3A and 5.3B shows the first order diffraction intensity during the formation of surface relief gratings on thin films of pMEA. The diffraction intensity follows the same exponential behavior as seen from the grating inscription on pDR1M thin films i.e. the diffraction intensity increases rapidly in the beginning of the illumination and after some minutes reaches saturation. Also the similar decrease in the diffraction intensity with successive increase in the temperature was found during temperature dependent inscription in pMEA as seen in case of pDR1M. The only difference is in the time required for the saturation of the process which is found to be higher than that of pDR1M. In case of high dipole moment pDR1M, the saturation of the grating inscription was found within few hundreds of seconds whereas for pMEA it was almost 5 times greater than that of required for pDR1M. This difference in time scale is due to the low dipole moment of azochromophore in pMEA which leads to the less isomerization cycles per unit time and hence affecting the orientation of the azo chromophore. The large variations in the diffraction efficiency observed during the inscription of grating at higher temperature are due to the local air turbulence within the closed chamber.

5.3 Rate of grating formation

5.3.1 Fluence Dependent rate of grating formation

Fluence is defined as the number of particles that intersects a given area. The rate of the grating formation can be treated as the speed of the grating formation process. The photo-orientation of the azobenzene chromophore depends upon variety of factors like bulkiness of azobenzene, rigidity of the polymer matrix, its chemical composition, linkage between the polymer and its backbone, free volume in the polymer etc.[5.12] The rate of the grating formation is extracted from the initial slope of the diffraction efficiency curve seen from the figures 5.1, 5.2 and 5.3, considering the first few seconds of illumination. The slope of the diffraction efficiency curve has been observed to vary with the parameters like intensity of the inscription laser, temperature during the inscription process and also on the polymer properties. The measured intensity I1(t) can be described by

$$I_1(t) = I_{sat}(T)(1 - e^{-t/\tau_p(T)})$$
(5.1)

where I_{sat} is the intensity after saturation and $1/\tau_p$ is the rate of the grating formation. This rate of grating formation has been extracted from the measurements at different inscription intensity of the laser, from the measurements described in figure 5.1.
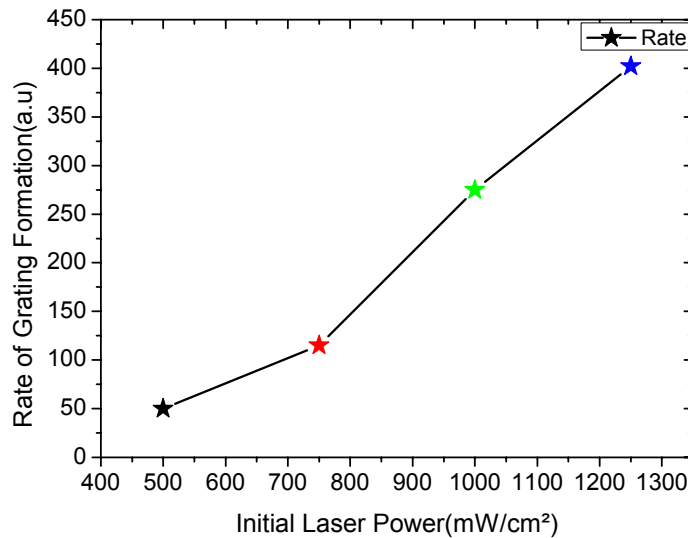

Figure5.4- Fluence Dependent rate of grating formation, measurements performed at room temperature.

Figure 5.4 shows the dependence of the rate of grating formation on the inscription intensity. It is observed that the rate of grating formation increases almost linearly with increase in the power density used for the inscription, for a given film thickness. In the scope of the current measurements, smaller rate of the grating formation is observed for initial power of 500mW/cm² compared to one observed for 1250mW/cm², where the laser intensity was maximum. From the above analysis, it can be concluded that the formation of surface relief grating is related to the fluence of the laser, taking into account the other parameters of the polymer remains constant like film thickness, ambient temperature etc.

5.3.2 Temperature Dependence rate of grating formation

Also, the rate of the grating formation varies inversely with the temperature during the inscription process. For the analysis purpose, one set of measurements from figure 5.1 (I_p=1000mW/cm²) has been considered. The rate of the grating formation has been extracted for different temperature dependent measurements and is plotted as shown in figure 5.5.
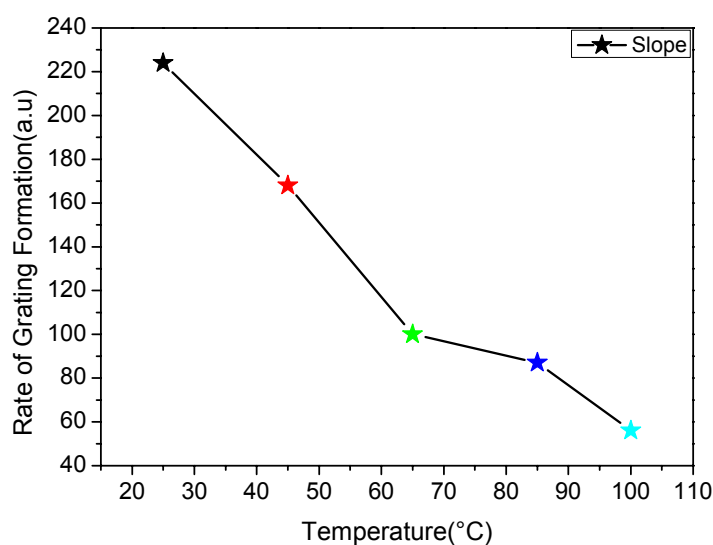
Figure5.5- Temperature dependent rate of grating formation.

The temperature dependence of the surface relief grating formation shows that the rate of the grating formation decreases with successive increase in the temperature. The rate of the grating formation is highest at T=25°C (about 70% higher) compared to the rate observed for T=100°C. The decrease in the rate at higher temperature manifests the decrease in the photo-orientation of the azochromophore at higher temperature.

5.3.3 Dipole moment dependent rate of SRG formation

The conclusions drawn from the fluence and temperature dependent rate of grating formation were explained considering the responses of the first order diffraction intensity under visible illumination of both the polymers under study i.e. pDR1M and pMEA. Whereas the comparison between the first order diffraction intensity of these two polymers shows that the rate of the grating formation is different for different polymers, as shown in figure 5.6 Even after normalizing both the curves with respect to the absorption maxima and to the factor corresponding to the difference in the power density.
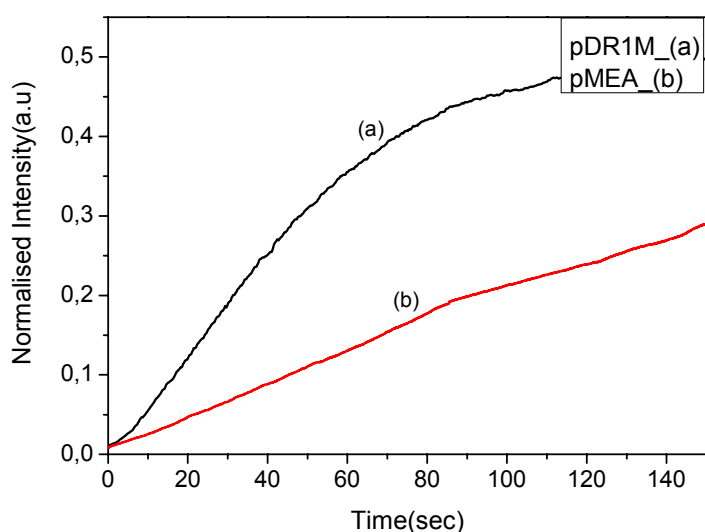

Figure 5.6- First order diffraction intensity during the process of grating formation at room temperature, normalised with respect to absorption maxima (a) pDR1M, (b) pMEA

This variation in the rate of the grating inscription has also been recorded in temperature dependent measurement. For further analysis, considering one set of measurements form pDR1M, I_p=1W/cm² (5.2, B) and pMEA, I_p=5W/cm² (5.3, B) the rate of the grating formation at different temperatures have been calculated. Prior to this, the inscription time is normalized with a factor of 13 as described in the section 5.2. Figure 5.7 shows the comparison between the rates of pDR1M and pMEA at different inscription temperatures.

From figure 5.7 it is observed that the rate of grating formation in pMEA is around 30% less than that in pDR1M at room temperature. This difference in the rate behaviour possibly arises due to less effective reorientation of chromophores in pMEA compared to pDR1M due to its low dipole moments[5.12a].
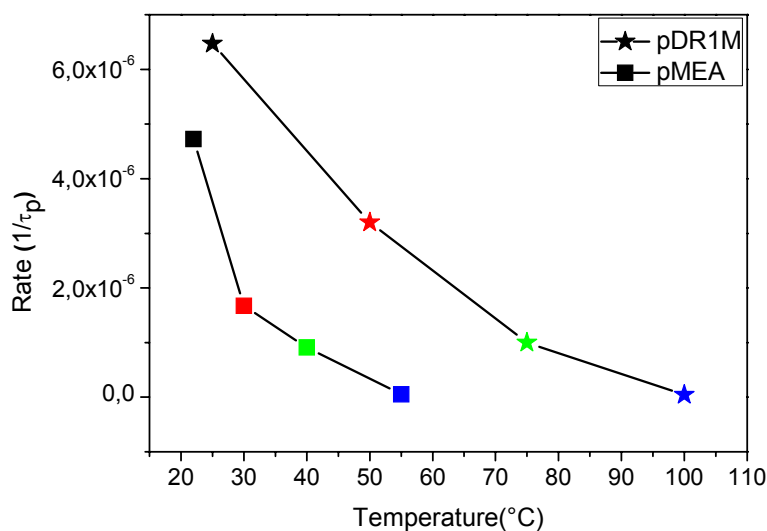
Figure 5.7- Rate of the grating formation in pDR1M and pMEA films at different inscription temperatures.

Thus the measurements reflect the strong influence of the polarity of azobenzene moieties on the process of grating inscription which intern responsible for the orientation mechanism of azochromophore.

5.4 Pulsed exposure measurements

Pulsed exposure measurements were previously studied [5.13,5.14,5.15] to understand the grating formation under time dependence in thin films of pDR1M. The typical response of the diffraction intensity under pulsed exposure is shown in the plots below. When the light is switched on, the diffraction intensity jumps to a certain value, then increases further under illumination, and slowly decays when the light is switched off after a jump back. The difference in intensity between two subsequent pulses reflects the plastic gain in SRG formation. We have studied the pulsed exposure under temperature dependent inscription of SRG and have recorded minute changes during the grating inscription under exposure and in the absence of light. Also we have studied the grating formation under different pulse durations for pDR1M and pMEA, the results are described below.

5.4.1 Pulse Exposure on pDR1M

Pulsed exposure on pDR1M was carried out for different pulse durations. The process of formation of surface relief gratings differs depending upon the pulse duration. This has helped in setting up the exact pulse length for the temperature dependent measurements.

The measurements were performed under similar conditions viz. power density at the sample surface, temperature, simply varying the pulse duration at room temperature. The plots are as shown in figure 5.8.
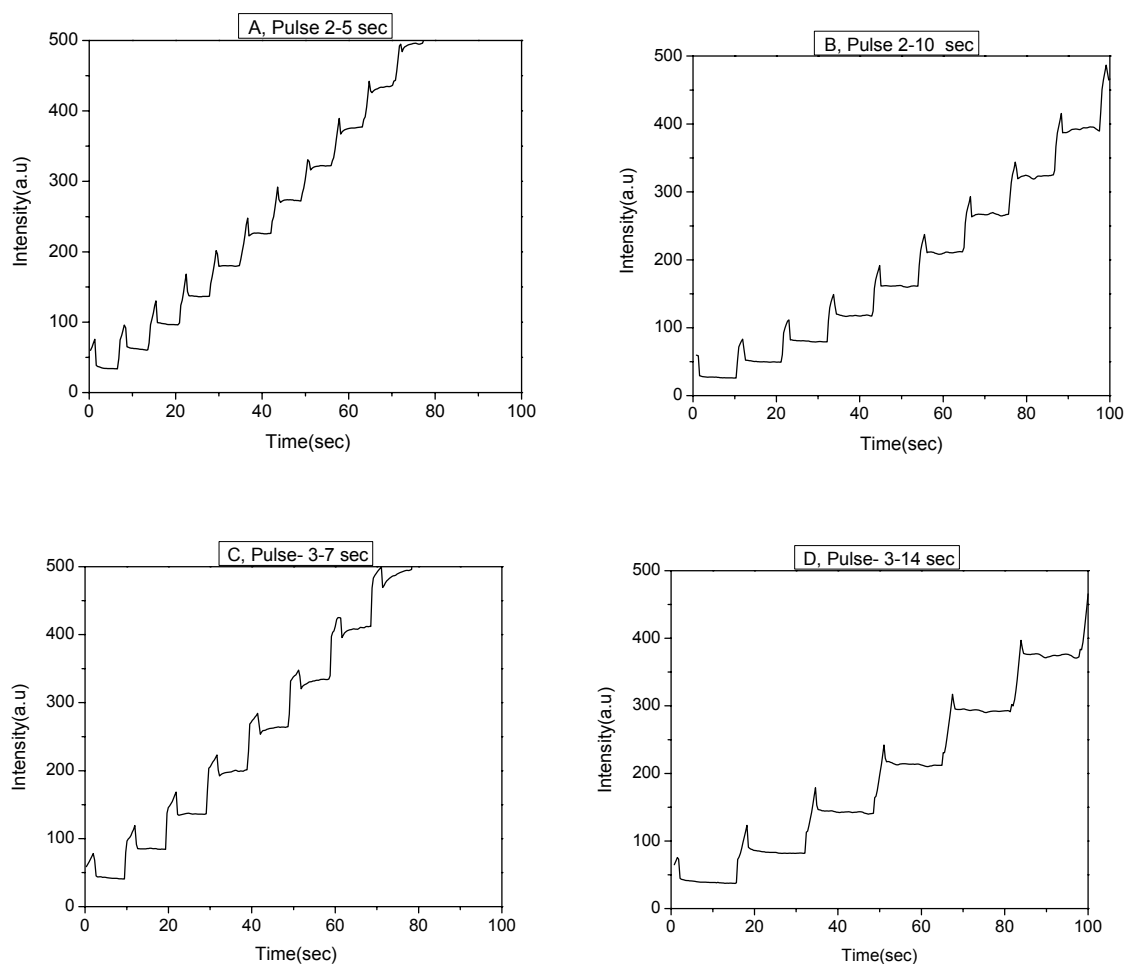

Figure 5.8 (A),(B,)(C),(D)- Pulsed exposure measurements on pDR1M with different pulse duration.

Figure 5.8(A) and 5.8(B) shows the response of the first order diffraction efficiency for a pulse of 2 sec exposure and 5 sec. and 10 sec. pause respectively. From these two plots it is seen that, when the pause time of the system was small, 5 sec, the diffraction intensity shows higher growth compared to the measurement where the pause time was 10 sec. This is due to the fact that, in a short pause time before the response of the polymer to actinic light would lose completely, the next pulse again induces the grating formation. The successive orientation of the system leads to the mass transfer of the polymer material with the uniform arrangement of the polymer chains with respect to the light polarization direction, which is nothing but the grating formation process. Hence the diffraction intensity is higher for small

pause time. Whereas when the pause time of the system is longer, the gratings relax to higher extent compared to previous case and consequently the plastic gain induced in successive pulse is small.

Similar behavior of diffraction efficiency was observed for an exposure pulse of 3 sec and pause time of 7sec. and 14 sec. figure 5.8(C) and figure 5.8(D) i.e. the plastic gain induced in successive pulse is higher for smaller pause time. Whereas, when the pause time of the system was small compared to its exposure time, after number of pulses the relaxation of the grating is no more observed, figure 5.8(a) and figure 5.8(c). Even though the light is switched off, the diffraction intensity signal increases instead of decaying in the absence of actinic light. This effect can be due to the momentum transfer within the polymer matrix after the number of pulses boosting the orientation mechanism.

Further increasing the exposure and pause time, the relaxation of the grating becomes more promising as shown in figure 5.8(E) and figure 5.8(F). The ultimate response of the grating formation was observed when the pause time was 23sec. as shown in the figure 5.8(F). But the accompanying plastic gain in every successive pulse was also higher due to the exposure time of 5 seconds.
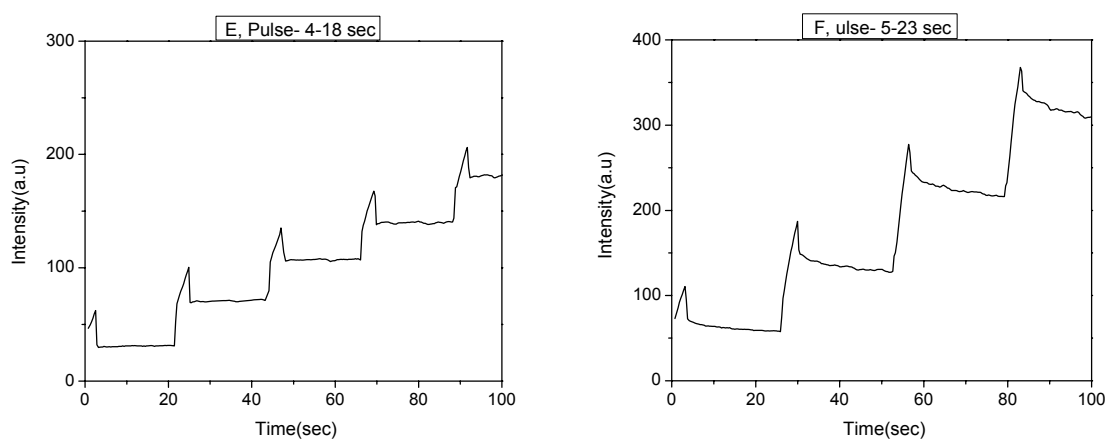
Figure 5.8 (E),(F)- Pulsed exposure measurements on pDR1M with different pulse duration.

Hence the typical response of the diffraction efficiency in terms of the plastic gain and relaxation of the system, (which, as per the assumption corresponds to the orientation and relaxation of the azobenzene chromophore) which were the two main parameters under the pulsed exposure study can be achieved by keeping the moderate exposure time and longer pause time. Therefore for the final temperature dependent pulsed exposure study, the exposure time was chosen to be 2sec. while the pause time was kept 20sec. for better resolved diffraction efficiency response.

5.4.2 Temperature dependent pulse exposure, pDR1M

The development of SRG under pulse like exposure was investigated using cyclic inscribing force by monitoring the first order diffracted intensity signal. The first order diffraction intensity signal was then normalized to the intensity of the incident radiation. Figure 5.9(a) shows the pulsed exposure study of pDR1M carried out at different temperatures. As described earlier, under pulse like exposure, the diffraction intensity increases under illumination, jumps back to a certain value when light is switched off-relaxes further in the dark time and the difference gives the plastic gain induced between the successive pulses. With increasing temperature, the induced plastic gain goes on decreasing, because as per the assumption the orientation mechanism of azochromophore is hindered at higher temperature, thereby affecting the generation of stress which leads to the grating formation. The relaxation of the system becomes more prominent with increasing temperature.
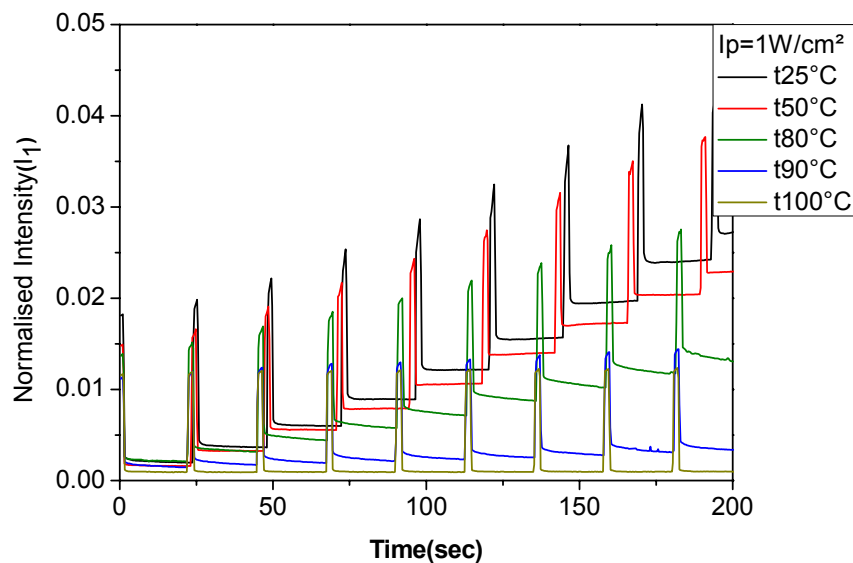
Figure 5.9- (a) Temperature dependence of first order diffraction efficiency during pulsed exposure of pDR1M

To study the relaxation of the gratings at higher temperature in the absence of light i.e. in the pause time, further measurements at higher temperature with a step of 5° have been performed. The range of the measurements was from 80°C to 110°C, as shown in figure 5.9(b). As seen from the figure the relaxation in the dark shows exponential behavior as long as the temperature is below 100°C. At this temperature no plastic gain and relaxation is found.

The gratings are purely elastic at this stage and exist only under light illumination. The atomic force microscope measurement of the samples at higher temperature also shows decreasing grating heights which is directly related to the induced plastic gain in every successive pulse. Above 100°C temperature, the response of the diffraction efficiency under pulsed exposure is almost the same as that of recorded for 100°C temperature, with a slight reduction in the jump under light illumination. This reduction in the jump is due to the excess softening of the polymer material near its glass transition temperature.
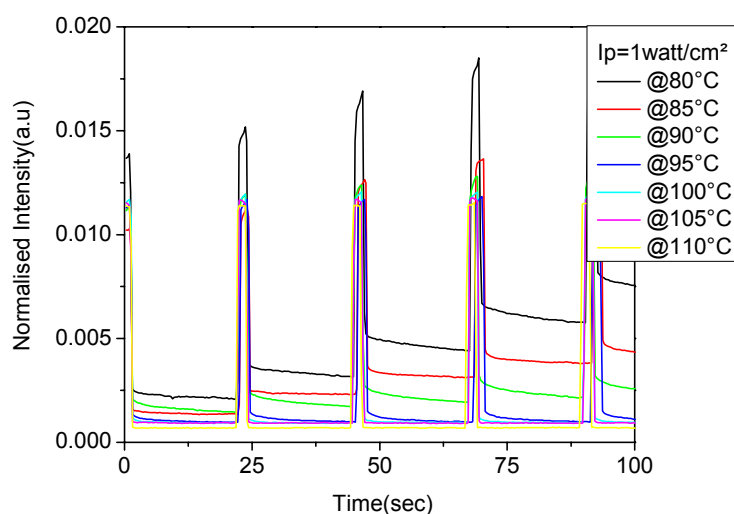

Figure 5.9- (b) Temperature resolved pulsed Exposure measurements on pDR1M.

The time dependence of scattered intensity during relaxation process can be represented by

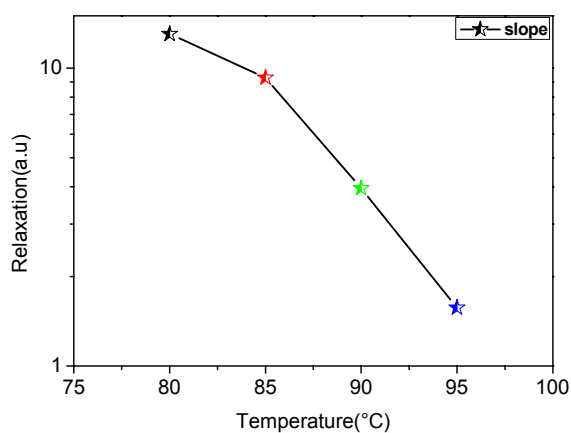$$I_2(t) = I_1(t)e^{-t/\tau_c(T)} \qquad (5.2)$$

Figure 5.9(c)- Temperature dependent rate of grating relaxation during pulsed exposure measurements on pDR1M.

The rate of grating relaxation, $1/\tau_c$ decreases with temperature as shown in figure 5.9(c) and is no more measurable at T=100°C. The rate of the grating relaxation is given by the slope of the diffraction efficiency curve in the dark.

The sudden changes in the polymer properties near its glass transition temperature which also affects the grating formation seen by lowest relaxation rate and negligible plastic gain at 100°C can also be seen from the plot of elastic and plastic gain verses number pulses as shown in the figure below.
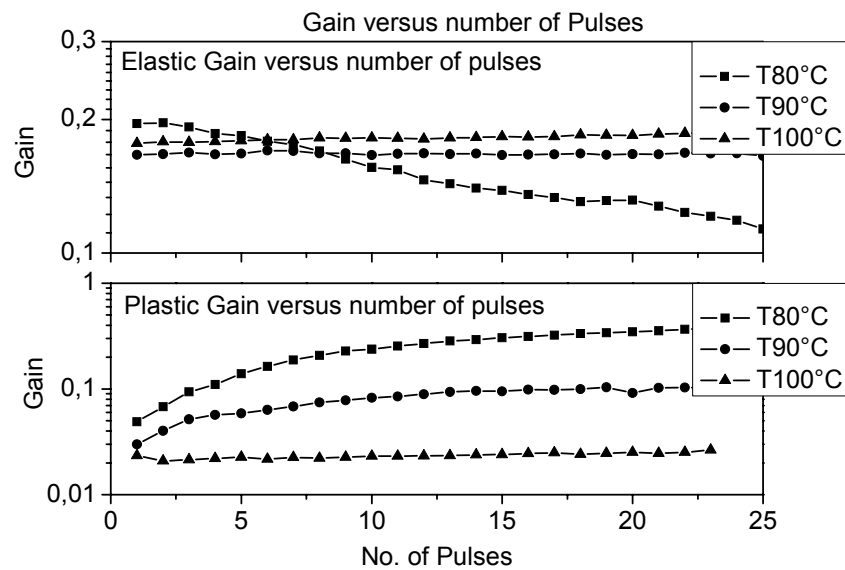
Figure5.10- Elastic and Plastic gain dependence of number of pulses.

The temperature dependence of plastic gain can be seen from the bottom part of the figure 5.10. One can see qualitatively similar behavior to that of the continuous exposure. The gain is accumulated from subsequent pulses. However, no plastic gain is observed for T=100°C. Also as seen from the upper part of the graph, decrease in the elastic gain at T=80°C with successive pulses is an indication of the induced plastic gain which is also seen from the bottom part of the graph at T=80°C. Negligible change observed in the elastic gain for T=90°C and for T=100°C in the upper part of the graph indicates the absence of plastic gain which corresponds to no grating formation. This is also observed by atomic force microscope measurements of the samples, where negligible grating formation was observed at this temperature.

5.4.3 Temperature dependent pulse exposure, pMEA

The pulsed exposure measurements on pDR1M have showed the formation and relaxation of gratings under illumination and in the absence of light respectively which can further be related to the reorientation and relaxation of the azobenzene chromophores as per the assumption. It has also been seen that, how the formation of gratings is prominent at room temperature and how the relaxation increases approaching the glass transition temperature upto a certain cross over temperature and after that very quick relaxation is observed. Similar pulse exposure measurements were also performed on low dipole moment pMEA to know the response of the first order diffraction intensity in terms of reorientation and relaxation. As seen from the continuous exposure measurements, the rate of the grating formation was lower in pMEA compared to high dipole moment pDR1M, hence the exposure and relaxation time was increased for pulsed exposure measurements on pMEA. Figure 5.11(a) shows the response of the first order diffraction efficiency during the measurements of pulse exposure on pMEA thin films for an exposure of 4sec. and relaxation of 30sec. the measurements were performed at room temperature and 40°C below its glass transition temperature.
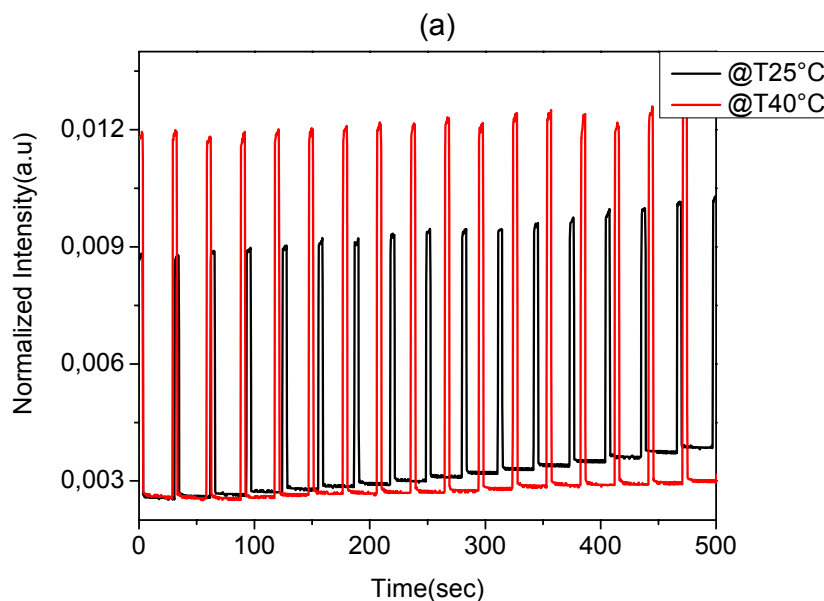
Figure 5.11(a) - First order diffraction efficiency response during pulsed exposure measurements on pMEA.

The response of the first order diffraction efficiency during the measurements of pMEA was similar to that of recorded for pDR1M pulsed exposure. The diffraction intensity shows a sudden jump under exposure and a reverse jump when the actinic light was switched off. The difference between the two pulses shows the induced plastic gain. But the relaxation of the

gratings was not observed at room temperature and neither at higher temperature. Also the degree of the induced plastic gain in successive pulse was very small compared to response of pDR1M. Since the assumed orientation process is slow in pMEA due to the low dipole moment, the magnitude of the induced stress due to this slower orientation is less in pMEA which intern limits the degree of the induced plastic gain. The induced plastic gain at room temperature can be seen in figure 5.11(a), after 5 pulses comparing with the red curve. The relaxation was not observed at room temperature measurements but it was expected to be observed at higher temperature due to the softening of the polymer. The measurements performed at T=40°C, well below glass transition temperature show very small relaxation seen by some variations in the diffraction intensity in the dark, which was still not able to measure in terms of the slope.

In order to reveal similar performance as that of pDR1M, the pulse width has to be taken larger in case of pMEA. Increasing the pulse width increases the degree of the induced plastic gain in successive pulse as seen in the figure 5.11(b)
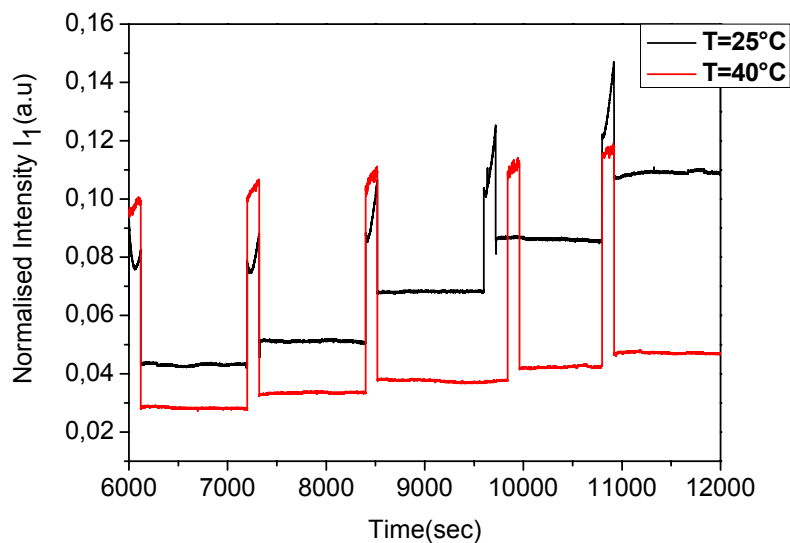
Figure5.11 (b) - Extended pulse exposure on pMEA

Still the relaxation was found to be negligible in case of pMEA. At 40°C temperature, well below glass transition temperature, even though the exposure time was larger, the induced plastic gain was found to be decreasing to a greater extent. This can be attributed to the combined effect of low dipole moments i.e. slow orientation and temperature effect which reduces the orientation probability. Even though the rate of grating inscription and the plastic gain induced in successive pulses was small for pMEA compared to pDR1M, the observed deformation at saturation level was observed to be approximately same at room temperature,

as the grating heights were found comparable at the saturation level for similar film thickness of pDR1M and pMEA. The AFM measurements for the identification of the grating height are discussed in the next session. This indicates that the orientation of the azochromophore plays a major role in the grating formation process.

From continuous exposure and pulsed exposure measurements it has been seen that the diffraction intensity increases linearly for first few seconds under illumination. Whereas, during the extended pulse exposure on pMEA it has been seen that the diffraction intensity shows a nonlinear behavior exactly after the first pulse. The extended pulse exposure measurements were carried out with the pulse of 120sec. and a relaxation of 1080sec. as shown in figure 5.11(c).
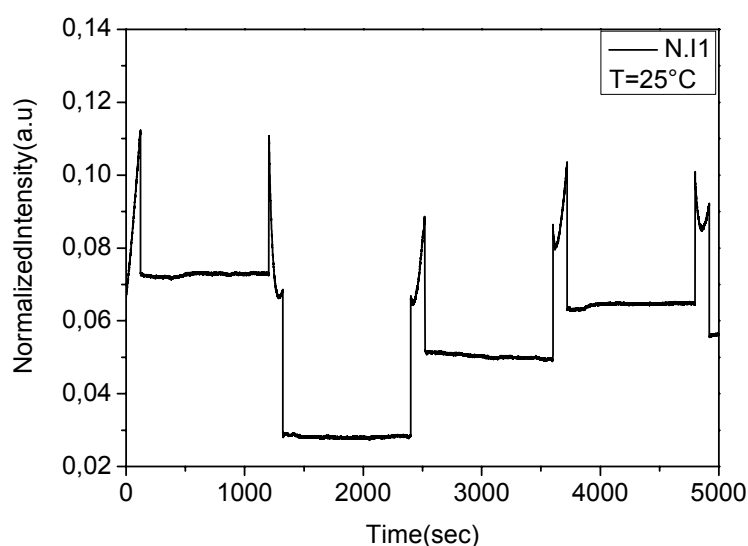
Figure5.11 (c) – Nonlinearity in the diffraction intensity, during the extended pulse exposure measurements on pMEA.

Under illumination, the diffraction intensity shows linear increase with time for the first pulse as seen from the figure5.11. It is then followed by a sudden decrease in the diffraction intensity and a relaxation when the light is switched off. After the first period, when the next pulse of light falls on the sample the diffraction intensity instead of increasing further shows a sudden decrease. With every successive pulse the induced nonlinearity goes on decreasing and after few pulses the diffraction intensity shows a typical response of the diffraction intensity as seen from the pulsed exposure measurements of pDR1M. Since, the effect was observed only for the first few pulses it can be related to the induced anisotropy in the polymer upon first irradiation cycle. For the confirmation of this statement, detailed single pulse exposure measurements were carried out on pMEA thin films. A polymer sample of

pMEA was exposed to light for 120sec. and allowed to relax in the dark for 1080sec. Probing the illuminated area of the sample in dark using 633nm He-Ne laser showed first order diffraction peaks as shown in the figure below. The probe beam direction was along 'Z' axis as shown in figure 5.12.
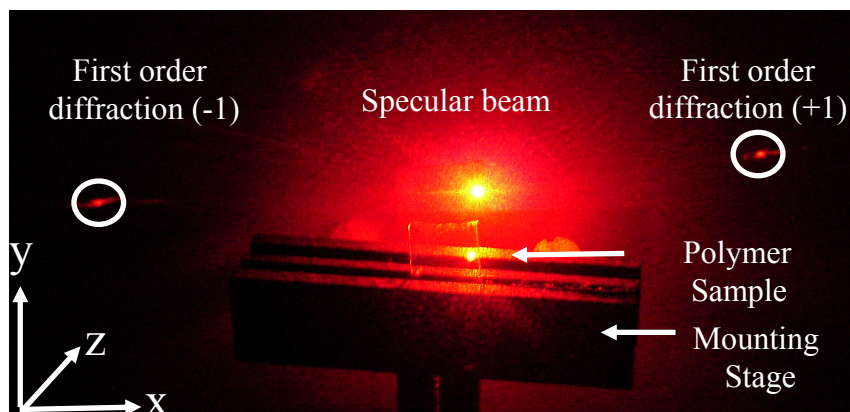
Figure5.12- Diffraction from a birefringence grating

Further exposing the sample to un-polarized light, the first order diffraction peaks were found to vanish suddenly probably due to the relaxation of the gratings. Such relaxation is possible because normally weak gratings get inscribed with in first pulse. Thus it can be concluded that the anisotropy was nothing but the induced birefringence gratings within the first pulse. The birefringence can normally be induced within the light sensitive polymers due to the initial anisotropy within the polymer material, e.g. a short pulse of polarized light which orients the chromophores with respect to the polarization direction. With successive pulses, the induced birefringence gets erased by further material movement which is not in phase with initial arrangement of macromolecules and hence the diffraction efficiency shows non linear behavior. At longer times, grating formation is dominant over induced birefringence.

In the comparative study of the induced birefringence on thin films of pDR1M, pMAEA, and pMEA having dipole moments in the order pDR1M>pMAEA>pMEA, the writing and relaxation rate of birefringence was in the order pDR1M>pMAEA>pMEA.[5.6] Due to the lower relaxation rate of birefringence in pMEA compared to pDR1M, the birefringence is preserved for a longer time in pMEA compared to pDR1M. As seen in our measurements, figure 5.11(c), as the first pulse induces the birefringence, the second and third pulse erases the induced birefringence due to the further material movement and this leads to

the anisotropy in the diffraction efficiency signal. Thus the slower writing and relaxation rate in pMEA compared to pDR1M are related to the low dipole moment and hence to the slow orientation process.

5.5 AFM characterization of grating samples

The ex-situ investigation of the surface relief grating samples inscribed at various temperatures was carried out using atomic force microscope. The obtained results in terms of the grating height also support the behavior of the first order diffraction intensity: mainly the grating height goes on decreasing approaching the glass transition temperature, as seen in the figure 5.13. From AFM characterization of the surface relief gratings inscribed on pDR1M thin films, it has been seen that gratings with maximum height were inscribed at room temperature (T=25°C), figure 5.13(A). Further increasing the temperature, the grating height was found to decrease successively. The trend was similar to that of the first order diffraction efficiency with respect to temperature observed in continuous exposure measurements and the induced plastic gain with respect to temperature in pulsed exposure measurements. At temperature near the glass transition temperature (T=100°C) of the polymer material, negligible grating formation was observed as seen from figure 5.13(B).

A   **B**

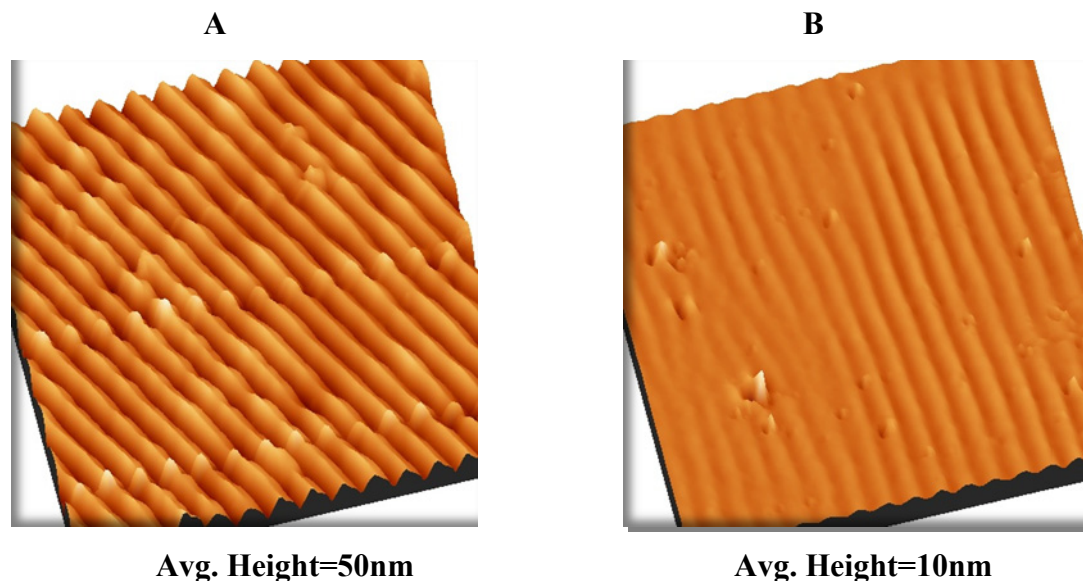**Avg. Height=50nm**   **Avg. Height=10nm**

Figure 5.13- AFM characterization of the grating samples on pDR1M, continuous exposure, (A) At Temperature=25°C, (B) At temperature=100°C

The ex-situ investigation of the gratings inscribed on pMEA thin films also shows similar trend of the decrease in the grating heights with respect to temperature and negligible grating
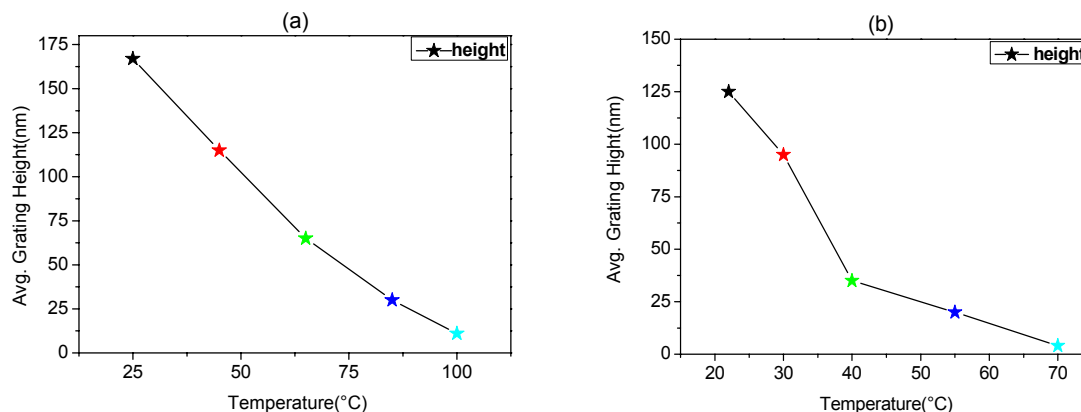
Figure 5.14- Decrease in the gratings heights with temperature, (a) pDR1M, (b) pMEA

heights near the glass transition, as seen in case of pDR1M. The behavior of grating height verses temperature is as shown in the figure 5.14.

5.6 Discussion

The time and temperature dependence of the grating formation discussed in this chapter can be explained in terms of the orientation approach.[5.16,5.17] In this approach, the mechanical stress appearing in the system under illumination with the polarized light is caused by reorientation of azobenzene back bone due to the photo-induced reorientation of chromophores. The probability P(Θ) that a chromophore is oriented at an angle 'Θ' with respect to the electric field vector E is shown to be described by the exponential function[5.17]

$$P(\Theta) \cong C \exp\left[-V(\Theta)/kT\right] \qquad (5.3)$$

where T is the absolute temperature, k is the Boltzmann constant and V(Θ) is the effective light induced potential. The inverse relation of the probability of orientation to that of temperature indicates that at higher temperature the orientation probability decreases consequently decreasing the total stress. Thus, temperature resolved continuous and pulsed exposure measurements performed on thin films of pDR1M indirectly support the main assumption of orientation approach, namely that the light induced orientation of chromophores is an initiator of the grating formation in azobenzene polymer films. Further, the comparison of the continuous and pulsed exposure measurements for azobenzene polymer with different rates of chromophore orientation i.e. azobenzene with different values of

permanent dipole moments namely, pDR1M and pMEA, also supports the orientation approach.

References

[5.1] C. L. Barrett, P. L. Rochon, and A. L. Natansohn *J. Chem. Phys*. 109, 1505, (1998)

[5.2] K. Sumaru, T. Yamanaka, T. Fukuda and H. Matsuda, *Appl. Phys. Lett*. 75, 1878, (1999).

[5.3] T. Fukuda, H. Mastuda, T. Shiraga, T. Kimura, M. Kato, N. K. Viswanathan, J. Kumar, and S. K. Tripathy, *Macromolecules* 33, 4220, (2000)

[5.4] Jayant Kumar, Lian L., X. L. Jiang, D. Y. Kim, T. S. Lee, and S. Tripathy, *Appl. Phys. Lett.*, **72,** pp.2096-2098, (1998).

[5.5] Bian S.P., Williams J. M., Kim D.Y., Li L. A., Balasubramanian S., Kumar J., and Tripathy S., *J. Appl. Phys*. **86**, pp. 4498-4508, (1999).

[5.5a] Marina Saphiannikova, Habilitationsschrift zur Erlangung des akademischen Grades, Feb (2007).

[5.6] M. S. Ho., A. Natansohn, C. Barrett, and P. Rochon, *Can. J. Chem*. **73**, 1773, (1995).

[5.7] C. Cojocariu, and P. Rochon. *Pure Appl. Chem*., **76**, 1479, (2004).

[5.8] M. S. Ho., A. Natansohn, C. Barrett, and P. Rochon, *Can. J. Chem*. **73**, 1773, (1995).

[5.9] C. Barrett, A. Natansohn, and P. Rochon *Chem. Mater*. **7**, 899, (1995).

[5.10] P. Rochon, E. Batalla, A. Natansohn. *Appl. Phys. Lett*., **66**, 136, (1995).

[5.11] D. Y. Kim, S. K. Tripathy, L. Li, J. Kumar. *Appl. Phys. Lett*., **66**, 166, (1995).

[5.12] Cristina Cojocariu and Paul Rochon *Pure Appl. Chem*. **76**, Nos. 7-8, 1479-1497, (2004).

[5.12a] Padmanabh U. Veer, Ullrich Pietsch, and Marina Saphiannikova *J. Appl. Phys.*, 2009

[5.13] M. Saphiannikova, T.M. Geue, O. Henneberg, K. Morawetz and U. Pietsch *J. Chem. Phys*. **120**, 1, (2004)

[5.14] T.M. Geue, M. G. Saphiannikova, O. Henneberg, and U. Pietsch, *Phys. Rev. E,* **65**, 052801, (2002)

[5.15] M. Saphiannikova, O. Henneberg, T. M. Geue, U. Pietsch, and P. Rochon, *J. Phys. Chem. B,* **108**, 15084, (2004).

[5.16] M. Saphiannikova, D. Neher. *J. Phys. Chem. B*, **109**, 19428, (2005).

[5.17] V. Toshchevikov, M. Saphiannikova, G. Heinrich., *J. Phys. Chem. B,* 113, 5031-5045, (2009) .

Chapter 6

Modeling visible light scattering data

6.1 Introduction

The experimental results of the time and temperature dependent measurements performed on the azobenzene polymers pDR1M and pMEA used for the comparative study have been presented in chapter 5. The results obtained from high dipole moment pDR1M and low dipole moment pMEA show a clear difference in the rate of the grating formation and the quantities such as relaxation of the chromophores in the absence of the inscribing light and induced stress.[1,2] This chapter deals with the MATLAB simulations carried out for the pulsed exposure measurements which were based on the viscoelastic approach.[3] The simulations were carried for pulsed exposure measurements performed on both the polymers i.e. pDR1M and pMEA. The obtained parameters give a quantitative comparison for the chromophore relaxation and light induced stress for both the polymer used in the experiment. Further, the viscoelastic approach has been modified to viscoplastic approach[4], which is the best suited approach to clarify the deformation(ε) of the polymer in the glassy state. Boltzmann superposition principal is utilized to describe the light induced stress produced by sequence of short pulses.

6.2 The viscoelastic model

The interference pattern of a polarized beam, at a certain angle results in a sinusoidal variation in the intensity or the direction polarization vector. In case of grating formation, the resultant vector varies along the grating period. Hence the force acting on polymer material should also vary sinusoidally along the same direction. Barrett et. al.[5] assumed that polymer is an incompressible viscous material and used the above force law to calculate the rate of the grating formation. With these assumptions, it was shown that the rate of the grating formation increases linearly with increase in the intensity and with the third power of the initial film thickness. The calculations were in good agreement with the experimental for the thin films. Further, Navier-Stokes equation was used to describe the flow of the material as discussed in chapter 3. That means the material was considered to be viscous material without any intrinsic relaxation time. But, considering the response of the first order diffraction intensity during the pulse exposure measurements (figure 6.1) the assumption of viscous flow fails to explain the relaxation in the absence of actinic light.
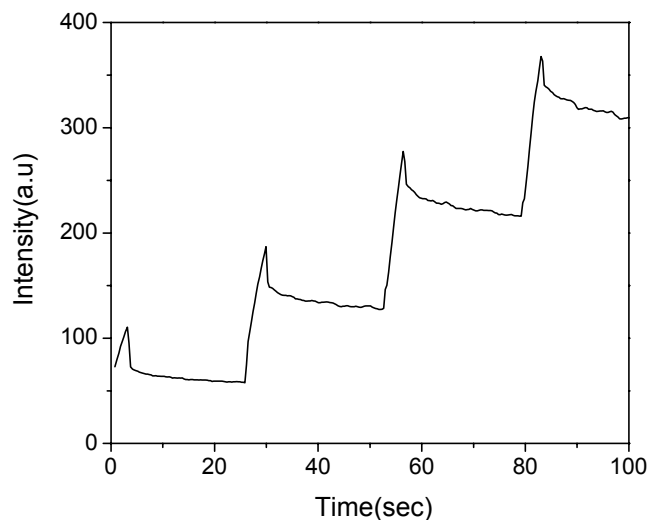
Figure 6.1- First order diffraction intensity during pulse exposure grating formation

Hence we consider the polymer material as an isotropic viscoelastic (VE) material with finite compressibility for the modeling of the visible light scattering data. The viscoelastic response is more promising near and above the glass transition temperature where the modulus of the polymer material is almost three orders of magnitude less than that of found at room temperature.[4,5.a]

6.2.1 Viscoelastic analysis

The stress strain equations in the viscoelastic analysis depend not only on the current stress and strain state, but also on the entire history of the development of these states. This behavior can be explained in terms of hereditary integrals as[4]

$$\sigma(t) = \int_0^t G(t - t') \frac{d\varepsilon(t')}{dt'} dt' \qquad (6.1)$$

where $\sigma(t)$ is the current stress and $\varepsilon(t')$ is the strain at a past moment of time t'. The time dependent relaxation modulus, $G(t)$, for materials with fading memory such as polymers can be described as an exponential series:

$$G(t) = \sum_{k=1}^N G_k \exp(-t / \tau_k) \qquad \text{and} \qquad G_0 = G(0) = \frac{E}{2(1+v)} \qquad (6.2)$$

where E is the Young's modulus, v is the Poisons ratio and τ_k are the particular relaxation times of the system.

Under application of constant stress, σ_0, a time dependent polymer deformation can be obtained from equation (6.1) using the Fourier Laplace transformation[6]

$$\varepsilon(t) = \sigma_0 \int \frac{d\omega}{2\pi\omega} \frac{e^{i\omega t}}{G^*(\omega)} \tag{6.3}$$

Where integration is performed in a complex plane and $G^*(\omega)$ is the complex shear modulus

$$G^*(\omega) = i\omega \int_0^\infty e^{-i\omega t} G(t) dt \tag{6.4}$$

Using equation 6.2, $G^*(\omega)$ can be written as

$$G^*(\omega) = \sum_{k=1}^{N} G_k \frac{i\omega\tau_k}{1 + i\omega\tau_k} \tag{6.5}$$

Substituting equation(6.5) into equation(6.3) gives the creep compliance of the material

$$J(t) = \frac{\varepsilon(t)}{\sigma_0} = \frac{t}{g_0} + \frac{g_1}{g_0^2} + \sum_{k=1}^{N-1} C_k \exp(-\omega_k t) \tag{6.8}$$

where $G_0 = \sum_{k=1}^{N} G_k$, $\quad g_0 = \sum_{K=1}^{N} G_k \tau_k$, $\quad\quad g_1 = \sum_{k=1}^{N} G_k \tau_k^2$, $\quad\quad C_k$ and ω_k are constants

depending upon G_k and τ_k.[3] The term g_0 can be identified as a stationary viscosity as

$$\sigma_0 = g_0 \frac{d\varepsilon(t)}{dt} \text{ at large t.[6]}$$

The sinusoidal force varying in X direction parallel to the grating vector for the grating inscription can be expressed as [4]

$$f_x = AV \exp\left(\frac{z - [h(x) + h_0]}{\mu}\right) \sin\left(\frac{2\pi x}{D}\right) \tag{6.9}$$

Here A is the force density which should be proportional to the laser power in the linear regime, h(x) is the height of SRG, h_0 is the initial film thickness, μ is the light penetration depth and D is the grating period. V is the sample volume equal to $h_0 D^2$. The inscribing force 'f_x' decays exponentially inside the film to account for the light absorption.

6.2.2 Grating formation under time dependent illumination

The development of surface relief gratings under pulse like exposure was reproduced using a cyclic external force applied as follows[4]

$$f = \begin{cases} f_x; 0 \le t \le t_1 \\ 0; t_1 \langle t \le T_c \end{cases} \tag{6.10}$$

where f_x is given by equation (6.9), t_1 is the pulse length and T_c is cycle length. The response to the complex loading history can be calculated using Boltzmann superposition principle[4]

$$\varepsilon(t) = \sum_t \Delta\sigma_i J(t - t_i) \tag{6.11}$$

where $\Delta\sigma_i$ is the change in stress after switching the light on(off), and *i* is the cycle number.

Experimentally, the relative deformation of the polymer film can be calculated using the specular and first order diffracted intensities[7] as

$$\varepsilon(t) = 2\left[\frac{I_1(t)}{I_0(t)}\right]^{0.5}\frac{\lambda_{red}}{\pi n_p L} \qquad (6.12)$$

where λ_{red} is the wavelength of the probing beam, $n_p = 1.66$ is the refractive index of azobenzene and L is the sample thickness. I_1 and I_0 are the first order diffracted and specularly reflected intensities. The value of the refractive index was taken the same for both the polymers.

6.3 Fitting Visible Light scattering data

The experimental deformation was calculated using equation (6.12) whereas the theoretical deformation was calculated by an appropriate expression for the creep compliance using equation (6.8) along with Boltzmann superposition principal, equation (6.11). Here we consider the viscoelastic model with two relaxation modes τ_1 and τ_2, and G_1 and G_2 are the modulus corresponding to τ_1 and τ_2. In this model the deformation depends linearly on the ratio σ/G_0, where σ is the stress (in our case it is the light induced stress) and G_0 is the elastic modulus of the used polymer. The elastic modulus of the polymer used in the experiment was considered to be 1GPa by taking into account its molecular weight which varied in the range of 7.6 to 11.5 Kg/mol (from 20 to 30 monomers).[3] Fittings have been performed for pulsed exposure data of pDR1M and pMEA taken at various temperatures. Figure 6.2 shows the deformation fittings carried out for pDR1M at various temperatures performed at the same inscribing intensity for the experiments described in chapter 5. Also fittings have been performed for the pulsed exposure data of pMEA obtained for room temperature measurements and near its glass transition temperature as shown in figure 6.3.

The comparison between the obtained parameters for pDR1M and pMEA has been carried out for further analysis.
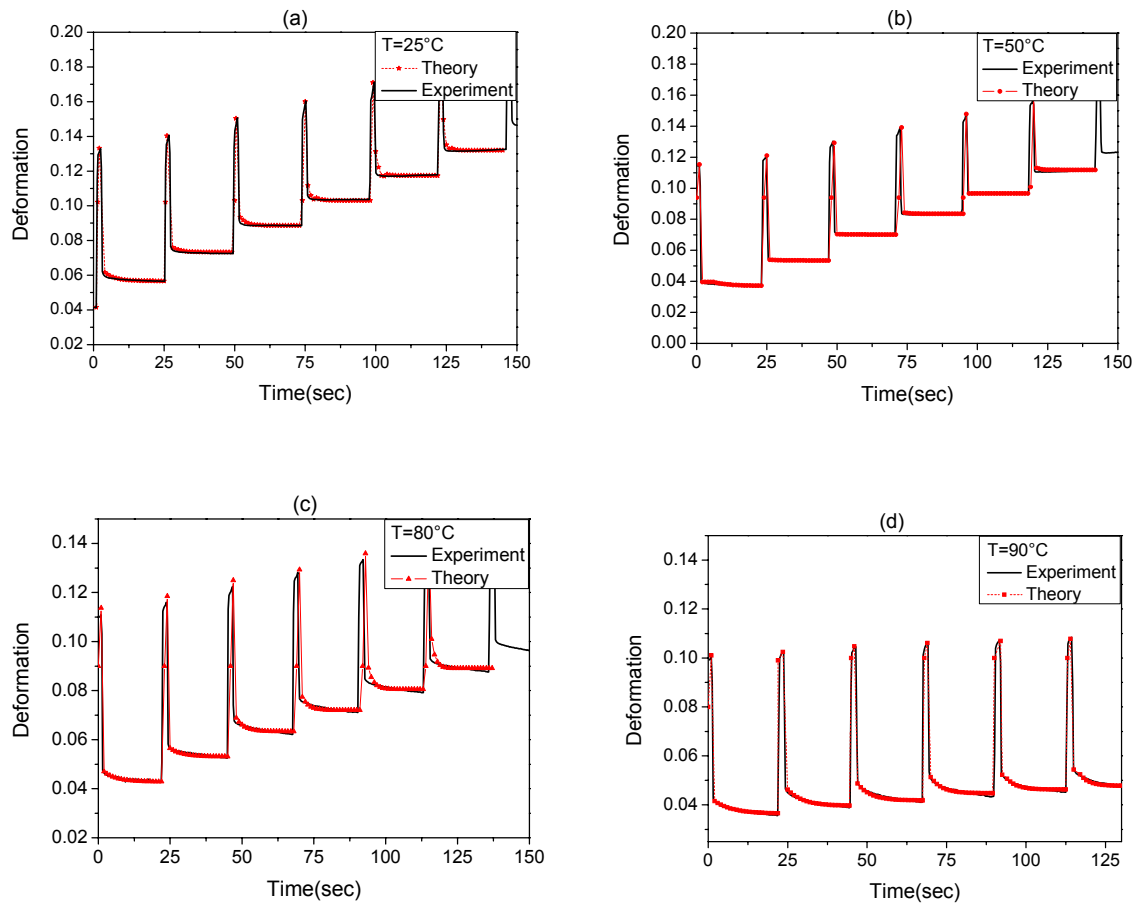
Figure 6.2- Fitting of pulsed exposure deformation on pDR1M, (a) Temperature 25°C, (b) Temperature 50°C, (c) Temperature 80°C, (d) Temperature 90°C.

Figure 6.2 (a), (b), (c), (d), and (e) shows the deformation fitting carried for pDR1M pulsed exposure measurements at temperature 25°C,50°C,80°C,90°C, and 100°C respectively. Depending upon the deformation and the observed relaxation during the experimental measurements, the parameters τ_1, τ_2 and G_1, G_2 and σ have found to vary with respect to temperature. The fittings performed for the pDR1M at T=100°C and for pMEA at T=25°C and T=40°C shows same behavior. But, considering the degree of deformation at various measurements the recorded stress shows considerable variation for those measurements. The fitting parameters for pDR1M at various temperatures are summarized in the table I.
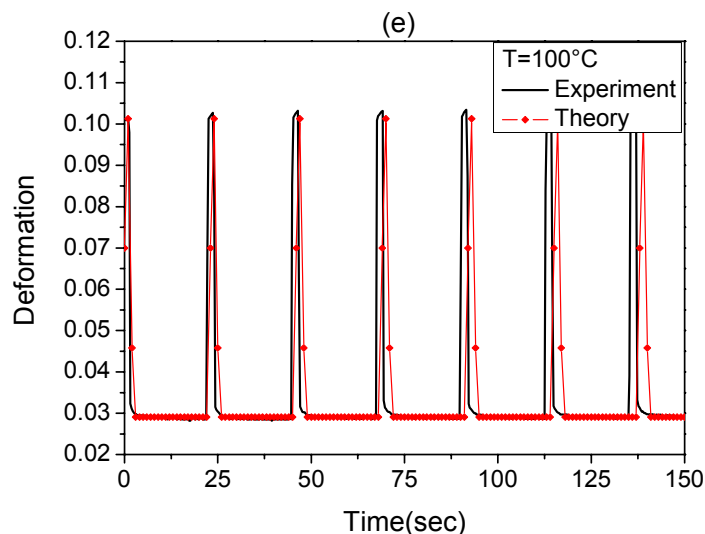
Figure 6.2- Fitting of pulsed exposure deformation on pDR1M, (e) Temperature 100°C.

The pMEA pulsed exposure measurements were carried out at T=25°C and at T=100°C along with its deformation fittings as shown in figure 6.3. Though the measurements look the same pictorially, the jump under the light exposure varies considerably at different temperature which shows variation in the deformation. The obtained parameters for pMEA at various temperatures are summarized in the table II.
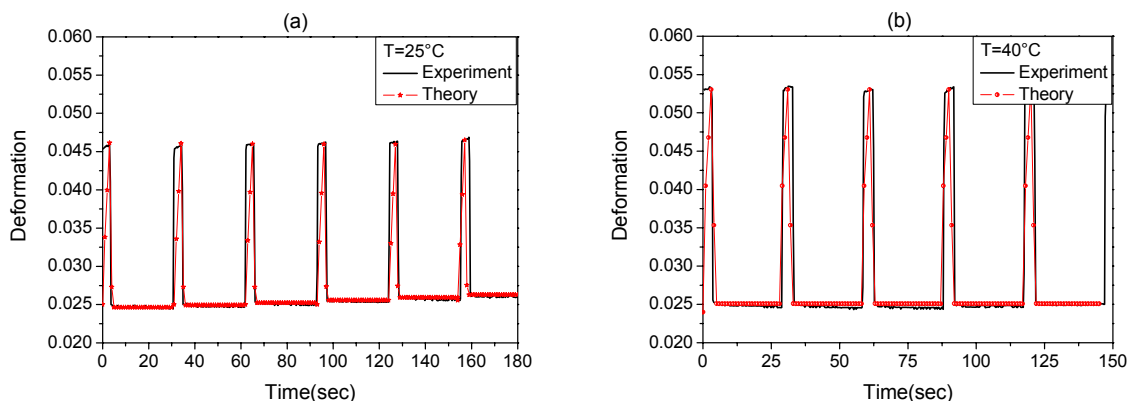
Figure 6.3-Fitting of pulsed exposure deformation on pMEA, (a) Temperature 25°C, (b) Temperature 40°C

The pDR1M and pMEA pulse data for first cycle were fitted with the set of five parameters as shown in Table I and Table II. The relaxation times τ_1 and τ_2 increase gradually up to a certain temperature near glass transition temperature, while the light induced stress was found to decrease. After this crossover temperature (T=90°C), at T $\approx T_G$, τ_1 achieves its highest value where as τ_2 and the light induced stress falls to its minimum. For the first cycle, since there

wasn't any significant difference in the deformation value at different temperature, the modulus of the polymer $G_0:(G1+G2)$ was unchanged. Following successive cycles both the relaxation times τ_1 and τ_2 decrease and reach to its minimum value upto the crossover temperature.

Table I - Fitting parameters for pDR1M

pDR1M Temperature(°C)	G_1 (GPa) modulus	τ_1 (sec) Ist relaxation	G_2 (GPa) modulus	τ_2 (sec) IInd relaxation	σ (GPa) Stress
25	0.52	1.7±0.05	0.48	3±0.1	0.105±0.002
50	0.60	3.2±0.1	0.40	4±0.2	0.094±0.001
80	0.6	3.2±0.1	0.4	6±0.2	0.09±0.001
90	0.75	3.2±0.05	0.25	8±0.2	0.08±0.001
100	0.8	6±0.01	0.2	0.1±0.01	0.07±0.001

Table II - Fitting parameters for pMEA

pMEA Temperature°C	G1(GPa) modulus	τ_1 (sec) Ist relaxation	G_2 (GPa) modulus	τ_2 (sec) IInd relaxation	σ (GPa) Stress
25	0.1	4.5±0.01	0.9	0.1±0.01	0.025±0.001
40	0.69	5.5±0.01	0.31	0.1±0.01	0.024±0.001

6.3.1 Discussion

Formation of surface relief gratings on azobenzene polymer film results in permanent deformation of the film at room temperature. This suggests that the light induced stress should be above the yield stress of the glassy polymer to achieve the permanent deformation. This light induced stress was found to decrease with increasing temperature as seen from the table I, for pDR1M. Above 100°C temperature, close to the glass transition temperature no permanent grating formation was observed (AFM measurements confirm the same, see figure 5.13). At this stage, the gratings were elastic and existed only under light illumination.

Table III – Material Properties of amorphous polymer.

Temperature	Phase state	Young's modulus	Viscosity
$T \ll T_G$	Glass=Solid	$E \sim 2\text{-}4 \ 10^9$ Pa	$\eta > 10^{15}$ Pa. s
$T > T_G$	Viscoelastic	$E \sim 10^6$ Pa	$\eta > 10^6$ Pa. s
$T \gg T_G$	Melt=Fluid	$E \sim 10^3 \text{-} 10^4$ Pa	$\eta > 10^3$ Pa. s

The modulus is represented by symbol E whereas in the table I and II it is represented by symbol G.

Considering the material properties of amorphous polymers as seen in table III, it is well-known that such materials become softer and their resistance to flow i.e. viscosity decreases upon heating towards the glass transition temperature[8]. Under these circumstances, the relaxation time of the system was found to increase gradually with temperature due to increasing softening. This is an indication of the gradual unfreezing of the molecular motion at higher temperature. This effect was observed from room temperature till T=90°C in case of pDR1M. Above this crossover temperature near T_G, the highest softening and probably the partial transition from glassy to viscoelastic state dominates the process of chromophore ordering seen by the lowest relaxation time and by negligible grating heights. Or it can be said that higher potential is needed to overcome the effect temperature, to keep the chromophores oriented. The parameters obtained for pMEA at room temperature (T=25°C) and at higher temperature (T=40°C) can be explained in the same frame.

The effect of low dipole moment manifests itself as increase of the time required for the saturation of SRG growth and decrease of the rate of grating formation observed in the case of pMEA. The low dipole moment of pMEA molecules, because of their less absorption reduces the effective trans-cis-trans isomerization cycles hence the rate of orientation in pMEA is considerably low compared to that of pDR1M.

The significant difference in the light induced stress for pDR1M (105MPa) and pMEA (25MPa) at room temperature is the consequence of the slower orientation rate of the chromophores in pMEA because of their low dipole moment. Since the accumulated stress within the polymer is the consequence of the statistical orientation of chromophore, the slower component in the writing process are related to the overall motion of the polymer matrix.

In the present model, in which the polymer is considered as an isotropic viscoelastic material, the stress relaxation modulus for two relaxation modes is represented as[7]

$$G(t) = G_1 e^{-t/\tau_1} + G_2 e^{-t/\tau_2}$$

(6.13)

The stress relaxation modulus is a measure of gradual decrease of stress when the material is held at constant strain. To understand the temperature dependent behavior of the stress relaxation modulus, the fitting parameters listed in the Table-I for first and second relaxation along with their modulus have been considered.
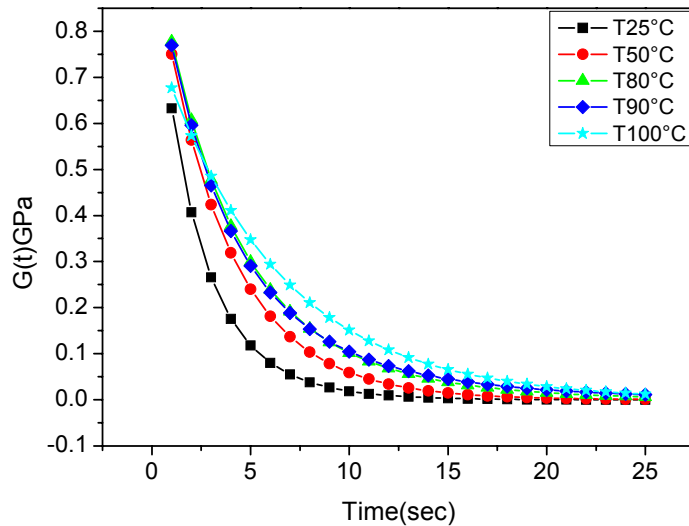

Figure 6.3(c) - Stress Relaxation modulus with respect to temperature.

Figure 6.3(c) shows a behavior of a stress relaxation modulus with change in the temperature with respect to time. At all temperatures the stress relaxation modulus G(t) relaxes to zero as for the viscoelastic materials. The lowering of the slope at different temperatures indicates that the external stress decreases faster with temperature.

6.4 Viscoelastic to Viscoplastic approach

Formation of surface relief gratings on azobenzene polymer film is nothing but the permanent deformation of the film in its glassy state far below its glass transition temperature. Such permanent deformation always requires a higher magnitude of stress than its yield stress. The yield stress for typical glassy polymer is σ_y ~50MPa and is independent of temperature for T<T_G[9] whereas the total stress obtained at room temperature from the simulation is around 100MPa for pDR1M (see table I). This indicates that there exists an additional stress than the yield stress which is responsible for the polymers plastic deformation. As per the assumption, the stress is originated from the orientation of chromophores and is named as light induced stress. Hence the proper description of the polymer deformation below the glass transition temperature is given by a viscoplastic model (= rate-dependent model with the yield stress):[1,4] In the present study, to simulate the pulsed exposure data we used however a simpler

viscoelastic model. Nevertheless, already this simple viscoelastic model allows to gain some insights into the real behavior of azobenzene material under illumination with polarized laser light. Roughly, the total external stress obtained from simulation data can be considered as the combination of yield stress and viscoplastic stress:

$$\sigma_{external} = \sigma_{yield} + \sigma_{viscoplastic}$$

Excluding the value of yield stress from the total external stress, Table I, the viscoplastic stress found to be decreasing gradually with increasing temperature leading to smaller deformation of polymer, seen by diminishing grating heights at higher temperature[1]. The value of the total external stress obtained for T=100°C (Table I) was found very close to the yield stress value where negligible deformation of the polymer film was observed[1], seen by the AFM measurements of the grating samples recorded near the polymers glass transition temperature.

The assumption behind the generation of the stress was the orientation of the azobenzene macromolecules due to the interaction with the polarized light. Hence the slower orientation rate leads to the smaller accumulation of the stress in pMEA. Hence we can conclude that the stress may vary depending upon the architecture of the polymer and it was also observed in the microscopic theory of light induced deformation in amorphous side-chain azobenzene polymers[9].

6.5 Summary

In this chapter, we have demonstrated that the phenomenon of surface relief grating formation on azobenzene polymer films is the consequence of the chromophore orientation which inturn is directly related to the dipole moment of the azobenzene material. The dipole moment of the azobenzene material is directly related to the effective trans-cis-trans isomerisation cycles and consequently to the orientation of azobenzene macromolecules. The high orientation rate in high dipole moment pDR1M leads to the high magnitude of the light induced stress and high order grating formation. The slower orientation and relaxation effect in pMEA reduces the effective isomerization cycles and thereby reduces the light induced stress and the rate of the grating formation. The light induced ordering of chromophores is found to be dominated by temperature induced disordering at higher temperatures.

References

[1] P. U. Veer, U. Pietsch, P. Rochon, and M. Saphiannikova *Mol. Cryst. Liq. Cryst.*, **486,** 66[1126], (2008).

[2] P. U. Veer, U. Pietsch, and M. Saphiannikova *J. Appl. Phys*. Accepted

[3] M. Saphiannikova, T. M. Geue, O. Henneberg, K. Morawetz, and U. Pietsch *J. Chem. Phys*. **120**, 1, (2004).

[4] Marina Saphiannikova, Habilitationsschrift zur Erlangung des akademischen Grades, Feb (2007).

[5] Barrett C. J., Rochon P. L., Natansohn A. L., *J. Chem. Phys.* **109**, 1505, (1998).

[5.a] Christopher Hall, *Polymer Materials* (1981).

[6] Doi M, Edwards S. F., *The Theory of Polymer Dynamics*, Clarendon Press: Oxford, 1986.

[7] M. Saphiannikova, O. Henneberg, T. M. Geue, U. Pietsch, and P. Rochon, J. Phys. Chem. B, **108**, 15084, (2004).

[8] Polymer Materials, Christopher Hall, The Macmillan press Ltd. 1981.

[9] V. Toshchevikov, M. Saphiannikova, G. Heinrich., J. Phys. Chem. B, **113**, 5032-5045 (2009).

[10] Buffeteau T, Lagugne-Labarthet F, Pezolet M, Sourisseau C, *Macromolecules*, **34**, 7514, (2001).

[11] Loucif- Saibi R, Nakatani K, Delaire J. A., Dumont M, Sekkat Z, *Chem. Mater*, **5,** 229, (1993) .

Chapter 7

Light induced Orientation of azobenzene chromophores

7.1 Introduction

The basic assumption of the light induced orientation of the azobenzene macromolecules due to the interaction with the polarized light can be well explained by the experiments performed in the scope of this thesis work. The pulsed exposure measurements have revealed the orientation and relaxation of the azobenzene chromophores whereas the temperature dependent continuous exposure measurements have revealed the ordering and disordering of the chromophores. The idea that the origin of the inscribing force during SRG formation may originate from the reorientation of the azobenzene moieties belongs to Pedersen et. al.[1]. The author, using Maier-Saupe[2] theory suggested that under illumination the azobenzene molecules orient parallel to each other which will increase their mutual attraction. The predictions were consistent with the nematic liquid crystals.[1] Further Bublitz et. al.[3] proposed that the orientation of the azo-chromophores along the grating vector leads to the deformation of the polymer film in that direction without providing any detailed macroscopic picture of the process. Further the magnitude of the light induced force was not predicted by any of the groups working on the investigation of the surface relief grating formation.

Herewith, I will be presenting the theories namely thermodynamic theory[4] and macroscopic theory[5] based on the orientation of the azobenzene chromophores which have predicted the magnitude of the inscribing force. The theories have explained the surface relief grating formation process in much more details.

7.2 Deformation of the Polymer Film

According to the microscopic theory of the light induced deformation,[5] the deformation ε is uniquely determined by the orientation distribution function of the oligomers $f(\theta, \psi)$ as

$$\varepsilon = \int d\Omega f(\Omega) w(\theta) \tag{7.1}$$

The probability $P(\Theta)$ that a chromophore is oriented at an angle Θ with respect to the electric field vector E is shown to be described by the exponential function[5]

$$P(\Theta) \cong C \exp\left[-V(\Theta, T)/kT\right] \tag{7.2}$$

where T is the absolute temperature, k is the Boltzmann constant and V(Θ, T) is the effective light-induced potential which may depend on temperature[6]. The microscopic orientation approach predicts that an azobenzene polymer film can either be stretched or uniaxially compressed along the polarization direction of the incoming light depending on the chemical architecture of azobenzene macromolecules[5]. This prediction is supported by the recent molecular dynamics simulation results, when the opposite sign of the light-induced deformation in LC and amorphous azobenzene polymer samples has been found by taking into account solely the effect of azobenzene reorientation[7,8].

Also from the temperature dependent SRG formation studies performed in the scope of this thesis, it can be seen that the magnitude of the irreversible elongation (i.e. the case when the light induced external stress (σ_{ext}) is higher than the yield stress of the polymer (σ_{yield}) rapidly decreases with increasing temperature and can disappear at certain temperature below the glass-transition temperature. At this stage no grating formation is observed[6]. The latter result has been concluded under assumption that light-induced potential V(Θ, T) that causes chromophore reorientation decreases with temperature following the decrease of the effective transition time between the trans and cis isomer states [6].

As mentioned earlier, the origin of the light induced stress is the statistical reorientation of the azobenzene chromophores. This orientation can be described in terms of the effective orientation potential as[7]

$$V_{eff}(\theta, T) = V_0 \cos^2 \theta_E \qquad (7.3)$$

where θ_E is the angle between the long axis of chromophore and the polarization direction $\mathbf{E}$. V_0 is the strength of potential given by[9]

$$V_0 = \frac{1}{2} \alpha v \tau(T) I_p \qquad (7.4)$$

where α is the absorption coefficient, v is the volume of azobenzene, τ is the effective transition time between two isomer states which depends on temperature T and I_p is the laser intensity. From UV/VIS spectra, the absorption coefficient α was found to be $1.22 \pm 0.03 \cdot 10^5$ cm^{-1} at $\lambda = 514$ nm for pDR1M.[10] The volume of azobenzene v is about 10^{-21} cm^3 and the transition time τ is estimated to be 10^{-3} s at room temperature.[9] Thus, for the laser intensity of 1 W/cm^2 we receive V_0 of about 10^{-19} J.

The magnitude of light induced stress can be estimated from the derivative of the free energy over deformation assuming that the medium is purely elastic.[4] It can be shown that at the very beginning of deformation

$$\sigma \sim nV_0 = \frac{1}{2} n\alpha\nu\tau(T)I_p \qquad (7.5)$$

where $n = 1.5 \cdot 10^{21}$ cm^{-3} is the number density of azobenzenes.[11] Using this value, we receive the light induced stress of about 100 MPa which is high enough to cause yielding of the glassy polymer film at room temperature. Also, during the fittings of the pulsed exposure data at room temperature the magnitude of the stress used was 105MPa[12]. Thus the magnitude of light induced stress estimated by the orientation approach was found to be sufficiently high to induce plastic deformation of the glassy polymer film.

7.3 Polarization dependence of SRG formation

The thermodynamic theory[4] based on the assumption of the reorientation of the azobenzene chromophores has explained the effect of the different inscription geometries i.e. the polarization dependence of the surface relief grating formation. The basic assumption of this theory is that, under homogeneous illumination, an initially isotropic sample should stretch itself along the polarization direction to compensate the entropy decrease produced by the photo-induced reorientation of azobenzene chromophores. The inscription of SRG is strongly dependent upon the polarization of the beam. Most groups report that two counter circularly polarized beams (cir-cir geometry) inscribe gratings of maximum diffraction efficiency followed by two P (p-p geometry) polarized beam while two S (s-s geometry) polarized beam produce gratings of minimum surface modulations.[13,14] The measurements performed during this thesis work also supports the conclusion drawn from the earlier studies as shown in figure 7.1. The dependence of the inscription geometry on the grating formation efficiency was investigated by two polarization states of the beam. The SRG recording was performed using circular and linear, S polarized beam.
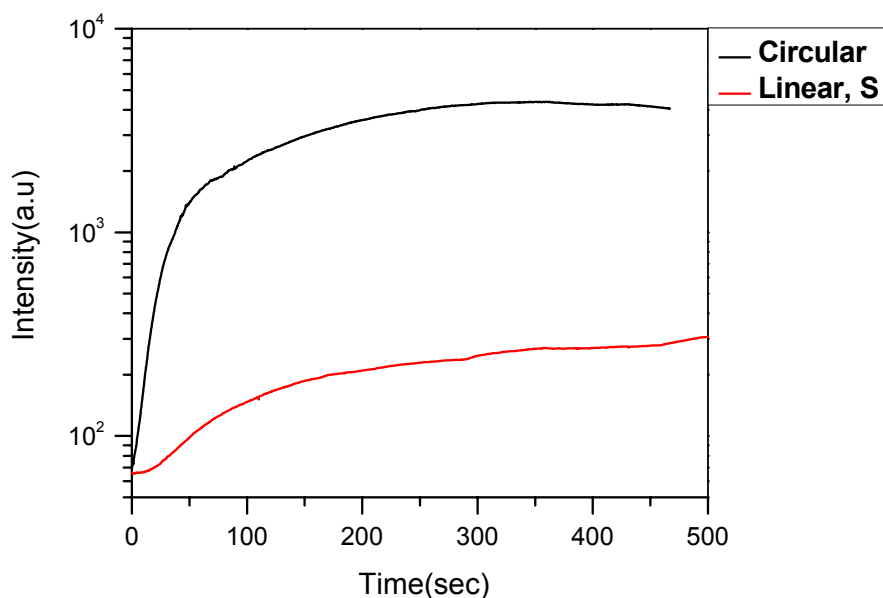
Figure 7.1- First order diffraction intensity during polarization dependence of the grating formation.

The interference pattern of linearly polarized light has intensity modulations whereas the direction of resultant filed vector remains constant. In case of interference pattern of circularly polarized light the intensity remains constant over a grating period whereas the resultant filed vector varies over grating period. Since the photo-addressing of the azobenzene chromophores is purely angular dependent[5], the variation in the resultant field vector of the polarized light in cir-cir geometry is much more effective for the photo-selection and orientation of the chromophores compared to the intensity modulations in s-s- or p-p geometry. The effect is clearly observable in the figure 7.1. For circular polarization of light, the rate of the grating formation is considerably high (around 75%) compared to the rate of grating formation found in S polarization of the light. The measurements were performed under the same power density of the inscribing laser at room temperature.

7.4 Grating inscription below room temperature

The temperature dependence of the surface relief grating formation has shown the decrease in the efficiency of the grating inscription approaching the glass transition temperature.[6,12] The decrease in the effective transition time, gradual unfreezing of the molecular motion with increase in temperature are the parameters which gets affected due to the increase in temperature.[6,12] Further, stronger effective light induced potential is needed to overcome the effect of temperature and to keep the azobenzene macromolecules oriented. The

effect of these factors lead to the decrease in the rate and efficiency of the grating formation at high temperature for the same intensity.

Contrary to this, it can be said that approaching a temperature below the room temperature the rate of the grating formation and the diffraction intensity should increase due to the induced rigidity in the polymer matrix below room temperature. The experimental sample which is always of few hundreds of nanometer thick in size will definitely be affected by small changes in temperature below the room temperature. A test measurement has been performed for the grating inscription below room temperature as shown in figure 7.2. The sample cooling was done by a peltier plate.
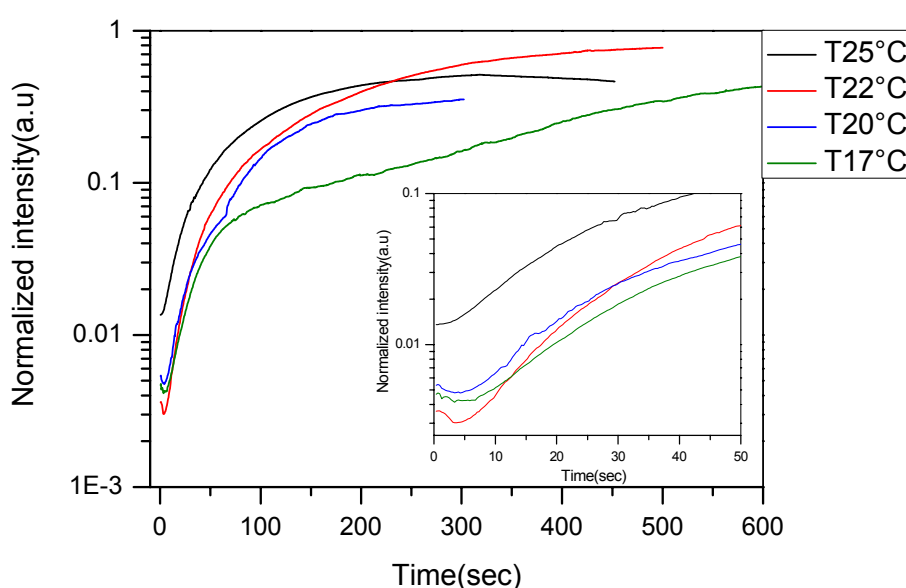

Figure 7.2- first order diffraction intensity during the process of grating formation, below room temperature

But it was very difficult to maintain a constant temperature during the course of the measurements since the second law of thermodynamics i.e. heat flows from hot body to cold body plays a major role in increasing the temperature of the cold side of the peltier plate. Still it was possible to cool the sample upto 17°C.

As seen from the figure 7.2, the diffraction intensity shows continuous increase for low temperature measurements, T=20°C and T=17°C compared to the saturation of SRG formation at room temperature. Also the second observation made in the SRG formation below room temperature is that, the diffraction intensity shows sudden decrease under illumination for first few seconds as seen in the inset of figure 7.2. The drop in the initial

intensity found to increase with decreasing temperature. Later the intensity increases exponentially with the SRG formation.

Further experimental modification is needed for the isolation of the two sides of the peltier plate to reach much lower temperature; to understand the phenomenon of SRG formation below room temperature.

References

[1] Pedersen T. G., Johansen P. M., Holme N. C. R., Ramanujam P. S., Hvilsted S., *Phys. Rev. Lett.* **80**, 89, 1998.

[2] Maier W.; Saupe A. Z.; *Naturforsch*, **14**, 882, 1959.

[3] Bublitz D.; Fleck B.; Wenke L.; *Appl. Phys. B.* **72**, 931, 2001.

[4] M. Saphiannikova, D. Neher. *J. Phys. Chem. B*, **109**, 19428, (2005).

[5] V. Toshchevikov, M. Saphiannikova, G. Heinrich., J. Phys. Chem. B, **113**, 5032-5045 (2009).

[6] P. Veer, U. Pietsch, P. Rochon, M. Saphiannikova, Mol. Cryst. Liq. Cryst., **486**, 66/[1114], 2008.

[7] J. Ilnytskyi, M. Saphiannikova, D. Neher, Cond. Matter Phys., **9**, 87 (2006).

[8] J. Ilnytskyi, D. Neher, M. Saphiannikova, M.R. Wilson, L.M. Stimson, Mol. Cryst. Liq. Cryst., **496**, 186 (2008).

[9] V. Chigrinov, S. Pikin, A. Verevochnikov, V. Kozenkov, M. Khazimullin, J. Ho, D.D. Huang, H.-S. Kwok. *Phys. Rev. E*, **69**, 061713, (2004).

[10] U. Pietsch, P. Rochon. *J. Appl. Phys.*, **94**, 963, (2003).

[11] O. Henneberg, In-situ Untersuchungen zur Entstehung von Oberflächengittern in Polymeren. PhD-Thesis Universität Potsdam, (2004)

[12] P. Veer, M. Saphiannikova, U. Pietsch, J. Appl. Phys. –accepted

[13] Viswanathan N. K., Kim D. Y., Bian S., Williams J., Liu W., Li L., Samuelson L., Kumar J., Tripathy S.K., *J. Mater. Chem.* **9**, 1941, 1999.

[14] Henneberg O., Panzner T., Pietsch U., Geue T., Saphiannikova M., Rochon P., Finkelstein K. Z. *Kristallogr,* **219**, 218, 2004.

Schematic representation of SRG formation

The formation of sinusoidal shaped surface relief gratings on azobenzene polymer thin films indicates that the force which is responsible for the grating formation should also vary sinusoidally. We follow orientation approach for the explanation of the grating formation process. As per the approach, the generation of the stress within the polymer film is due to the statistical orientation of the azobenzene chromophore upon interaction with the polarized light. This orientation is caused by the multiple trans-cis-trans isomerization cycles upon homogeneous illumination of actinic light corresponding to the polymers absorption spectra. The successive orientation cycles lead to the generation of the stress. The stress distribution is according to the intensity or electric field pattern resulting from the interference of two polarized beams used for the grating inscription. The orientation mechanism starts at the surface of the polymer film since grating formation is a surface initiated process[1]. The inscribing force decays exponentially inside the film with respect to the light absorption as shown in figure 1. The schematic representation of the SRG formation is as shown in the figure below.
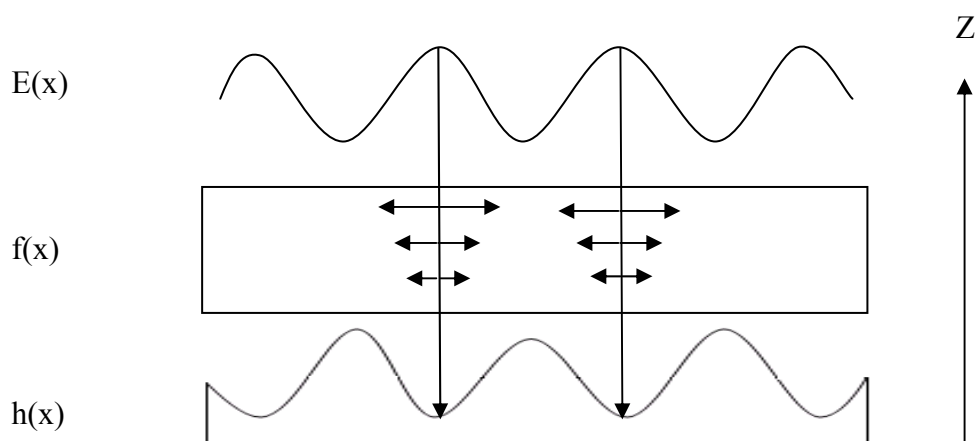

Figure1- Schematic representation of the surface relief grating formation.

The schematic represented here is according to the grating inscription in circular-circular geometry on amorphous azobenzene polymer films, studied in this thesis work. The schematic is divided into three parts; first part shows the electric filed variation resulting from the interference of right and left circularly polarized light along X axis. The second part shows the stress generated within the polymer film following the resultant electric filed variation and the third part shows the grating inscribed on the polymer film. The electric field vector is parallel to the grating vector along X axis.

As seen from the figure1, the sinusoidally varying field vector generates sinusoidally varying force within the polymer film and that leads to the material transport away from the illuminated area. The process thus leads to the π shift of surface relief grating with respect to the interference pattern, in case of amorphous polymer material.

In case of liquid crystalline material, as per the Maier-Saupe theory by Pedersen et. al [2] the grating peaks corresponds to the illuminated regions contrary to π shift of gratings found in amorphous polymer material.

References

[1] Nirmal. K. Viswanathan, Srinivasan Balasubramaniam, Lian Li, Jayant Kumar and Sukant. K. Tripathy *J. Phys. Chem. B*, **102**, 6064, (1998).

[2] T. G. Pedersen, P. M. Johnsen, N. C. R. Holme, P.S. Ramanujam, S. Hvilsted. *Phys. Rev. Lett.*, **80**, 89, (1998).

Summary and conclusion

1. Formation of surface relief gratings (SRG) on azobenzene polymer thin films is due to the ordered arrangement of azobenzene chromophores with respect to the light polarization. The resultant field vector of the light plays a role of director for the arrangement of the azobenzene macromolecules.

2. The temperature dependent continuous exposure and pulsed exposure measurement results can be well explained under the assumption of orientation of azobenzene chromophores upon interaction with the polarized light leading to the generation of mechanical stress necessary for the grating formation.

3. The comparative study between high dipole moment pDR1M and low dipole moment pMEA supports the assumption of the orientation mechanism during SRG formation. The low dipole moment pMEA showed smaller rate and longer inscription time for SRG formation compared to high dipole moment pDR1M due to effectively low orientation mechanism.

4. For a typical value of power density, the estimated light induced stress is 100MPa and the stress obtained from the simulation of deformation data is 105MPa. The obtained values of light induced stress are in good agreement with each other and found enough to deform the polymer in its glassy state.

5. The literature value of the yield stress is 50MPa and the light induced stress (viscoplastic stress + yield stress) obtained near T_G where very weak grating formation was observed was found to be 70MPa. Thus the light induced stress diminishes with temperature and at one stage it becomes less than the yield stress. At this stage no grating formation is possible.

6. Formation of SRG leads to the alteration of the mechanical properties of the azobenzene polymer film. The spatially resolved hardness measurements revealed that the crests of SRG show about 50% increase in hardness relative to the original film. The reason behind this increased hardness is the uniform arrangement of polymer chains at the crests of the gratings compared to troughs. The hardness measurements confirm the rearrangement of polymer chains during SRG formation.

Appendix A

Matlab program for the calculation of polymer deformation under pulsed exposure.

```matlab
%% Inputs initialization


clear all;
sigma_visco = 0.02;      %stress in GPa
sigma_yield = 0.05;      %stress in GPa
k = 0:1:3;               %number of pulses
T = 25;                  %time period in sec
t = 0:1:23;              %time


for i=1:2:max(k)+1
    n=i-1;
    a(i)=T*k(i);
    a(i+1)=T*k(i)+2;    % Exposure
end;


G0 = 1;             %modulus of azobenzene
tou(1)=6;           %first relaxation time
tou(2)=0.1;         %second relaxation time
G(1) = 0.8*G0;      %modulus corresponding to first relaxation time
G(2) = 0.2*G0;      %modulus corresponding to second relaxation time


%% stationary viscosity

g0 = sum(G.*tou);
g1 = sum(G.*tou.^2);
w0 = (1/(G0*tou(1)*tou(2)))*g0;


%% Time dependent deformation

for n=1:max(t)+1
    result(n)=0.0;
        for m=1:max(k)+1
                tx=(n-1)-a(m);
                Gam =(sigma_visco+sigma_yield)*((tx/g0)+(g1/g0^2)+
(exp(-w0*tx)/(G0*w0^2)*(-w0+(1/tou(1)))*(-w0+(1/tou(2)))));
                if tx<0    Fi=0;
                else       Fi=1;
            end
        result(n)=result(n)+(-1)^(m-1)*Gam*Fi;
        end
end

plot(t,result);
data=[t;result];
fid=fopen('file1.txt','wt');
fprintf(fid,'%6.2f %12.5f \n',data);
fclose(fid);
```

Acknowledgement

I would like to express my gratitude to all those who gave me the possibility to complete this thesis.

I am deeply indebted to my research adviser **Prof. Dr. Ullrich Pietsch** for giving me an opportunity to contribute to the development of science and technology. His help, stimulating suggestions and encouragement helped me in all the time of research and for writing of this thesis. I am thankful to him for introducing me to such a potential material which has lots of applications being a light sensitive material.

I am greatly thankful to **Dr. Marina Saphiannikova** for her timely help and guidance throughout the period of this research work. Her intensive research in the same topic for last many years, her research papers and habilitation thesis has helped me a lot to gain a deeper insight into the very complicated grating formation process.

I would like to give my special thanks to **Prof. Dr. Paul Rochon** for many fruitful discussions during the course of this thesis work and being the inventor of this surface relief grating formation phenomenon. I am thankful to him for an idea of a vacuum chamber for the temperature dependent inscription of surface relief gratings to avoid the air turbulence . Small part of the experimental work was performed at his research lab at Royal Military College, Kingston, Canada. I would like to thank him for all the technical support during that period.

I would like to thank my family members, my parents, my brother and sister for their encouragement to achieve higher education.

Last but not least I would like to thank all the present and former members of solid state physics group of Prof. Dr. Ullrich Pietsch.

Eidesstattliche erklärung

Hiermit versichere ich die vorliegende Arbeit selbstständig und unter ausschließlicher Verwendung der angegebenen Literatur und Hilfsmittel erstellt zu haben.

Die Arbeit wurde bisher in gleicher oder ähnlicher Form keiner anderen Püfungsbehörde vorgelegt und auch nicht veröffentlicht.

Siegen